

THERIS

2000

This is to certify that the

dissertation entitled

ELECTROSPRAY IONIZATION - COLLISIONALLY ACTIVATED DISSOCIATION MASS SPECTROMETRIC ANALYSIS OF CHARGED DERIVATIVES OF PEPTIDES

presented by

Nalini Sadagopan

has been accepted towards fulfillment of the requirements for

Ph.D. degree in Chemistry

MSU is an Affirmative Action/Equal Opportunity Institution

0-12771

LIBRARY Michigan State University

PLACE IN RETURN BOX to remove this checkout from your record.

TO AVOID FINES return on or before date due.

MAY BE RECALLED with earlier due date if requested.

DATE DUE	DATE DUE	DATE DUE

6/01 c:/CIRC/DateDue.p65-p.15

ELECTROSPRAY IONIZATION - COLLISIONALLY ACTIVATED DISSOCIATION MASS SPECTROMETRIC ANALYSIS OF CHARGED DERIVATIVES OF PEPTIDES

Ву

Nalini Sadagopan

A DISSERTATION

Submitted to
Michigan State University
in partial fulfillment of the requirements
for the degree of

DOCTOR OF PHILOSOPHY

Department of Chemistry

1999

ABSTRACT

ELECTROSPRAY IONIZATION - COLLISIONALLY ACTIVATED DISSOCIATION MASS SPECTROMETRIC ANALYSIS OF CHARGED DERIVATIVES OF PEPTIDES

By

Nalini Sadagopan

Collisionally activated dissociation (CAD) tandem mass spectrometry (MS/MS) is a useful tool in obtaining protein sequence information. CAD of peptides often yields a mixture of fragment ions retaining either the N-terminus or C-terminus; a further complication usually results from the lack of a continuous series of ions. In contrast, charged derivatives of peptides, where the charge is fixed on one terminus, yield a series of ions retaining only one terminus and hence simpler CAD mass spectra.

This dissertation describes electrospray ionization (ESI)-CAD-MS/MS analysis of peptides derivatized with [tris(2,4,6-trimethoxyphenyl)phosphonium] acetyl (TMPP⁺-Ac), to provide a fixed charge at their N-terminus; ESI-CAD-MS/MS is readily interfacable with separation techniques like liquid chromatography. Based on the results obtained from model peptide derivatives, ESI-in-source-fragmentation (ISF)-MS and ESI-CAD-MS/MS analyses of peptides after TMPP⁺-Ac-derivatization give a continuous and simple series of *a_n and *b_n ions. Most amino acid residues fragment to form *a_n and *b_n ions, however, some specific amino acid residues (e.g., proline, aspartic acid, asparagine etc.) either do not fragment or fragment to give additional ions, which could disrupt the continuity in the series. Recognition of these characteristic patterns is useful

when an unknown sequence is to be determined using this methodology. The application of this derivatizing procedure to tryptic digests of proteins as analyzed by LC-MS is presented.

The impact of charge-derivatization on methods for determining post-translational modification such as phosphorylation is described. Results from studying model phosphopeptides after charge-derivatization show simplification of the spectral series. Phosphoserine and phosphothreonine lose H₃PO₄ predominantly, while phosphotyrosine predominantly loses HPO₃ when present in the charge-derivatized peptide. Similar results are also observed in underivatized phosphopeptides.

Studies on the fragmentation mechanisms of charged derivatives of peptides using deuterium labeling by MALDI-PSD-MS and ESI-CAD-MS/MS show that the migration of the amide hydrogen via a 1,2 elimination process is the major fragmentation pathway in the formation of the ${}^{*}a_{n}$ and ${}^{*}b_{n}$ ions. However, fragmentation at the site of the proline residue to yield ${}^{*}a_{n}$ during the ESI-CAD-MS/MS studies is possibly due to a β -hydrogen shift.

.

Dedicated in loving memory of my Dad......

ACKNOWLEDGMENTS

I would like to express my deepest gratitude to Prof. J.Throck Watson. He was a great mentor and inspired me in many ways. He helped me think through problems critically, and fundamentally.

Thanks to Prof. Allison my second reader, who read through my thesis and provided critical insight. I really enjoyed working with him as a TA during my stay at graduate school.

I also would like to acknowledge the other members of my committee, Professors

Stanley Crouch, Rawle Hollingsworth and Ned Jackson of the Chemistry department.

Many thanks to Charles Ngowe, Jennifer Smith and Jianfeng Qi for their friendship during my stay at MSU.

Words cannot describe how thankful I am to my sweet daughter Shilpa. I am so happy that I was able to have her during my graduate studies. Rishi, my husband, has been so supportive and encouraging during my studies despite his busy schedule. I could not have come this far without their cooperation.

I would also like to thank my parents-in-law, mother, sister and brother for their constant encouragement.

TABLE OF CONTENTS

LIST OF TABLES.	ix
LIST OF FIGURES	x
CHAPTER 1: INTRODUCTION: ELECTROSPRAY IONIZATION TANDEM MA	ASS
SPECTROMETRY AND ITS USE IN THE ANALYSIS OF CHARGED	
DERIVATIVES OF PEPTIDES	
I. Preface	
II. Analytical Techniques and Chemical Procedures	
A) Desorption/Ionization (D/I) Techniques	
B) Electrospray Ionization	
a) Charged-residue Mechanism	
b) Ion Evaporation Mechanism	
C) Collisionally Activated Dissociation Tandem Mass Spectrometry	
D) Triple Quadrupole and Ion Trap Mass Spectrometers	
E) Charged Derivatives for Analysis by Mass Spectrometry	
a) Quaternary Ammonium Derivatives	
b) Quaternary Phosphonium Derivatives	
c) N-terminal Derivatives With High Proton Affinities	
d) The Ideal Charged Derivative	
III. Conclusions	
IV. References	32
CHAPTER 2: ANALYSIS OF TRIS(2,4,6-TRIMETHOXYPHENYL)PHOSPHONI	T IN A
ACETYL DERIVATIVES OF PEPTIDES BY ELECTROSPRAY IONIZATION	.OIVI
FOLLOWED BY QUADRUPOLE OR ION TRAP MASS SPECTROMETRY	27
I. Introduction	
A) Role of Mass Spectrometry in Protein Sequencing	
B) Nomenclature of Fragment Ions Formed From Collisionally Activated	3 /
Dissociation	20
C) FAB-CAD-MS and MALDI-PSD-MS Studies of TMPP ⁺ -Ac-Peptides	20
II. Experimental	
A) Preparation of Charged Derivatives.	
B) Mass Spectrometry	
a) In-source Fragmentation (ISF) MS	
b) MS/MS	
c) MALDI-MS	
III. Results and Discussions.	
A) In-source Fragmentation of the TMPP ⁺ -Ac Derivatives of Peptides	
B) MS/MS of the TMPP ⁺ -Ac Derivatives of Peptides	
a) Triple Quadrupole Mass Spectrometer	
b) Ion Trap Mass Spectrometer.	

C) Comparison of the Fragmentation of the TMPP*-Ac Derivatives of Pepti	
ISF vs. MS/MS	
D) Comparison of the Fragmentation of the TMPP ⁺ -Ac Derivatives of Pepti	
Triple Quadrupole vs. Ion Trap	
E) Speculation of the Fragmentation Pathways of TMPP ⁺ -Ac-Peptides	
F) Characteristic Fragmentation Behavior of Some Amino Acid Residues	
G) Comparison of the Fragmentation of the TMPP ⁺ -Ac Derivatives of Pepti	
ESI-ISF vs. MALDI-PSD and FAB-CAD	
H) ESI-CAD-MS/MS Study of TMPP ⁺ -Ac Derivatized Tryptic Digests	
IV.Conclusions	
V. References	8/
CHAPTER 3: EFFECT OF CHARGE-DERIVATIZATION IN THE	
DETERMINATION OF PHOSPHORYLATION SITES IN PEPTIDES BY ESI-C	`A D_
MS/MS	
I. Introduction.	
II. Experimental.	
III. Results.	
A) Fragmentation of Phosphorylated Tyrosine Residue Containing	
Derivatives by CAD-MS/MS	
B) Fragmentation of Phosphorylated Serine Residue Containing	
Derivative by CAD-MS/MS	
C) Fragmentation of Phosphorylated Threoine Residue Containing	
Derivative by CAD-MS/MS	
D) Fragmentation of Doubly Phosphorylated Peptide Derivative Con	ntaining
Threonine and Tyrosine Residues by CAD-MS/MS	
E) In-Source-CAD-MS of Phosphopetide Derivatives in an Ion Tra	
Spectrometer	111
F) Multiply Phosphorylated Peptides From β-casein	115
IV. Conclusions.	
V. References	120
CHAPTER 4: MECHANISMS OF FRAGMENTATION OF PEPTIDES	
CHARGE-DERIVATIZATION BY ESI-CAD-MS/MS AND MALDI-PSD-MS	123
I. Introduction	
A) Collisionally Activated Dissociation of Protonated Peptides	
B) Fragmentation of Charged Derivatives	
C) Current Studies	
II.Experimental	
A) Peptides Synthesis	
B) Derivative Synthesis	
C) MALDI-MS	
D) ESI-CAD-MS/MS	
III. Results	
A) Analysis of the unlabeled TMPP ⁺ -Ac-VGVAPG	
B) Results From Peptides with Deuterium Label at the α- Carbon	142

a) Deuterium Label at the α- Carbon of Glycine	142
b) Deuterium Label at the α- Carbon of Valine	147
C) Results From Peptides with Deuterium Label at the β- Carbons	149
a) Deuterium Label at the β- Carbon of Valine	149
b) Deuterium Label at the β- Carbon of Alanine	150
D) Results From Peptides with Deuterium Label on the Amide Nitrogens	151
a) Mechanism of Formation of the a _n ion due to the Shift of an	Amide
Hydrogen	155
b) Mechanism for Formation of the (*a ₆ +2) Ion Due to the Shift of C-	termina
Hydrogen Atom	156
c) Mechanism for Formation of the b _n Ion Due to the Shift of an	Amide
Hydrogen	157
d) Mechanism for Formation of the (*b _n +H ₂ O) Ion From the *b _n Ion	159
e) Mechanism for Loss of the C-terminal Residue	160
E) Genesis of *a _n and *b _n ions due to Cleavage at the Site of the Proline Resid	ue162
V.Conclusions	167
IV.References	168

LIST OF TABLES

Table 2.1 Peptides Studied by ESI-CAD-MS After TMPP ⁺ -Ac Derivatization	42
Table 2.2 Proteins Studies by LC-MS After Tryptic Digestion and Derivatization	.43
Table 3.1 List of Phosphopeptides Used in the Study	.97
Table 4.1 List of Labeled Peptides	33
Table 4.2 Ions Observed for d ₂ -TMPP ⁺ -Ac-VG ^α VAPG	46
Table 4.3 Ions Observed for d ₂ -TMPP ⁺ -Ac-V ^α GV ^α APG	48
Table 4.4 Ions Observed for d ₂ -TMPP ⁺ -Ac-V ^β GV ^β APG	49
Table 4.5 Ions Observed for d ₃ -TMPP ⁺ -Ac-VGVA ^β PG1	51
Table 4.6 Ions Observed for d_6 -TMPP ⁺ -Ac-V ^{η} G ^{η} V ^{η} A ^{η} PG ^{η}	54
Table 4.7 List of m/z values for *a ₅ and *b ₅ Ions Observed From the Labeled Variants of TMPP*-Ac-VGVAPG	

LIST OF FIGURES

Figure 1.1 The ESI source5
Figure 1.2 Mechanism of ion formation in ESI as proposed by Dole
Figure 1.3 The components of a quadrupole mass spectrometer
Figure 1.4 The ion trap mass spectrometer
Figure 1.5 Trimethylammonium derivatiation scheme
Figure 1.6 Trialkylammonium-acetyl derivatization scheme
Figure 1.7 Quaternary ammonium derivatization using thiocholine iodide
Figure 1.8 C5Q derivatization reaction
Figure 1.9 Triphenylphosphonium ethyl derivatization reaction
Figure 1.10 TMPP ⁺ -Ac derivatization scheme24
Figure 1.11 Reaction schemes of Renner and Spiteller
Figure 1.12 SPA derivatization reaction
Figure 2.1 Nomenclature for peptide fragmentation during CAD39
Figure 2.2 Reaction of TMPP ⁺ -Ac reagent with the N-terminus of a peptide40
Figure 2.3 ESI-ISF mass spectrum of TMPP ⁺ -Ac-MNYLAFPRM-amide. The inset shows the portion containing peaks due to fragment ions from cleavage at the asparagine (N) residue
Figure 2.4 ESI-CAD-MS/MS spectrum of TMPP ⁺ -Ac-GGSLYSFGL-amide, doubly-charged precursor at m/z 736 in a triple quadrupole mass spectrometer at a collision energy of 65 eV
Figure 2.5 ESI-CAD-MS/MS spectrum of singly-charged precursor of GNLWATGHFM-amide in an ion trap mass spectrometer at 30% relative collision energy

Figure 2.6 ESI-CAD-MS/MS spectrum of singly-charged precursor of TMPP ⁺ -Ac-GNLWATGHFM-amide in an ion trap mass spectrometer at a relative collision energy of 60%
Figure 2.7 ESI-CAD-MS/MS spectrum of doubly-charged precursor of TMPP ⁺ -Ac-GNLWATGHFM-amide in an ion trap mass spectrometer at a relative collision energy of 35%
Figure 2.8 A comparison of the fragmentation of TMPP ⁺ -Ac-GGSLYSFGL-amide by A) In-source fragmentation, B) CAD-MS/MS in a triple quadrupole (doubly-charged precursor) C) CAD-MS/MS in an ion trap (singly-charged precursor) mass spectrometers
Figure 2.9 In-source fragmentation of TMPP ⁺ -Ac-GGSLYSFGL-amide followed by m/z analysis of fragment ions in an ion trap mass spectrometer
Figure 2.10 ESI-source-CAD mass spectrum of TMPP ⁺ -Ac-VGVAPG in a single-quadrupole mass spectrometer. Spectrum shows a series of *a _n ions, except for cleavage at the site of proline (*a ₅)
Figure 2.11 Structure of proline (P) residue
Figure 2.12 Structure of threonine (T) residue
Figure 2.13 Structure of aspartic acid (D) residue
Figure 2.14a Mechanism for the formation of b _n ion due to fragmentation at D65
Figure 2.14b Mechanism for the formation of *c _n ion due to fragmentation at D65
Figure 2.14c Mechanism for the formation of ${}^{\bullet}c_{n-1}$ ion due to fragmentation at D66
Figure 2.15 Portion of the ESI-ISF- mass spectrum of TMPP ⁺ -Ac-APGDIRYVHPF, showing the fragmentation pattern of aspartic acid residue (D)
Figure 2.16 Structure of asparagine (N) residue
Figure 2.17 Structure of glutamine (Q) residue69
Figure 2.18 Portion of the ESI-ISF-MS spectrum of TMPP ⁺ -Ac-APSGAQRLYGFGL-amide. Fragmentation at the glutamine residue (Q) results in a [•] c _{n-1} ion. Fragment ions containing the arginine residue (R) show loss of ammonia
Figure 2.19 Structure of histidine (H) residue71

Figure 2.20 ESI-ISF mass spectrum of TMPP ⁺ -Ac-VHLTPVEK showing characteristic fragmentation of H residue and T residue at positions 2 and 4 respectively
Figure 2.21 Structure of arginine (H) residue
Figure 2.22 A comparison of the fragmentation of TMPP ⁺ -Ac-GMDSLASFGGL-amide by ESI-ISF-MS, MALDI-PSD-MS and FAB-CAD-MS respectively
Figure 2.23 LC-MS results of the TMPP ⁺ -Ac-derivative mixture of the tryptic digest of cytochrome-C. Top panel shows the chromatogram for the separation mixture. Bottom panel shows the ESI-ISF mass spectrum of a peptide derivative (residues 80-86), TMPP ⁺ Ac-MIFAGIK
Figure 2.24 ESI-CAD-MS/MS of TMPP ⁺ -Ac-IFVQK, peptide derivative from tryptic digest of cytochrome-c, in an ion trap mass spectrometer at 55% relative collision energy
Figure 2.25 ESI-CAD-MS/MS of a peptide derivative from cytochrome-c tryptic digest with a precursor mass of 1179 Da at a relative collision energy of 60%
Figure 2.26 ESI-CAD-MS of TMPP ⁺ -Ac-YLDSR, peptide derivative from the tryptic digest of glucagon, showing the characteristic fragmentation pattern of aspartic acid residue D
Figure 2.27 A comparison of ESI-ISF mass spectrum (top panel) with MALDI-PSD spectrum (bottom panel) of TMPP ⁺ -Ac-GFFYTPK, a peptide derivative from the tryptic digest of insulin chain-B
Figure 3.1 Structures of amino Acid residues serine (S), threonine (T), and tyrosine (Y) respectively90
Figure 3.2 Loss of phosphoric acid via a six-membered transition state in peptides containing phosphorylated serine, and threonine residues
Figure 3.3 a) Possible elimination of H ₃ PO ₄ from tyrosine phosphate. b) Dehydration of an aromatic alcohol vs. an aliphatic alcohol
Figure 3.4 ESI-CAD-MS/MS spectrum of the doubly-charged precursor of LKRAyLG-amide at 25% (relative collision energy full scale of 5 eV)
Figure 3.5. ESI-CAD-MS/MS spectrum of TMPP ⁺ -Ac-LKRAyLG-amide, singly-charged precursor m/z 1471, at 50% relative collision energy
Figure 3.6. ESI-CAD-MS/MS spectrum of TMPP ⁺ -Ac-LKRAsLG-amide, singly-charged precursor m/z 1395.5, at 50% relative collision energy

Figure 3.7a ESI-CAD-MS/MS spectrum of LKRAtLG-amide, singly-charged precursor m/z 837, 30% relative collision energy
Figure 3.7b ESI-CAD-MS/MS spectrum of TMPP ⁺ -Ac-LKRAtLG- amide, singly-charged precursor m/z 1409.5, 50% relative collision energy
Figure 3.8 ESI-CAD-MS/MS spectrum of TMPP ⁺ -Ac-KIGEGtyGVVYK, doubly-charged precursor m/z 1024, 35% relative collision energy. The boxed notations indicate the fragments retaining the phosphate moiety
Figure 3.9 ESI-source-CAD-MS spectrum of TMPP ⁺ -Ac-LKRAyLG-amide, at a capillary voltage of 70 V and tube lens offset of 50V
Figure 3.10 Abundance of fragment ions formed from TMPP ⁺ -Ac-LKRAyLG-amide by source-CAD-MS
Figure 3.11 Abundance of fragment ions formed from TMPP ⁺ -Ac-LKRAyLG-amide by CAD-MS/MS
Figure 3.12 Structure of *c _n ions formed from TMPP*-Ac derivatives of peptides115
Figure 3.13 MALDI-TOF mass spectrum of the tryptic digestion mixture of β -casein. The peak at m/z 3125 represents a protonated phosphopeptide with four phosphates. The peaks at m/z 3027 and 2939 represent the protonated singly and doubly dephosphorylated forms of the peptide RELEELNVPGEIVEsLsssEESITR respectively
Figure 4.1a Mechanism of fragmentation of protonated peptides to form y _n ions126
Figure 4.1b Mechanism of fragmentation of protonated peptides to form b _n ions127
Figure 4.2 Protons that could possibly shift during charge-remote fragmentation of a peptide bond
Figure 4.3. Plausible structures of fragment ions formed from fixed-charged derivatives130
Figure 4.4. Mechanism of *a _n ion formation by amide hydrogen shift in TMPP*-Acpeptides
Figure 4.5. Structure of the proline residue
Figure 4.6a ESI-source-CAD mass spectrum of TMPP ⁺ -Ac-VGVAPG in a single-quadrupole mass spectrometer. Spectrum shows a series of *a _n ions, except for cleavage at the site of proline (*a ₅)
Figure 4.6b MALDI-PSD mass spectrum of TMPP ⁺ -Ac-VGVAPG. The spectrum shows a series of *a _n ions except for cleavage at the site of the proline residue(*a ₅)139

Figure 4.6c FAB-CAD-MS/MS spectrum of TMPP ⁺ -Ac-VGVAPG (Adapted from reference 21). Peak represented by a ₅ corresponds to cleavage at the proline residue140
Figure 4.7 ESI-CAD-MS/MS spectrum of TMPP ⁺ -Ac-VGVAPG in an ion-trap mass spectrometer
Figure 4.8a ESI-source-CAD mass spectrum of TMPP ⁺ -Ac-VG $^{\alpha}$ VAPG, species B, in an ion trap mass spectrometer. Fragment ions ${}^{*}\mathbf{a_{2}}$ ${}^{*}\mathbf{a_{6}}$ are shifted by 2 Da corresponding to the retention of the deuterium label on the α -carbon during fragmentation
Figure 4.8b ESI-CAD-MS/MS spectrum of TMPP ⁺ -Ac-VG ^α VAPG, species B, in an ion trap mass spectrometer at 35% relative collision energy. Fragment ions ${}^{*}a_{2}$ - ${}^{*}a_{6}$ are shifted by 2 Da corresponding to the retention of the deuterium label on the α-carbon during fragmentation.
Figure 4.8c MALDI-PSD mass spectrum of TMPP ⁺ -Ac-VG $^{\alpha}$ VAPG, species B. Fragmentions ${}^{*}\mathbf{a_2} - {}^{*}\mathbf{a_6}$ are shifted by 2 Da corresponding to the retention of the deuterium label on the α -carbon during fragmentation
Figure 4.9 Full scan mass spectrum of the amide hydrogen labeled species of TMPP ⁺ -Ac-VGVAPG. Completely deuterium exchanged precursor is represented by the peak at m/z 1077.5

Chapter 1

INTRODUCTION

ELECTROSPRAY IONIZATION TANDEM MASS SPECTROMETRY AND ITS USE IN THE ANALYSIS OF CHARGED DERIVATIVES OF PEPTIDES

I. Preface

The goal of this chapter is to introduce the analytical techniques and concepts that are primarily used in obtaining the results discussed in this dissertation. Electrospray ionization (ESI), one of the desorption ionization (D/I) techniques, is presented in section B. Structural information of the ions formed by ESI is obtained from their collisionally activated dissociation (CAD). CAD is described in section C. The fragments that are obtained from CAD are analyzed by triple quadrupole and ion trap mass spectrometers. Section D of this chapter focuses on these mass spectrometers. The main crux of this dissertation is to study the fragmentation of fixed charge derivatives; history of charged derivatives and their study by various DI/-mass spectrometry (MS) is discussed in the section E of this chapter.

II. Analytical Techniques and Chemical Procedures

A) Desorption/Ionization (D/I) Techniques:

Mass spectrometry has been used in the structural elucidation of small organic molecules for several decades [1]. The analyte, which has a significant vapor pressure (10⁻² mm of Hg) at room temperature, is ionized and fragmented by energy absorbed

from 70 eV electrons. The resultant ionic species are then separated based on their physical properties such as momenta, or m/z values in the mass analyzer. Thus the technique itself has two major components, one involves the ionization source and the other involves the mass analyzer. Hence, if a molecule is non-volatile and thermally labile it cannot be transferred into the gas phase without degradation. Therefore, it is not suitable for mass spectrometric analysis. Ingenious scientists realized this shortcoming of the electron ionization technique in the late 1970's, when the need to analyze the mass of biomolecules was identified. These researchers paved way for the D/I techniques. These techniques are briefly discussed in the following sections with a major focus on electrospray ionization (ESI). Most of the results presented in this dissertation are based on ESI.

Biomolecules such as peptides and nucleotides have very low vapor pressure and are non-volatile. The idea of transferring non-volatile compounds into the gas phase without decomposition was originally put forth by *Beuhler et al.* [2]. Based on the rate theory for unimolecular decomposition they proposed that sufficiently rapid heating could vaporize complex molecules before decomposition occurred. This led to the development of "pyrolysis MS" by *Meuzelaar et al.* [3]. Later, the same group used laser photons to flash desorb the non-volatile large molecules. These kinds of techniques are described by *Fenn et al.* as "energy sudden", since the analyte instantaneously achieves high-energy density [4]. These experiments can be called the forerunners of the current D/I techniques.

Fast atom bombardment (FAB) is the first D/I technique used in conjunction with MS for the analysis of biomolecules up to 5000 Da in molecular weight [5]. Since then

other "energy sudden" techniques such as fast ion bombardment (FIB) [6] and plasma desorption (PD) [7] have evolved. These techniques are based on generating ions from a surface that cannot be continuously replenished. However, the development of continuous-flow-FAB presented a continuously renewed surface to the incident fast atoms [8].

LD became well known due to the efforts of Karas and Hillenkamp; they showed the effect of a matrix that assists in the energy transfer from the photons to the analyte [9]. This technique called matrix-assisted laser desorption ionization (MALDI) is "softer" than the other "energy sudden" techniques described earlier. The wavelength of the laser and the composition of the matrix (small organic molecules) play an important role in this D/I processes. This technique has gained attention in the last few years and is primarily used with a time-of-flight mass spectrometer. The use of a reflectron with this technique has also allowed for the analysis of fragment ions produced from metastable decomposition of the precursor ion during its flight in the field-free region [10]. This technique is termed post-source decay (PSD) and is widely used in determining the sequence of peptides and nucleotides.

Field desorption (FD) involves desorbing ions from analytes with the assistance of very strong electrostatic fields. *Inghram and Gomer* [11] first used it as an ionization source for MS. Later on *Beckey* modified the technique to produce higher currents from analyte ions [12]. Emitter electrodes are used to desorb analytes into the gas phase in vacuum. This technique is tedious and can be used only with magnetic sector mass analyzers since the ions emerging from the ion source have kV's of kinetic energy.

The other form of field desorption involves production of ions from solutions at atmospheric pressure rather than in vacuum. It is most generally called atmospheric ionization (API). It is also called electrospray ionization (ESI) or thermospray ionization (TSI) depending on the design of the source. However, in both cases the formation of droplets and the subsequent formation of ions are assumed to be the same. The following sections will concisely describe the history of ESI and mechanism of ion formation in ESI.

B) Electrospray Ionization:

Malcolm Dole and his coworkers were the first to report ESI in 1968 [13]. They pioneered the experiments which explain the mechanism for ion formation in ESI. Figure 1.1 describes ESI in its widely accepted form [14]. The solution, which contains the analytes in their ionic form, is nebulized into a high electric field gradient from a capillary (held at 3.5 – 5 kV) with a typical inner diameter of 100 μm and a flow rate of 1-10 μL/min. The charged analyte accumulate at the tip of the capillary, and the electrohydrodynamics of the solution result in the formation of a "Taylor cone". Droplets with an initial diameter of 1μm are then formed from the Taylor cone by the process of budding [15]. These typical droplets contain numerous charged analytes (150,000 for a concentration of 500 fmol/ μL) [16].

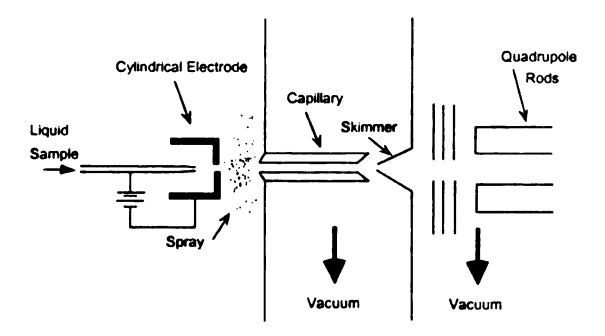


Figure 1.1. The ESI source.

The mechanism by which the individual analyte ions are released from the droplet is explained by two theories.

a) Charged-residue Mechanism:

Dole proposed the charged-residue mechanism. It states that as the charged droplets progress through the electric field, solvent molecules evaporate due to the effect of the drying gas, and the droplet shrinks in size. At one point, the number of charges on the droplet is high and hence there is a very high coulombic repulsion that exceeds the surface tension that holds the droplet together. This results in the "coulombic explosion" of the droplet. These explosions occur repeatedly, which result in the ejection of individual charged analyte molecules [13]. This theory was substantiated by *Chapman*'s mobility experiments [17]. Figure 1.2 presents Dole's mechanism of ion formation in ESI [14].

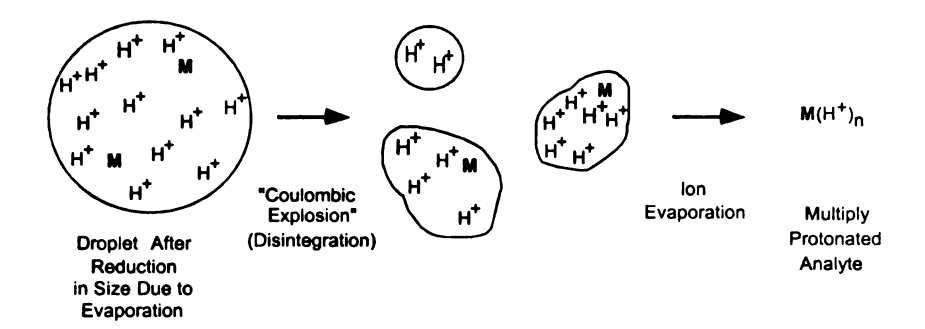


Figure 1.2. Mechanism of ion formation in ESI as proposed by Dole.

b) Ion Evaporation Mechanism:

Thomson and Iribarne [18] first proposed the field-assisted ion evaporation mechanism. Later, this was applied for the ion generation for biomolecules by Fenn et al. [19]. This mechanism suggests that a charged part of the molecule penetrates the surface of a droplet. The coulomb repulsion between this part of the molecule and the droplet surface would pull the entire charged molecule out of the droplet. The macromolecule plays an active role in ionization in this mechanism whereas it is passive in the mechanism proposed by Dole [20].

Although, *Dole's* mechanism is widely accepted, the ion evaporation mechanism has still not been ruled out as a possibility. Whatever the mechanism of ion formation, the multiply charged individual analytes are then analyzed by the mass spectrometer. The formation of multiple-charged analyte ions is advantageous since this allows the usage of a mass spectrometer such as a quadrupole or an ion trap, which has a limited mass range capability (up to 2000).

There are several reviews and tutorials explaining the process of electrospray and its advantages over the existing ionization mechanisms [21,22]. One of the advantages is that the sample need not be volatile; however it should be ionizable. The other advantage is that ionization occurs at room temperature and at atmospheric pressure. This eliminates the possibility of sample degradation during ionization, because there is no need for extreme heating. This aspect has been pursued in using ESI-MS for the study of non-covalent interactions between molecules [23].

The major advantage is its compatibility with separation techniques such as liquid chromatography. The effluent from such a separation technique could be directed into the inlet of the ESI-MS, and samples can be directly analyzed. Modern mass spectrometers with specially designed sources could tolerate flow rates of even 1 mL/min, at a higher flow of sheath gas. On the other hand, in order to improve the efficiency of ionization, there has been much focus on the miniaturization of the ESI device. A report by Wilm and Mann has served as an introduction to this area of research [16]. Based on theoretical calculations and experimental evidence, they conclude that by using a capillary of 1-3 µm, droplets as small as 180 nm could be formed. The source was operated at 580-800 V as opposed to 3.5-5 kV in a conventional device. Using such a construction, a 1-uL aliquot of solution was sprayed for ca. 45 min., which amounts to a flow rate of < 25 nL/min. The overall effect was that the ionization and transmission efficiencies were improved by several orders of magnitude. It was also shown that signal could be detected from a solution of concentration as low as 0.05 pmol/uL. Additionally, the micro electrospray device or the nanospray is more stable than the conventional source and is moderately tolerant to salts. This idea has been

commercialized and there are several vendors who provide nanospray devices. These are highly useful in analyzing very small amounts (femtomoles to attomoles) of biomolecules such as protein derived from biological sources [24].

C) Collisionally Activated Dissociation Tandem Mass Spectrometry:

Structure elucidation of an analyte after ionization is possible in MS by collisionally activated dissociation (CAD). Ions leaving the source can be classified based upon their lifetime relative to the transient time from the ion source to the detector. Ions with a lifetime greater than 10⁻⁶ sec. are considered stable and reach the detector before they can fragment. Ions with a lifetimes less than 10⁻⁷ sec. are unstable and fragment before leaving the ionsource. Ions with lifetime between 10⁻⁶ and 10⁻⁷ sec. are considered metastable as they fragment sometime after leaving the source and before reaching the detector. The ion with a lifetime longer than 10⁻⁶ sec, the stable ion, is selected and activated before it fragments. The intact ion is energetically activated which results in its fragmentation. The fragment ions thus formed are mass analyzed. Rules governing the fragmentation for various molecules have been derived. For example, the types of bonds that can be cleaved and the ions that could be obtained from a peptide are well defined [25,26]. Thus, from the fragment ion masses and from using the specific guidelines for the type of analyte, the structure could be determined. The scientific community also uses the term collision-induced dissociation (CID) interchangeably with CAD.

The process of CAD is specific since a precursor is chosen and is selectively activated. The availability of tandem mass spectrometers allows one to perform MS/MS.

The term MS/MS implies that there are two scans performed. The first process is a full scan for the entire m/z range to isolate the precursor of interest. The isolated precursor is activated by collision with a neutral target gas admitted to the reaction region, during which a portion of its translational energy coverts into internal energy. The excess internal energy in the analyte is then channeled via the vibrational modes, which results in the unimolecular decomposition of the activated ion. Only a fraction of the ion kinetic or translational energy (E_{lab}) is converted into its internal energy. This is given by the energy of center-of-mass (E_{com}) which is dependent on the mass of the target gas (m_t) and the mass of the precursor (m_p) [27].

$$E_{com} = E_{lab}[m_t/(m_t + m_p)]$$

Consequently, an increase in the ion kinetic energy (E_{lab}) increases the available energy for ion fragmentation (E_{com}). The second scan involves the mass analysis of the fragments formed after CAD.

CAD is classified as high-energy (HE) or low-energy (LE) based upon the energy imparted to the precursor. The precursor is activated with keVs of energy in HE-CAD, whereas it is activated with less than 200 eV in LE-CAD. HE- CAD is usually performed in the magnetic sector or hybrid instruments. The primary excitation in this collision energy region is electronic. The kinetic-to-internal energy conversion occurs most efficiently when the collision interaction time and the internal period of the mode that undergoes excitation are comparable [28]. The interaction time of the precursor and the target in such cases is in the order of 10⁻¹⁵ sec. This corresponds to a vertical electronic transition. Generally, gas such as argon or xenon is used in these studies to enable efficient internal energy transfer. Although keV's of energy are supplied to the precursor

ion, only 1-4 eV of energy is acquired by the ion during its stay in the HE collision cell [29,30].

LE-CAD is usually performed in the triple quadrupole or ion trap mass spectrometers. The lifetime of the target-precursor complex is only 10^{-14} sec. and hence the ions excitation is usually vibrational. The energy that is deposited on the ion is lower than in HE-CAD. However, the collision yields are higher than in HE-CAD because of the multiple collisions that can occur in these processes. The effective energy gained by the precursor ion is about 2.3 eV [27]. Dependent on the mass spectrometer, the tandem process could occur in time or space. For example, in the triple quadrupole MS, it occurs in space, while in the ion tap mass spectrometer it occurs in time. There are several books describing the operational principles of these two mass spectrometers [31,32]. It is beyond the scope of this dissertation to describe the triple quadrupole and the ion trap mass spectrometers in their entirety. However, their basic operation and the differences between these two mass spectrometers will be discussed in the following section.

Based on the above description, the energetics involved in HE- and LE-CAD processes vary; thus, significantly different fragmentation of the precursor occurs. It has been reported that while it is possible to generate d_n ions, formed due to cleavage of side chains from peptides from HE-CAD, it is not very commonly observed during LE-CAD [33]. The pathways involved in the formation of the same product ions from a precursor by these two processes (HE-CAD and LE-CAD) could be different, too.

D) Triple Quadrupole and Ion Trap Mass Spectrometers:

The transmission quadrupole and the ion trap mass spectrometers are dynamic devices, in which the ion trajectories are influenced by a set of time-dependent forces.

Ions in such quadrupole fields experience strong focusing to the center of the device. The motion of the ions in quadrupole fields is described mathematically by the solutions to a second-order linear differential equation described by *Mathieu* [31].

The transmission quadrupole is made of four hyperbolic rods that are electrically connected as shown in Figure 1.3. RF and DC voltages are superimposed on the rods to create a hyperbolic electric field. At any one set of voltages, only ions of a particular m/z value have stable trajectories inside the device and they eventually reach the detector. An analytical scan is performed by increasing the RF and DC voltages at a constant ratio. The relationship between the voltages and the m/z values are derived based on the Mathieu's equations. Thus, the device could be termed as a filter based on the m/z value of the ions. In order to obtain structural information of the ions, a triple quadrupole is used [34]. There are three transmission quadrupoles aligned linearly. The first stage allows the transmission of a precursor with a particular m/z value into the second stage. The second stage is a RF-only device (non-mass selective) which contains the target gas such as argon. The RF-only mode allows in better focusing of the precursor ions. The precursor ions are kinetically accelerated while arriving into the high-pressure collision cell and collisions with the target gas result in their fragmentation. The third stage performs a full scan to analyze the m/z values of the fragment ions resulting from the CAD process. The fragmentation efficiencies of this device are high because of the considerable distance traveled by the ion in the collision cell. Rapid speeds are achievable for the precursor and product scan mode in the transmission quadrupole. The ability to switch between masses makes multiple selected reaction monitoring

experiments practical. Thus, these devices are widely used in experiments for quantitating a single component in highly complex mixture.

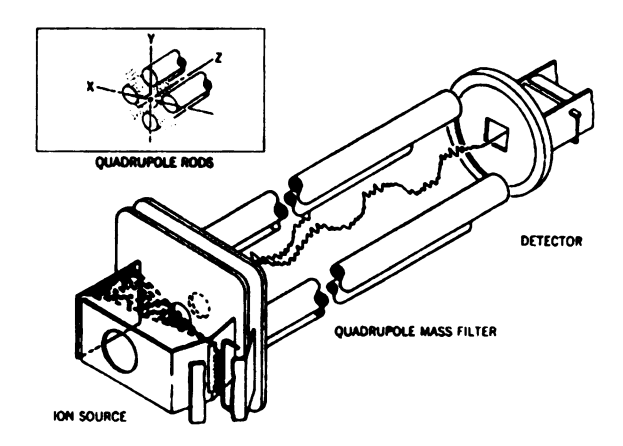


Figure 1.3. The components of a quadrupole mass spectrometer.

The ion trap mass spectrometer is also a quadrupole device composed of three electrodes (Figure 1.4). There are two end-cap electrodes and a ring electrode. Application of a RF potential to the ring electrode while maintaining the end-cap electrodes at ground establishes a 3D quadrupole field in the trap. Helium is usually used as the gas in the trap, which serves to "cool" the ions as well as to cause CAD. The analytical scan is performed by operating the trap in the mass-selective instability mode where the ions are rendered unstable and are ejected out of the trap in the order of increasing m/z. CAD is performed in the trap by "resonance-excitation". The precursor ion of interest is isolated in the trap while all the other ions are ejected. A supplemental AC voltage ("tickle") whose frequency corresponds to the fundamental frequency of the precursor ion is applied through the end-cap electrodes [32]. The ion is thus energetically activated, which results in collisions with the helium gas. Thus fragments are formed, which are then mass analyzed by performing a product ion scan in the trap.

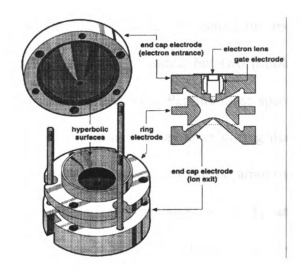


Figure 1.4. The ion trap mass spectrometer.

The reaction times in the transmission quadrupoles and the ion trap quadrupoles are different. In the trap, the residence times of the ions are in the order of milliseconds whereas in the transmission quadrupole it is less than 100 µsec. Thus, considerably more collisions will occur in the trap (which also depend on the pressure in the cell) and hence higher energies can be deposited but in smaller increments [35]. This is often not the case because, helium is the collision gas and hence the activating collisions are relatively inefficient [36]. Moreover, because of the long reaction times, an ion that has accumulated sufficient internal energy to decompose by a lower-energy process may not survive to undergo another activating collision. Thus, the ion trap mass spectra are reflective of fragment ions produced from low-energy processes than those spectra produced from a transmission triple quadrupole device [37]. These characteristics are also observed in the CAD-MS/MS results for the charged derivatized peptides as shown in the following chapters.

E) Charged Derivatives for Analysis by Mass Spectrometry:

The introduction of the new desorption ionization techniques and MS/MS revolutionized mass spectral analysis of peptides, but two problems remained: lack of sensitivity and difficulty in data interpretation. Peptide mass spectra can be complicated due to the many types of fragment ions that can arise during desorption/ionization and CAD-MS/MS. The peptide fragments observed can be amino-terminal fragments (a_n, \mathbf{b}_n , \mathbf{c}_n , and \mathbf{d}_n ions), carboxy-terminal fragments (\mathbf{x}_n , \mathbf{y}_n , \mathbf{z}_n , \mathbf{v}_n , and \mathbf{w}_n ions), or internal fragments. The extent of charge localization influences the types of fragment ions produced [38]. Charge-derivatized peptides have complete charge-localization and produce fragments with the charge retained at the site of derivatization. Charged derivatives were developed to simplify and direct the fragmentation of peptides. Thus, formation of a series of one ion type from charged derivatives facilitates the interpretation of their mass spectra. Charged peptide derivatives form fragment ions through charge-remote mechanisms (i.e., the site of the charge is remote from where the cleavage of the bond occurs) [39,40]. As a result, specific types of fragment ions are observed. Several types of derivatives were developed to lower the detection limits of peptide analytes. Some of these derivatives contained nonpolar functionalities to increase the surface activities of peptides during analysis by FAB and LSIMS [41-43]. Other derivatives generated preformed ions, a condition that increased ionization efficiencies of many analytes during analysis by desorption/ionization techniques [44].

Protonated peptides and charged peptide derivatives differ in mass depending on the type of derivatization. The nomenclature used here for the fragment ions of chargederivatized peptides corresponds to the nomenclature of protonated peptides when the mass difference in (singly-charged) precursor ions is taken into account, but an asterisk is added to denote the presence of the derivative moiety. For example, the N-terminal fragment ion resulting from cleavage of the $CH(R_n)$ -CO bond is called an a_n ion when it arises from a protonated peptide and is called an a_n ion when it arises from a charged derivative.

Charge derivatization limits the types of fragment ions generated from peptides. Derivatization at the N-terminus causes N-terminal charge-remote fragments to be observed and derivatization at the carboxy-terminus (C-terminus) causes C-terminal fragment ions to be observed. High-energy CAD of N-terminal charged derivatives produces primarily $*a_n$ and $*d_n$ ions plus a few $*b_n$ and $*c_n$ ions [45] while C-terminal charged derivatives produce primarily y_n*-2 , y_n* , v_n* and w_n* ions [46, 47]. This section will focus on derivatives that localize a charge on the N-terminus of a peptide to control its fragmentation during analysis by MS or MS/MS.

The vast majority of charged derivatives were developed for use with FAB or LSIMS desorption/ionization techniques. Most of these papers were published between the mid 1980's and the mid 1990's. Charge-remote fragmentation mechanisms require greater internal energies than charge-directed fragmentation mechanisms [48] and are most readily formed by high-energy CAD. Many instruments during this period made use of high-energy CAD, which can provide the internal energies necessary to induce charge-remote fragmentation. Derivatization to increase analyte signal intensity was also more important when FAB or LSIMS was used, because the response of many peptides could be increased by increasing their hydrophobicity [41-43].

The use of charged derivatives with plasma desorption (PD) has been quite limited [49,50] mainly because PD was never as widely used as FAB or LSIMS. However, the high internal energies of ions generated by PD produce abundant fragment ions without the use of CAD-MS/MS techniques.

Only recently [51-57] have charged derivatives been applied to the analysis of peptides by matrix-assisted laser desorption/ionization (MALDI). MALDI has detection limits for peptides and proteins that are several orders of magnitude lower than those obtained with FAB or LSIMS, hence there was little incentive to develop derivatization approaches to increase signal intensities of the analytes. Additionally, before the development of post-source decay (PSD), most MALDI instruments were incapable of generating and observing fragment ions of peptides. The spectra of underivatized peptides obtained by MALDI-PSD have been observed to resemble those obtained by LSIMS low-energy CAD [58]. PSD is an effective technique for forming fragment ions of charged derivatives, and now charge derivatization to control fragmentation is an attractive option.

The analysis of charged derivatives by electrospray ionization (ESI) has received limited attention [59-62]. This is due to the belief that it would be difficult to form charge-remote fragment ions during analysis by ESI because ions are produced with lower internal energies than those formed by LSIMS[48], and because the majority of electrospray instruments use low-energy CAD to form fragment ions for analysis by tandem mass spectrometry.

a) Quaternary Ammonium Derivatives:

In 1984, *Kidwell* and coworkers reported the development of several derivatization approaches. The first approach to N-terminal derivatization used methyl iodide to form a trimethylammonium derivative as shown in Figure 1.5 [63,64].

Figure 1.5. Trimethylammonium derivatization scheme.

This derivatization approach had low yields, so another approach involving successive derivatization of the peptide N-terminus with chloroacetyl chloride followed by reaction with triethylamine to give a triethylammonium derivative was proposed as shown in Figure 1.6A.

NH₂-Peptide-COOH

$$i, ii$$
 R_3 -N-CH₂C-NH-Peptide-COOH

 R_2

Reagents: $i = \text{Hal-CH}_2\text{C-R}_1$ $ii = R_2$ -N-R₄

A) Hal = Cl, R₁ = Cl, R₂ = R₃ = R₄ = Et

B) Hal = Cl, R₁ = Cl, R₂ = R₃ = R₄ = CH₃

C) Hal = I, R₁ = OC(O)CH₂I, R₂ = R₃ = CH₃, R₄ = CH₃, C₆H₁₃, or C₈H₁₇

Figure 1.6. Trialkylammonium-acetyl derivatization scheme.

Both of these derivatization approaches derivatized unprotected lysine side-chains as well. The derivatized peptides were randomly cleaved with acid or enzymes to generate a series of derivatives differing by the number of residues present. The cleavage products were then esterified and acetylated to suppress ionization of the underivatized fragments. These mixtures were analyzed by secondary ionization mass spectrometry

(SIMS), the precursor of FAB and LSIMS. The derivatives had detection limits in the low nanogram (picomole) range; detection limits were not given for the underivatized peptides. Data were presented only for peptides containing three or fewer residues.

Stults et al. presented a selective procedure for attaching a quaternary ammonium group to the peptide N-terminus [65]. 1-30 nmol of peptide were reacted with iodoacetic anhydride followed by thiocholine iodide, each at a controlled pH as shown in Figure 1.7.

Figure 1.7. Quarternary ammonium derivatization using thiocholine iodide.

The pH control allowed selective derivatization of the N-terminus by exploiting differences between the pK_a of the N-terminus and those of the basic amino acid sidechains. However, protection of free cysteines was required to prevent derivatization [67]. The reactions were complete in a few hours, but the products had to be purified by HPLC prior to analysis. Analysis by FAB or LSIMS followed by CAD-MS/MS gave typical N-terminal charge-remote fragment ions, but the spectrum was complicated by the loss of trimethylamine from several ions.

Vath and Biemann proposed another procedure for attaching a trimethylammonium group to the N-terminus of a peptide [67]. The procedure involved reaction of approximately one nmol of peptide with chloroacetyl chloride followed by trimethylamine as shown in Figure 1.6B. This two-step procedure involved a total

reaction time of three hours. The signal intensity of the derivative was approximately one-half that generated from an equal amount of the underivatized peptide during analysis by FAB-MS. The derivative gave common charge-remote fragmentation products when analyzed by FAB-CAD-MS/MS.

Stults et al. developed a similar reaction scheme for attaching a dimethylalkylammonium (DMAA) group at the peptide N-terminus [68]. The derivatization involved reaction of at least 100 pmol of peptide with iodoacetic anhydride followed by reaction with a dimethylalkylamine as shown in Figure 1.6C. derivatization required a total reaction time of about two hours and gave overall yields of 60-80%. The pH control of the iodoacetylation gave 70-90% selectivity for the Nterminus over the \varepsilon-amino group of lysine, but cysteine residues had to be protected to prevent derivatization. The presence of a nonvolatile buffer and excess reagents necessitated HPLC cleanup prior to analysis by mass spectrometry. The derivatives were analyzed by FAB-high-energy-CAD-MS/MS or by LSIMS-high-energy-CAD-MS/MS. The dimethylhexylammonium and dimethyloctylammonium derivatives of a hexapeptide yielded signal intensities that were stronger by a factor of 2-5 compared to those from the underivatized peptide. The increase in signal intensity is presumably the result of increased surface activity; however, such enhancements were not observed during analyses of larger peptides (a 14-mer and a 19-mer). The trimethylammonium derivative gave a slight decrease in signal intensity compared to that for the underivatized peptide. The derivative gave abundant N-terminal charge-remote fragments and a small loss of the hexyl group from the dimethylalkylammonium functionality. Stults has applied this derivatization technique to prepare peptide derivatives with a dimethylhexylammonium

group at the N-terminus for analysis by ESI [59]. The signal from the derivative was a factor of 2-5 less intense than that from the underivatized peptide when analyzed by ESI-MS. The doubly-charged ions of the underivatized peptide [M + 2H]²⁺ and the derivative [C + H]²⁺ were used as precursors for analysis by ESI-low-energy CAD-MS/MS. In contrast to the product ion spectrum of the underivatized peptide, the product ion spectrum of the derivative gave primarily *a_n and *b_n ion peaks with no C-terminal fragment ion peaks observed. The presence of abundant *b_n ions is in contrast to the fragmentation patterns observed by high-energy CAD [45]. This derivatization technique was also used by *Dongré et al.* to prepare the trimethylammonium acetyl derivative of leucine enkephalin for analysis by electrospray surface-induced dissociation tandem mass spectrometry (ESI-SID-MS/MS) [48].

Bartlet-Jones et al. developed another derivatization approach (Figure 1.8) to attach a trimethylammonium functionality to the peptide N-terminus [51].

Figure 1.8. C5Q derivatization reaction.

This derivative has been named "C5Q", presumably because it consists of a five-carbon chain and a quaternary ammonium group. The C5Q derivatization reaction was complete in 10 minutes and was performed on 20-50 fmol of peptide; 50 fmol of derivatized peptide was readily observed by MALDI. This derivatization approach was studied in detail in a later paper [55]. MALDI-PSD analysis of the derivatized peptide with a C-terminal arginine residue generated several y_n ions. Derivatization of Lys and

Arg side-chains was recommended to reduce their basicity. The chemistry used to block lysine side-chains results in cleavage of the N-terminal residue. The blocking of lysine, derivatization of the N-terminus, and modification of arginine required four reaction steps and more than four hours with quantities of 5-10 pmol of peptide. HPLC was required to remove excess reagents. When basic side-chains were modified, only N-terminal fragment ions were produced, primarily *a_n and *b_n ions. Abundant *b_n fragment ions have not usually been observed for other charge-derivatized peptides analyzed by high-energy CAD [45] or MALDI-PSD [54,56]. However, *b_n ions have been observed in the MALDI-PSD spectra of charge-derivatized peptides when very high laser powers were used for desorption [54]. When *Hines et al.* analyzed peptides derivatized with the C5Q reagent [52], several *a_n fragment ion peaks and one *b_n fragment ion peak were observed in the MALDI-PSD spectrum, but the most abundant fragments were immonium ions and ions presumably resulting from a combination of backbone cleavage and the loss of trimethylamine from the derivative ([*a_n-59] and [*b_n-59] ions).

b) Quaternary Phosphonium Derivatives:

Wagner et al. presented an approach for attaching a triphenylphosphonium group to either the N-terminus or the C-terminus of a peptide [46]. For the N-terminal derivative, approximately one nmol of peptide was reacted with 2-bromoethyl-triphenylphosphonium bromide at pH 9 for 3 hours at 37°C, as shown in Figure 1.9A.

Figure 1.9. Triphenylphosphonium-ethyl derivatization reaction.

The derivatization reactions gave greater than 75% yield [47], but with some difficulty in reproducibility. These derivatives provided both charge localization and enhanced surface activity on the FAB matrix. As a result, the fragmentation was simplified and the signal intensity increased relative to that obtained from the underivatized peptides. The detection limit of some peptide derivatives was below 5 picomoles. Both derivatives produced abundant charge-remote fragments arising from the derivatized terminus. However, when a peptide containing a disulfide bond was derivatized at the N-terminus, the mass spectrum provided less structural information than the spectrum of the native peptide [69]. The derivatization reaction used pH control to prevent reaction with basic side chains, but it required removal of the buffer salts prior to analysis; this procedure was later modified to eliminate the need for nonvolatile With the new procedure, the peptide was reacted with buffers [70]. vinyltriphenylphosphonium bromide in a mixture of acetonitrile and pyridine as shown in Figure 1.9B. This new procedure eliminated the need for sample cleanup, but the pH control was uncertain and allowed the possibility of reaction with basic side-chains.

Bunk and Macfarlane reported the N-terminal derivatization of bradykinin with vinyltriphenylphosphonium bromide as shown in Figure 1.9B [49]. The reagents were combined in a pH 9.0 buffer solution and allowed to react at room temperature overnight. The derivatives under went metastable decay to produce N-terminal fragments, with *a_n ions dominating, when analyzed by plasma desorption mass spectrometry (PD-MS). A peak for the protonated derivative [C + H]²⁺ and a few C-terminal fragments were also observed. Although an increase in N-terminal fragmentation was observed, the data obtained by PD-MS analysis of the derivatives gave unsatisfactory results especially when larger peptides were derivatized and analyzed [50]. The triphenylphosphonium group was readily cleaved through a reverse Michael-type reaction, which led to a decrease in sequence-specific fragment ions. Also, the derivative formed primarily metastable fragments, that produced broader peaks than the fragment ions obtained from underivatized peptides.

Liao and Allison reported that charge derivatization of a hexapeptide led to signal enhancement when analyzed by MALDI [71]. They used the procedure of Wagner et al. to prepare both the N- and C-terminal ethyltriphenylphosphonium derivatives. A one-pmol sample of the underivatized peptide gave no signal when analyzed by MALDI, but both the N- and C-terminal derivatives produced strong signals at the one-pmol level.

Huang et al. introduced a derivatization procedure that attaches a tris(2,4,6-trimethoxyphenyl)-phosphonium (TMPP⁺-Ac) group to the peptide N-terminus [53]. At least 10 pmol of peptide were combined with S-pentafluorothiophenyl [tris(2,4,6-trimethoxyphenyl)-phosphonium]acetate bromide and p-(dimethylamino)pyridine (DMAP) for 15 minutes at room temperature as shown in Figure 1.10.

NH₂-Peptide-COOH

TMPP⁺-CH₂-C — NH-Peptide-COOH

Reagent =
$$TMPP^+$$
-CH₂-C — S — F F F

TMPP⁺ = $TMPP^+$ = TMP

Figure 1.10. TMPP⁺-Ac derivatization reaction.

The reaction gave yields in excess of 90% for most peptides, but a few peptides have yields as low as 64%. The reaction mixture usually does not require purification prior to analysis by FAB or MALDI. In addition, peptides composed primarily of amino acid residues with nonpolar side-chains showed significant signal enhancement upon derivatization and analysis by FAB or MALDI. When the derivatization is performed at a controlled pH of 8.2, derivatization will occur at the N-terminus with no derivatization of lysine side-chains. The spectra of the derivative obtained by FAB-high-energy CAD-MS/MS show a strong series of charge-directed fragments. When TMPP⁺-Ac derivatized peptides were analyzed by LSIMS-CAD-MSⁿ with a quadrupole ion trap instrument, abundant *b_n+H₂O ions were produced in addition to a series of *a_n ions [72].

The TMPP⁺-Ac derivative (Figure 1.10) has been used to direct the fragmentation of peptides during analysis by MALDI-PSD [53,54]. The spectra consist of a strong series of *a_n ions plus a few *b_n, *c_n, and *d_n ions. The *d_n ion peaks in the MALDI-PSD spectra are less intense than those in the FAB-high-energy CAD-MS/MS spectra.

The TMPP⁺-Ac reagent has been used to derivatize protein digests at the 25 pmol level [73]. This reagent was also used to derivatize peptides located in an electrophoretic gel or membrane [56]. The modified peptides were then analyzed by MALDI and MALDI-PSD directly from the gel or membrane on a modified sample plate.

The TMPP⁺-Ac derivative has also been applied to peptide analysis by electrospray using an elevated cone voltage to promote in-source fragmentation [62]. With the cone set at a typical potential of 37 V, the peptide derivatives did not fragment significantly and the derivatives were observed as the doubly-charged derivative [C + H]²⁺. When the cone voltage was raised to 100 V, extensive fragmentation occurred and the doubly-charged derivative was not observed. The fragmentation produced primarily *a_n and *b_n ions with some *c_n and *d_n ions produced as well. This pattern is similar to the fragmentation of another charged derivative analyzed by ESI-low-energy CAD-MS/MS [59].

c) N-terminal Derivatives With High Proton Affinities:

In addition to derivatives with a fixed charge, several N-terminal derivatives have been developed with high proton affinities. The basic groups provide some degree of charge localization, but there is potential for protonation at other sites or for proton transfer to other sites. These derivatives are analogous to peptides with basic residues (Arg, His, or Lys) at the N-terminus. As a result, the nomenclature used for these derivatives will be the same as that used for underivatized peptides.

Renner and Spiteller [38] reported N-terminal derivatization schemes using dansylchloride, as shown in Figure 1.11A, and 2-bromo-5-(dimethylamino)benzene sulfonyl chloride as shown in Figure 1.11B.

NH₂-Peptide-COOH Ar-SO₂-NH-Peptide-COOH

Figure 1.11. Reaction schemes of Renner and Spiteller.

Although these derivatives did not have a fixed charge, the aromatic amine was preferentially protonated during analysis by FAB. The derivatives had greater signal intensities and an increase in fragmentation (without CAD) compared to the underivatized peptides. The FAB-MS analysis of the dansyl derivative produced only N-terminal fragments ($\mathbf{a_n}$ and $\mathbf{b_n}$), but the second derivative produced $\mathbf{a_n}$, $\mathbf{b_n}$, and $\mathbf{y_n}$ ions. The $\mathbf{a_n}$ and $\mathbf{b_n}$ ions arising from the second derivative produced two peaks for each ion, as a result of the ⁷⁹Br and ⁸¹Br isotopes. These isotope peaks allowed the N-terminal fragments be distinguished from the C-terminal fragments. The chemistry employed would likely also derivatize basic side-chains as well as the N-terminus of the peptide.

Sherman et al. [60] have used N-hydroxysuccinimide-2-(3-pyridyl)acetate (SPA) to derivatize the peptide N-terminus, as shown in Figure 1.12, in preparation for analysis by ESI-MS; this chemistry was optimized by Cárdenas et al. [61].

Figure 1.12. SPA derivatization reaction.

The N-pyridylacetyl functionality is not charged, but it does have a slightly increased proton affinity compared to that of the peptide N-terminus. The derivatives were analyzed by ESI-MS/MS on a triple quadrupole instrument [60] or by ESI-MSⁿ on a quadrupole ion trap instrument [61]. The spectrum of the derivative contains both N-terminal fragment (\mathbf{b}_n and \mathbf{a}_n) peaks and C-terminal fragment (\mathbf{y}_n) peaks. However, the \mathbf{b}_n fragment ion peaks of the derivative are more intense than the corresponding \mathbf{b}_n fragment ion peaks of the underivatized peptides. The optimized reaction occurs in four minutes and gives yields in the range of 80-100% for peptides that do not contain lysine or tyrosine. The reagent reacts with the side-chain of lysine and reacts to a lesser extent with the side-chain of tyrosine. Reactions with the side-chains produce derivatives having multiple N-pyridylacetyl functionalities. This derivatization has been used on peptides having as many as 15 residues.

Naven et al. [57] used MALDI-PSD to study peptides derivatized with SPA (Figure 1.12). The derivatization was performed on as little as 50 fmol of peptide. The procedure was also applied to tryptic peptides electroblotted onto a PVDF membrane. The reaction was essentially quantitative at the N-terminus and the lysine side-chains. The PSD spectra contained peaks for a series of abundant \mathbf{b}_n ions and some \mathbf{a}_n and \mathbf{y}_n ions.

d) The Ideal Charged Derivative:

The ideal charged derivatization approach would have several attributes. The chemistry should occur rapidly with high product yield without unwanted derivatization of peptide side-chains. The derivatives should not require purification prior to analysis. The derivative should be compatible with all mass spectrometry ionization and

fragmentation techniques. The ideal derivative would have a lower detection limit than the underivatized peptide. The derivative should have a fixed charge and produce a series of charge-remote fragments upon analysis by tandem mass spectrometry. The derivative moiety should not fragment during analysis by tandem mass spectrometry because that fragmentation might complicate the mass spectrum and reduce the intensity of the other fragment ion peaks.

Three of the derivatization approaches discussed come closer to the ideal than the others. They are the dimethylalkylammoniun acetate (DMAA) derivatization reported by Stults et al. (Figure 1.6C), the C5Q derivatization of Spengler et al. (Figure 1.8) and the [tris(2,4,6-trimethoxyphenyl)-phosphonium] acetate (TMPP⁺-Ac) derivatization reported by Huang et al. (Figure 1.10). These approaches utilize highly specific chemistry to attach a fixed charge to the N-terminus of the peptide in high yields.

The DMAA derivatization is performed with commercially available reagents. The C5Q and TMPP⁺-Ac derivatization reagents must be synthesized, but the TMPP⁺-Ac reagent, and possibly the C5Q reagent, is stable for months. The TMPP⁺-Ac derivatization occurs in one fifteen-minute step, the DMAA derivatization occurs in two steps requiring a total of two hours, and the C5Q derivatization between twenty minutes (without side-chain derivatization) and four hours (with derivatization of Lys and Arg). The amount of peptide required for the derivatization reactions has been reported as 100 pmol for DMAA, 10 pmol for TMPP⁺-Ac and 5-10 pmol for the C5Q derivatization. However, the C5Q derivatization procedure can be performed on sub-picmolar quantities of peptide if neither Lys nor Arg need derivatization. All three reactions occur with high yields and are selective for the N-terminus when the pH of the reaction mixture is

controlled. The DMAA and C5Q derivatizations usually require purification by HPLC to remove excess reagent. Such purification usually is not required for the TMPP⁺-Ac derivatization when the reaction mixture is analyzed by FAB or MALDI, but it is required in analyses by ESI.

The TMPP⁺-Ac derivative has been analyzed successfully with FAB, ESI, and MALDI techniques. The DMAA derivatives have only been analyzed by FAB and ESI, but they are probably compatible with MALDI. Likewise, the C5Q reagent has only been analyzed by MALDI, but should be compatible with FAB and ESI.

DMAA derivatives give a small increase in signal intensity in some conditions and a small decrease under others. No loss of signal intensity was observed for C5Q derivatization, but the relative signal intensities of underivatized and derivatized peptides were not reported. For most peptides, the TMPP⁺-Ac derivative has only a small effect on signal intensity, but some hydrophobic peptides have shown a significant signal enhancement upon derivatization. All of the derivatives have detection limits in the low picomole to sub-picomole range.

Because the derivative moieties have fixed charges, the fragment ions produced from these derivatives are believed to form by charge-remote mechanisms. FAB-high-energy-CAD-MS/MS analysis of the DMAA and TMPP⁺-Ac derivatives produces primarily *a_n and *d_n plus a few *b_n and *c_n ions. In addition, the DMAA derivative loses the alkyl group to generate a peak that can complicate the high-mass end of the spectrum. When TMPP⁺-Ac derivatives are analyzed by MALDI-PSD, a dominant series of *a_n ions is produced and a few *b_n, *c_n and *d_n ions are produced. Peptides derivatized with C5Q (including modification of Lys or Arg) are reported to form

primarily *a_n and *b_n ions, but also *c_n and *d_n ions to a lesser extent. In a preliminary study by *Hines et al.*, a C5Q derivative was reported to form primarily *a_n-59 and *b_n-59 ions. The differences in these fragmentation patterns are difficult to explain. Perhaps the laser power (or some other experimental parameter) is causing the differences in fragmentation as has been documented in one case of fragmentation of charged derivatives during analysis by MALDI-PSD. The C5Q derivative moiety has a smaller head group than the TMPP*-Ac moiety, and the C5Q moiety has a flexible five-carbon chain. These differences might allow the formation of secondary structures in which the charge can interact with the peptide backbone to influence fragmentation behavior.

When DMAA and TMPP⁺-Ac derivatives are analyzed by ESI, primarily $*a_n$ and $*b_n$ ions are generated plus a few $*c_n$ and $*d_n$ ions.

III. Conclusions

Although most of these charged derivatives have been studied by FAB-CAD-MS and MALDI-PSD-MS, there has been very little focus in using ESI-CAD-MS/MS for the study of these charged derivatives. The fragmentation pattern of peptides in ESI-CAD-MS/MS is equally complicated as in the other two techniques. Study of the charged derivatives of peptides by ESI-CAD-MS/MS could provide reliable and easily interpretable spectra. It is known that charged derivatives require high-energy for their fragmentation. However, fragmentation of these charged derivatives in the low-energy regime (< 200 eV) has been observed [59]. These factors have been the major driving force behind the study of the TMPP⁺-Ac charged derivatives by ESI-CAD-MS/MS reported in this dissertation. Chapter 2 presents a systematic study of the TMPP⁺-Ac derivatives of peptides. Attempts are made to derive rules for fragmentation behavior of various amino acid residues when present in the TMPP⁺-Ac derivatized peptide sequence. Results from the fragmentation of these charged derivatives in a quadrupole vs. an ion trap mass spestrometer are compared. Chapter 3 presents the application of the TMPP⁺-Ac charge- derivatization towards identifying the sites of phosphorylation in a peptide. Chapter 4 focuses on understanding the basic mechanism of charge-remote fragmentation under LE conditions at the molecular level using the TMPP+-Ac derivatives of deuterium labeled peptides.

IV. References

- 1. Budzikiewicz,H.; Djerrasi, C.; Williams, D.H. "Mass Spectrometry of Organic Compounds" *Holden Day*, San Francisco, 1967.
- 2. Beuhler, R.J.; Flanigan, E.; Green, L.J.; Friedman, L. J. Am. Chem. Soc., 1974, 96, 3990.
- 3. Meuzelaar, H.L.C.; Posthumus, M.A.; Kistemaker, P.G.; Kistemaker, J. Anal. Chem., 1973, 45, 1546.
- 4. Fenn, J.B.; Mann, M.; Meng, C.K.; Wong, S.F. Mass Spec. Rev., 1990, 9, 37.
- 5. Barber, M.; Bordoli, R.S.; Sedgwick, R. D.; Tyler, A. N. J. Chem. Soc., Chem. Commun., 1981, 325.
- 6. Honig, R.E. Int. J. Mass Spectrom. Ion Phys., 1985, 66, 31.
- 7. Sundqvist, B.U.R.; Macfarlane, R.D. Mass Spec. Rev., 1985, 42, 421.
- 8. Caprioli, R.M. Mass Spec. Rev., 1987, 6, 237.
- 9. Karas, M.; Hillenkamp, F. Anal. Chem., 1988, 60, 2299.
- 10. Spengler, B.; Kirsch, D.; Kaufmann, R.; Jaeger, E. Rapid Commun. Mass Spectrom., 1992, 6, 105.
- 11. Ingrhram, M.; Gomer, R.J. J. Chem. Phys., 1954, 22, 1279.
- 12. Beckey, H.D. Principles of Field Ionization and Field Desorption Mass Spectrometry. Pergamon, Oxford, 1977.
- 13. Dole, M.; Mack, L.L.; Hines, R.L.; Mobley, R.C.; Ferguson, L.D. Alice, M.B. J. Chem. Phys., 1968, 49, 2240.
- 14. Watson, J.T. Introduction to Mass Spectrometry, Lippincott-Raven, Philadelphia, 1997.
- 15. Bruins, A.P.; Covey, T.R.; Henion, J.D. Anal. Chem., 1987, 59, 2642.
- 16. Wilm, M.; Mann, M. Int. J. Mass Spectrom. Ion Processes, 1994, 136, 167.
- 17. Chapman, S. S. Phys Rev., 1937, 52, 184.
- 18. Thomson, B.A.; Iribarne, J.V. J. Chem. Phys., 1979, 71, 4451.

- 19. Fenn, J.B. J. Am. Soc. Mass Spectrom., 1993, 4, 524.
- 20. Mann, M. Org. Mass Spectrom., 1990, 25, 575.
- 21. Siuzdak, G. Proc. Natl. Acad. Sci. USA, 1994, 91, 11290.
- 22. Loo, J. Bioconjugate Chem., 1995, 6, 644.
- 23. Smith, R.D.; Light-Wahl, K.J. Biol. Mass Spectrom., 1993, 22, 493.
- 24. Wilm, M.; Shevchenko, A.; Houthaeve, T.; Breit, S.; Schweigerer, L.; Fotsis, T.; Mann, M. Nature, 1996, 379, 466.
- 25. Roepstorff, P.; Fohlman, J. Biomed. Mass Spectrom, 1984, 11, 601.
- 26. Biemann, K. Nomenclature for Peptide Fragment Ions. Methods in Enzymology, Ed. J.McCloskey, 1990, 193, 886.
- 27. Busch, K.L.; Glish, G.L.; McLuckey, S.A. Mass Spectrometry/ Mass Spectrometry: Techniques and Applications of Tandem Mass Spectrometry, VCH, New York, 1988.
- 28. Benyon, J.H.; Boyd, R.K.; Brenton, A.G. Adv. Mass Spectrom., 1986, 10A, 437.
- 29. Neumann, G.M.; Derrick, P.J. Org. Mass Spectrom., 1984, 19, 165.
- 30. Wysocki, V.H.; Kenttamma, H.I.; Cooks, R.G. Int. J. Mass Spectrom. Ion Processes, 1985, 75, 181.
- 31. Dawson, P.H. (ed.) Quadrupole Mass Spectrometry and Its Applications, Elselvier New York, 1976.
- 32. March, R.E.; Todd, J.F.J. Fundamentals of Ion Trap Mass Spectrometry, CRC press, Boca Raton, 1995.
- 33. I. A. Papayannopoulos *Mass Spectrom*. Rev., 14, 49-73 (1995).
- 34. Yost, R.A.; Enke, C.G. J. Am. Chem. Soc. 1978, 100, 2274.
- 35. Brodbelt, J.; Kenttamma, H.I.; Cooks, R.G. Org. Mass Spectrom., 1986, 23, 6.
- 36. Alexander, A.J.; Boyd, R.K Int. J. Mass Spectrom. Ion Processes, 1989, 90, 211.
- 37. Hayes, R.N.; Gross, M.L Collision-Induced Dissociation Methods in Enzymology, Ed. J.McCloskey, Academic Press, 1990, 193, 337.
- 38. Renner, D.; Spiteller, G. Biomed. Environ. Mass Spectrom., 1986, 13, 405.

- 39. Gross, M. L. Int. J. Mass Spectrom. Ion Processes, 1992, 118/119, 137.
- 40. Jensen, N. J.; Tomer, K. B.; Gross, M. L. J. Am. Chem. Soc., 1985, 107, 1863
- 41. Falick, A. M.; Maltby, D. A. Anal. Biochem., 1989,182,165.
- 42. Ligon, W.V. Anal. Chem., 1986, 58, 485.
- 43. Naylor, S.; Findeis, A. F.; Gibson, B. W.; D. H. Williams J. Am. Chem. Soc., 1986, 108, 6359.
- 44. Busch, K. L.; Unger, S. E.; Vincze, A.; Cooks, R. G.; Keough, T. J. Am. Chem. Soc., 1982, 104.1507.
- 45. Zaia, J.; Biemann, K. J. Am. Soc. Mass Spectrom., 1995,6, 428.
- 46. Wagner, D. S.; Salari, A.; Gage, D. A.; Leykam, J.; Fetter, J.; Hollingsworth, R.; Watson, J. T. Biol. Mass Spectrom., 1991, 20, 419.
- 47. Watson, J. T.; Wagner, D. S.; Chang, Y. S.; Strahler, J. R.; Hanash, S. M.; Gage, D. A. Int. J. Mass Spectrom. Ion Processes., 1991, 111, 191.
- 48. Dongré, A. R.; Jones, J. L.; Somogyi, Á.; Wysocki, V. H. J. Am. Chem. Soc., 1996, 118, 8365.
- 49. Bunk, D. M.; Macfarlane, R. D. Int. J. Mass Spectrom. Ion Processes, 1991, 111, 55.
- 50. Bunk, D. M.; Macfarlane, R. D. Int. J. Mass Spectrom. Ion Processes, 1993, 126, 123.
- 51. Bartlet-Jones, M.; Jeffery, W. A.; Hansen, H. F; Pappin, D. J. C. Rapid Commun. Mass Spectrom., 1994, 8, 737.
- 52. Hines, W.; Peltier, J.; Hsieh, F.; Martin, S. Proceedings of the 43rd ASMS Conference on Mass Spectrometry and Allied Topics, Atlanta, Georgia, May 21-26, 1995.
- 53. Huang, Z.-H.; Wu, J.; Roth, K. D. W.; Yang, Y.; Gage, D. A.; Watson, J. T. *Anal. Chem.*, 1997, 69, 137.
- 54. Liao, P.-C.; Huang, Z.-H.; Allison, J. J. Am. Soc. Mass Spectrom., 1997, 8, 501.
- Spengler, B.; Leutzenkirchen, F.; Metzger, S.; Chaurand, P.; Kaufmann, R.; Jeffery, W.; Bartlet-Jones, M.; Pappin, D. J. C. Int. J. Mass Spectrom. Ion Processes., 1997, 169/170, 127.

- 56. Strahler, J. R.; Smelyanskiy, Y.; Lavine, G.; Allison, J. Int. J. Mass Spectrom. Ion Processes, 1997, 169/170, 111.
- 57. Naven, T. J. P.; Jeffery, W. A.; Bartlet-Jones, M.; Rahman, D; Pappin, D. J. C. *Proceedings of the 45th ASMS Conference on Mass Spectrometry and Allied Topics*, Palm Springs, California, June 1-5, 1997.
- 58. Rouse, J. C.; Yu, W.; Martin, S. A. J. Am. Soc. Mass Spectrom., 1995, 6, 822.
- 59. Stults, J. T. Proceedings of the 40th ASMS Conference on Mass Spectrometry and Allied Topics, Washington, DC, May 31-June 5, 1992.
- 60. Sherman, N. E.; Yates, N. A.; Shabanowitz, J.; Hunt, D. F.; Jeffery, W.; Bartlet-Jones, M.; D. J. C. Pappin, *Proceedings of the 43rd ASMS Conference on Mass Spectrometry and Allied Topics*, Atlanta, Georgia, May 21-26, 1995.
- 61. Cárdenas, M. S.; van der Heeft, E.; de Jong, A. P. J. M. Rapid Commun. Mass Spectrom., 1997, 11, 1271.
- 62. Sadagopan, N.; Wu, J.; Yang, Y.; Huang, Z.-H.; Watson, J. T. Proceedings of the 45th ASMS Conference on Mass Spectrometry and Allied Topics, Palm Springs, California, June 1-5, 1997.
- 63. Kidwell, D. A.; Ross, M. M.; Coulton, R. J. J. Am. Chem. Soc., 1984, 106, 2219.
- 64. Kidwell, D. A.; Ross, M. M.; Coulton, R. J. Springer Ser. Chem. Phys.: SIMS 4, 1984, 36, 412.
- 65. Stults, J. T.; Halualani, R.; Wetzel, R. Proceedings of the 37th ASMS Conference on Mass Spectrometry and Allied Topics, Miami Beach, Florida, May 21-26, 1989.
- 66. Wetzel, R.; Halualani, R.; Stults, J. T.; Quan, C. Bioconjugate Chem., 1990, 1, 114.
- 67. Vath, J. E.; Biemann, K. Int. J. Mass Spectrom. Ion Processes, 1990, 100, 287.
- 68. Stults, J. T.; Lai, J.; McCune, S.; Wetzel, R. Anal. Chem., 1993, 65, 1703.
- 69. Chang, Y. S.; Gage, D. A.; Watson, J. T. Biol. Mass Spectrom., 1993, 22,176.
- 70. Wagner, D. S. Ph.D. Dissertation, Michigan State University, East Lansing, MI (1992).
- 71. Liao, P.-C.; J. Allison J. Mass Spectrom., 1995, 30, 511.
- 72. Lin, T.; Glish, G. Proceedings of the 45th ASMS Conference on Mass Spectrometry and Allied Topics, Palm Springs, California, June 1-5, 1997.

73. Huang, Z.-H.; Shen, T.S.; Wu, J.; Gage, D. A.; Watson, J. T. Anal. Biochem., 1999, 268, 305.

Chapter 2

ANALYSIS OF TRIS(2,4,6-TRIMETHOXYPHENYL)PHOSPHONIUM ACETYL DERIVATIVES OF PEPTIDES BY ELECTROSPRAY IONIZATION FOLLOWED BY QUADRUPOLE OR ION TRAP MASS SPECTROMETRY

I. Introduction

A) Role of Mass Spectrometry in Protein Sequencing:

Determining the amino acid sequence of proteins continues to be of great interest in today's scientific community especially due to the rapidly progressing human-genome project [1]. In addition, it is of importance to the pharmaceutical industries where recombinant proteins are being developed for therapy, diagnosis, and prophylaxis of human disease [2]. Usually, protein sequences are either deduced from the cDNA sequence, or determined by Edman sequencing. Although the DNA sequence provides the primary amino acid sequence, initiated at the methionine codon and terminated at the stop codon, it does not give any information regarding the post-translational modifications of the protein, which occur in the cytoplasm [3]. Phosphorylation, disulfide bond formation, deamidation, and glycosylation are several such important posttranslational events that modify the protein structure outside the nucleus. The Edman degradation method is very sensitive, but is only unidirectional; it is also difficult to obtain sequence information if the N-terminus is acylated or blocked due to other modifications. In cases where results from the previously mentioned techniques are ambiguous or incomplete, mass spectrometric information can be complementary.

B) Nomenclature of Fragment Ions Formed From Collisionally Activated Dissociation:

The nomenclature for fragmentation of peptides under mass spectrometric ionization methods has been clearly defined [4]. When a peptide is subjected to collisionally activated dissociation (CAD), the fragments produced are dependent on the position of the most basic residue (if any) in the sequence or protonation of any given amide group. In the latter case, due to charge-mediated fragmentation, a mixture of ion types is produced, predominantly b and y ions, and some a, c, x, and z ions. This is depicted pictorially in Figure 2.1. In cases where there is a \(\beta\)-methylene unit in the side chain, d and w ions are also possible. This multitude of ion types complicates the spectrum, and requires a great scrutiny to interpret the spectrum. In an effort to obtain a simple spectrum, charged derivatives of the peptides (as defined in chapter 1) could be prepared and subjected to fragmentation to generate predominantly one type of ions. This generally occurs via charge-remote fragmentation, which is also likely when a basic residue is located on either terminus. Most of the charged derivatives studied so far have been shown to produce *a_n ions [5]. The results presented in this chapter are those of Nterminally derivatized peptides. The fragment ions contain a charged group at the Nterminus, and will be referred to as a_n -type ions (* a_n) instead of a_n ions. Similarly, the other charge-derivatized N-terminal containing fragments will be denoted as *b_n, *c_n, and *d_n ions

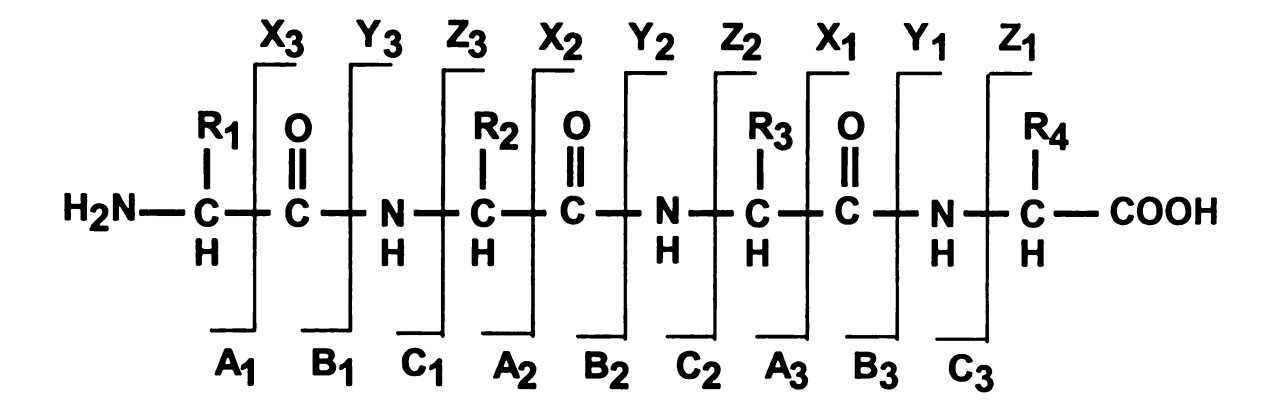


Figure 2.1. Nomenclature for peptide fragmentation during CAD.

C) FAB-CAD-MS and MALDI-PSD-MS Studies of TMPP*-Ac-Peptides:

Although a number of charge-derivatizing reagents have been described, most of them have disadvantages [5]. One of the charge-derivatizing reagents that was developed to avoid the disadvantages of other existing reagents, contains a tris[2,4,6-trimethoxyphenyl]phosphonium acetyl (TMPP+-Ac) cation [6]. The structure of the TMPP+-Ac reagent and its coupling reaction with the N-terminus of a peptide are shown in Figure 2.2; the reagent selectively derivatizes the N-terminus of the peptides at the picomole level, with only a 5-fold molar excess, at room temperature. Studies of TMPP+-Ac-peptides by fast atom bombardment-CAD (FAB-CAD) [6] and matrix-assisted laser desorption/ionization – post-source decay (MALDI-PSD) [7] have demonstrated that it is possible to correlate the CAD spectrum of a TMPP+-Ac-peptide to its structure. TMPP+-Ac derivatives of peptides have also been studied by FAB-CAD in an ion trap mass spectrometer [8].

Figure 2.2. Reaction of TMPP⁺-Ac reagent with the N-terminus of a peptide.

TMPP⁺-Ac derivatization can be applied to protein digests. The lypophilized tryptic digest of proteins like cytochrome-c can be treated directly with the TMPP⁺-Ac reagent, and analysis of derivatized tryptic fragments by MALDI-PSD can be used to obtain sequence information [9]. Whereas a simple mixture of TMPP⁺-Ac tryptic peptides can be analyzed directly by MALDI-PSD, preliminary separation is usually required for proteins larger than 10 kDa because a larger excess of the TMPP⁺-Ac reagent is used for derivatization. This excess reagent may suppress the signal in MALDI, and hence HPLC is necessary. Such practical issues create a pressing need for the analysis of these charged derivatives by electrospray ionization (ESI). An obvious advantage is the possibility of LC-MS based on ESI. Hence, it was of great interest to study the fragmentation pattern of the TMPP⁺-Ac-peptides using ESI-MS.

There have been many studies on the fragmentation pattern of charged derivatives by FAB [6,8,10-18] and MALDI [7,19-23]. However, there are only a few studies based on ESI of charged derivatives [24-28]. There have been several high-energy studies of

peptide fragmentation with ESI. High-energy CAD of multiple-charged ions from ESI has been used to study the parameters of charge location and charge state [29]. Wysocki and coworkers have reported ESI-surface induced dissociation (SID) studies of peptides [30]. Since ESI is more commonly used with triple quadrupole and ion trap mass spectrometers, it is of interest to study the low-energy CAD of such ESI-generated ions. This paucity of such studies by ESI prompted our investigation of the fragmentation of TMPP+-Ac derivatives by ESI via in-source fragmentation (ISF) and MS/MS (low-energy CAD) with a comparison to results from FAB-CAD and MALDI-PSD. Such studies would also provide insight to the fragmentation pathways of charged derivatives when ionized by ESI and fragmented under low-energy conditions.

II. Experimental

A) Preparation of Derivatives:

Peptides and proteins used in the experiments were purchased from Sigma and were dissolved in acetonitrile/water (1:1 v/v). Peptides were N-terminally derivatized using TMPP⁺-Ac-SC₆F₅ bromide reagent synthesized as described elsewhere [6]. Table 2.1 shows the list of peptides that were used for this study.

Table 2.1. Peptides Studied by ESI-CAD-MS After TMPP⁺-Ac Derivatization:

Peptide	Sequence	Mass of Derivative
		(C ⁺)
Chemotactic Elastin	VGVAPG	1071.4
Osteocalcin Fragment	FYGPV	1196.5
Peptide	VGGYGYAK	1444.6
Allatostatin III	GGSLYSFGL-amide	1472
Hb-S peptide	VHLTPVEK	1495.7
Buccalin	GMDSLAFSGGL-amide	1626
Lutenizing hormone	HWYGLRPG-amide	1644.8
Angiotensin II	APGDRIYVHPF	1845
Neuromedin	GNLWATGHFM-amide	1704.7
Cardioactive peptide-B	MNYLAFRPM-amide	1715
Dynorphin Fragment	YGGFLRKYPK	1802.1
Human Renin Inhibitor	PHPFHFFYK	1892.1
Allatostatin I	APSGAQRLYGFGL-amide	1907.9

The peptide solution was mixed with a 5-fold molar excess of the derivatizing reagent in the presence of dimethylaminopyridine (DMAP). The reaction was allowed to occur at room temperature for 15 min. After derivatization, the reaction mixture was analyzed by HPLC to separate the derivatized peptide from any underivatized peptide and hydrolyzed derivatizing reagent. A C₁₈ column (4.8 x 250mm) from Vydac was used.

Separation was performed using a gradient elution program from 25% to 60% of acetonitrile/water/TFA (90%/10%/0.1% v/v/v) (solvent B) over 30 min at 1mL/min using a Waters Millenium system. Solvent A was water/0.1% TFA (v/v). Fractions corresponding to the derivatized peptides were collected manually, and dried under reduced pressure; they were reconstituted in acetonitrile/water (1:1 v/v) when needed.

Three proteins, as shown in Table 2.2 were tryptically digested and the peptide fragments were TMPP⁺-Ac derivatized.

Table 2.2. Proteins Studied by LC-MS After Tryptic Digestion and Derivatization:

Protein	Molecular Weight
Insulin Chain -B	3400.9
Glucagon	3482.8
Cytochrome-C	11702.6

Proteins were digested using 10% (w/w) of trypsin (sequencing grade) to protein, at 37° C for periods of 30 min to 2 h in a phosphate buffer (50mM) at pH 8.2. Once digested, the mixture of peptide fragments was derivatized *in situ*, using the TMPP⁺-Ac derivatizing reagent at a 10-fold molar excess over the estimated number of peptide fragments. For example, if 1 nmole of a protein were digested, and 3 fragments were produced, then there would be 3 nmoles of peptides, so 30 (3 X 10) nmoles of the derivatizing reagent would be used. The mixture was allowed to react at room temperature for 15 min. The derivatized tryptic fragments were separated by HPLC (gradient program used was the same as described previously). The fractions were

collected manually (the R_t's of the TMPP⁺-Ac-peptides were between 28 and 37 min, while those of the underivatized peptides were between 12 and 20 min), and subsequently analyzed by ESI-MS on the Fison's platform. Alternatively, the derivatized digest mixture was analyzed directly by LC-MS using the LCQ.

B) Mass Spectrometry:

a) In-source Fragmentation (ISF) MS:

The purified TMPP⁺-Ac-peptides were analyzed by a Fison's VG platform ESI-MS. Samples (10 pmol/µL) were flow injected with acetonitrile/water (1:1) as the mobile phase (10 µL/min). Nitrogen was used as the drying gas, and the capillary was typically held at 3.5 kV. The quadrupole mass analyzer was operated at 3 scans/sec over a range of m/z 200-2000. Increasing the cone voltage in the ESI source to 100 V induced fragmentation of the peptide derivatives. This is referred to as in-source fragmentation (ISF). When no fragmentation was desired, the cone voltage was maintained at 37 V.

In-source fragmentation (ISF) was also performed in the Finnigan LCQ, where TMPP⁺-Ac derivatives were fragmented in the atmospheric region by increasing the capillary and the tube lens offset voltages simultaneously to 59 V and 40 V from initial values of 25V and 10 V, respectively.

b) MS/MS:

CAD-MS/MS of the TMPP⁺-Ac derivatized peptides was performed using two different instruments. A triple quadrupole mass spectrometer, API 2000, manufactured by PE-SCIEX, with an ESI source was used in one case. The peptide derivative (in acetonitrile/water/0.1%formic acid, 10 pmol/μL) was infused at a flow rate of 5 μL/min

into the ion spray source held at 5 kV. The precursor ion selected in the first quadrupole was collisionally activated in the second stage. Nitrogen was used as the collision gas. The third quadrupole was scanned to detect product ions, in steps of 0.3 m/z for a dwell time of 1 msec. Optimum conditions for efficient fragmentation were determined by using a "ramp parameter" feature of the software. Fragmentation of singly-charged ions of the TMPP⁺-Ac derivatives occurred at accelerating potential differences (corresponding to lab frame collision energies in eV) of 50–70 V.

A Finnigan LCQ, an ESI-ion trap mass spectrometer, was also used to obtain CAD information on the TMPP⁺-Ac derivatives (acetonitrile/water/1%acetic acid, 10 pmol/μL) both by infusion of the sample (3 μL/min) and by LC-MS. The source was held at 4.3 kV, and helium was used as the CAD gas. MSⁿ was performed, where n=1,2,or 3. Fragmentation of singly-charged TMPP⁺-Ac derivatives occurred at relative collision energies of 60-70% of a maximum of 5 eV (LAB). LC instrumentation included the Alliance system from Waters corporation, and the Symmetry (from Waters) HPLC column (2.1x150 mm). Solvents were pumped at a flow rate of 200 μL/min. The solvent composition and gradient are the same as described earlier. Approximately 10 pmol of the derivatized, digested protein were loaded on the HPLC column for LC-MS.

c) MALDI-MS:

MALDI spectra were obtained with a Voyager Elite reflectron time-of-flight mass spectrometer (Perseptive Biosystems) using an accelerating voltage of 22 kV. The mass spectrometer was equipped with a 337-nm nitrogen laser. A saturated solution of α -cyano-4-hydroxycinnamic acid, prepared in acetonitrile/water (1:1,v/v), was used as the

matrix. A 1-μL aliquot of the sample (5 picomoles/μL) was mixed with an equal volume of the matrix solution on the sample plate, and the mixture dried in air. PSD data were obtained when the mass spectrometer was operated in the reflectron mode. Several PSD spectra, each optimized for a different range of m/z values for the fragment ions, were obtained and "stitched" together to yield the composite spectrum.

III. Results and Discussions

A) In-source Fragmentation of the TMPP*-Ac Derivatives of Peptides:

Infusion of the TMPP⁺-Ac derivatives of the peptides into the ESI source, at a cone voltage of 37 V, usually produced doubly-charged ions. This is not unusual because, along with the fixed charge on the TMPP⁺-Ac head group, there could be protonation on a basic residue in the peptide. In larger peptides, triple-charged species are also observed. However, in the case of TMPP⁺-Ac-VGVAPG, only a singly-charged ion is observed (the charge is the one carried by the phosphonium moiety), due to the presence of amino acids containing non-polar side chains. In the case of the VG-platform instrument, which has a single quadrupole mass analyzer, the only means to obtain fragmentation and hence structural information is by CAD in the source. In-source fragmentation (ISF) of the charged derivatives of peptides is observed at elevated cone voltages. A recent article elaborately describes the in-source fragmentaion of various peptides in a similar instrument, now called the micromass platform (29). By elevating the cone voltage, the potential difference between this electrode (the cone) and the counter electrode at ground is increased. Thus, the species travelling through this region undergo a drastic increase in kinetic energy, approximately tens of eV's for a singly-charged species, which results in fragmentation of the precursor ions. In our studies, a cone voltage setting of 100 V was sufficient to fragment peptide derivatives with 6 - 12 amino acids to yield discernible *an ions. Peptide derivatives with fewer amino acids fragmented at a lower cone voltage, and those with more than 12 amino acids required a higher cone voltage. ISF of the TMPP⁺-Ac derivatized peptide produces a series of $*a_n$ ions, with a few $*b_n$ ions and $*c_n$ ions.

Derivatized peptides containing amino acid residues with side chains tend to yield $*d_n$ ions in some cases. As an example, Figure 2.3 shows the ESI-ISF mass spectrum for TMPP⁺-Ac-MNYLAFPRM-amide at a cone voltage of 100 V. The spectrum consists of peaks corresponding to an almost complete series of $*a_n$ ions, along with a low abundance series of $*b_n$ ions.

While most peptides always give a complete series, it cannot be guaranteed. The intensity of the peaks due to fragment ions of high-m/z seems to be lower than that of the peaks due to low-m/z fragments. This may be either due to the mass discrimination effect inherent to the quadrupole mass analyzer, or simply that the low-mass fragments are formed preferably over high-mass fragments.

B) MS/MS of the TMPP⁺-Ac Derivatives of Peptides:

a) Triple Quadrupole Mass Spectrometer:

The ESI source of the API/SCIEX instrument produced both doubly- and singly-charged ions of the intact peptide derivative under the given conditions, and CAD was performed on both types of ions. Regardless of whether the singly- or the doubly-charged species was selected as the precursor, the product ion spectrum was the same, i.e., in both cases peaks were observed at the same m/z values, although the peak intensities differed by as much as 40% at a given m/z value. Since the ion count for the doubly-charged species was higher than that for the singly-charged species, the MS/MS spectrum of the former had better S/N. Fragmentation of the precursor ions occurred at lab-frame collision energies of 60-70 eV. A series of *a_n ions was observed from fragmentation of either the singly- or doubly-charged ions, along with a few *b_n and *c_n ions.

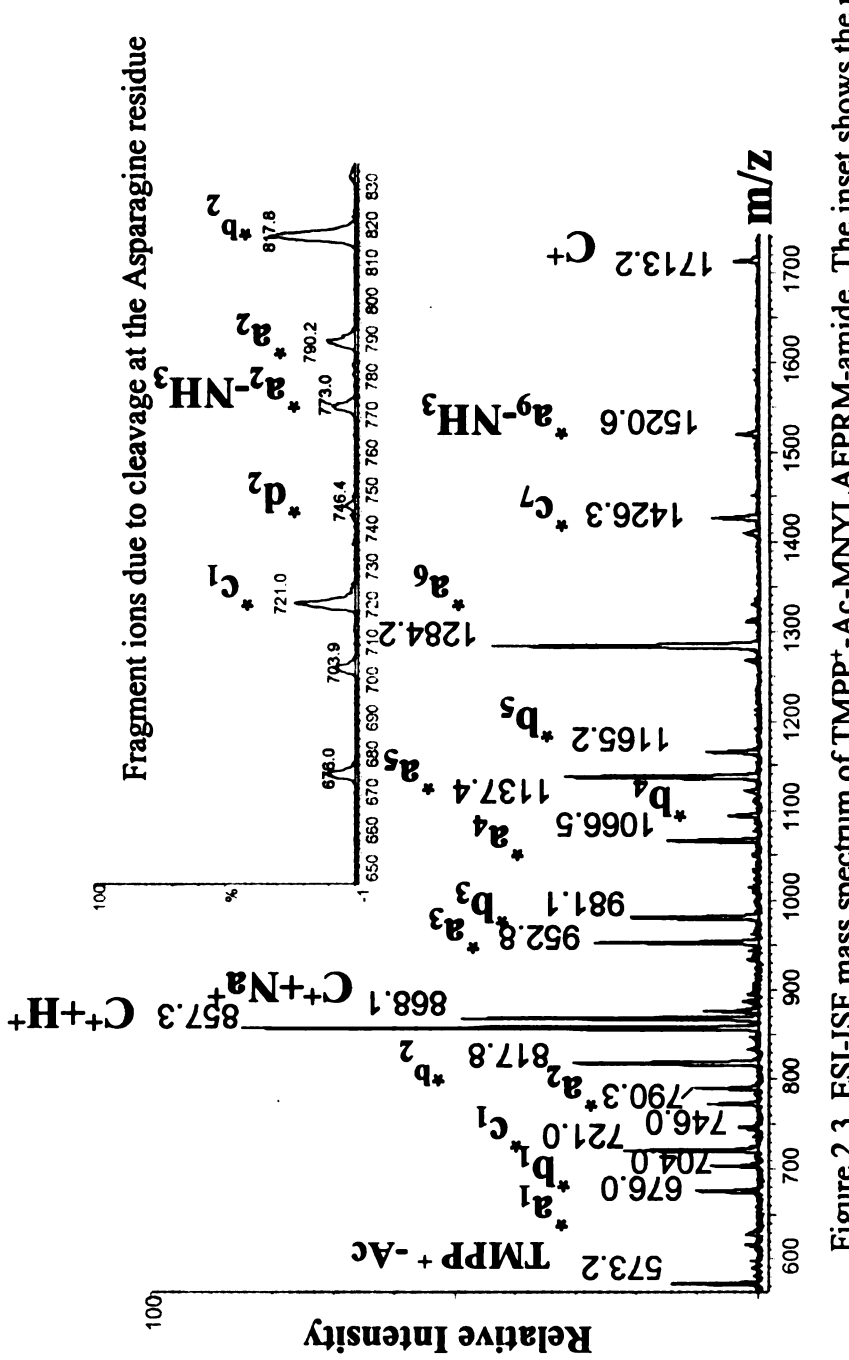


Figure 2.3. ESI-ISF mass spectrum of TMPP+-Ac-MNYLAFPRM-amide. The inset shows the portion containing peaks due to fragment ions from cleavage at the asparagine (N) residue.

A representative spectrum, for the CAD of TMPP⁺-Ac-GGSLYSFGL-NH₂ in the triple quadrupole, as observed from the doubly-charged precursor (m/z 836) is shown in Figure 2.4. It is readily noticeable that a complete series of *a_n ions is formed, along with some *b_n ions.

b) Ion Trap Mass Spectrometer:

Figure 2.5 shows the ESI-CAD-MS/MS spectrum of the underivatized peptide (singly-charged) Neuromedin-B. Figure 2.6 shows the MS/MS spectrum for the TMPP⁺-Ac-derivative of the same peptide, obtained from the singly-charged species (1704 Da). The spectrum from the underivatized species shows both C-terminal (e.g., m/z 433, m/z 592, m/z 662 etc.) and N-terminal ions (e.g., m/z 682, m/z 700, m/z 837 etc.) along with some internal fragments (e.g., m/z 514). The spectrum from the derivatized peptide shows peaks corresponding to N-terminal fragments. The chemistry during the fragmentation in the trap is rich, as represented by many more fragment ions than seen during fragmentation of similar peptides in the quadrupole mass spectrometer. There are peaks corresponding to loss of water and ammonia from the precursor and the fragment ions, which are low energy processes that occur commonly in the trap.

The type of fragment ions produced from the TMPP⁺-Ac charged derivatives of peptides in the LCQ mass spectrometer are different, depending on selection of either the singly- or the doubly-charged intact species as the precursor. An example spectrum for the fragmentation of the doubly-charged TMPP⁺-Ac-GNLWATGHFM-NH₂ in the ion trap is shown in Figure 2.7. This can be compared with the MS/MS spectrum from the singly-charged precursor in Figure 2.6.

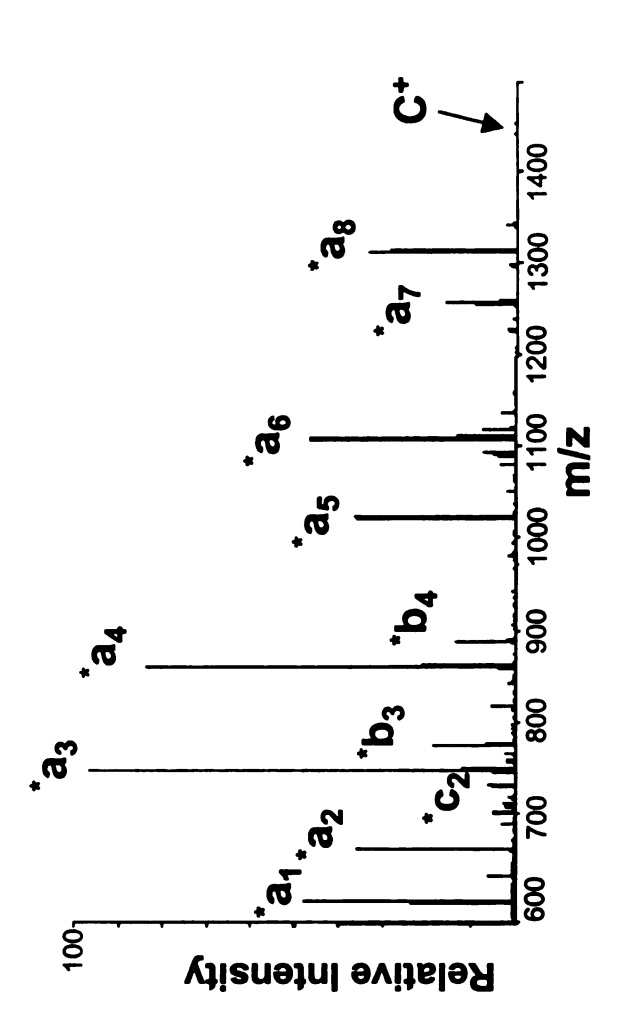
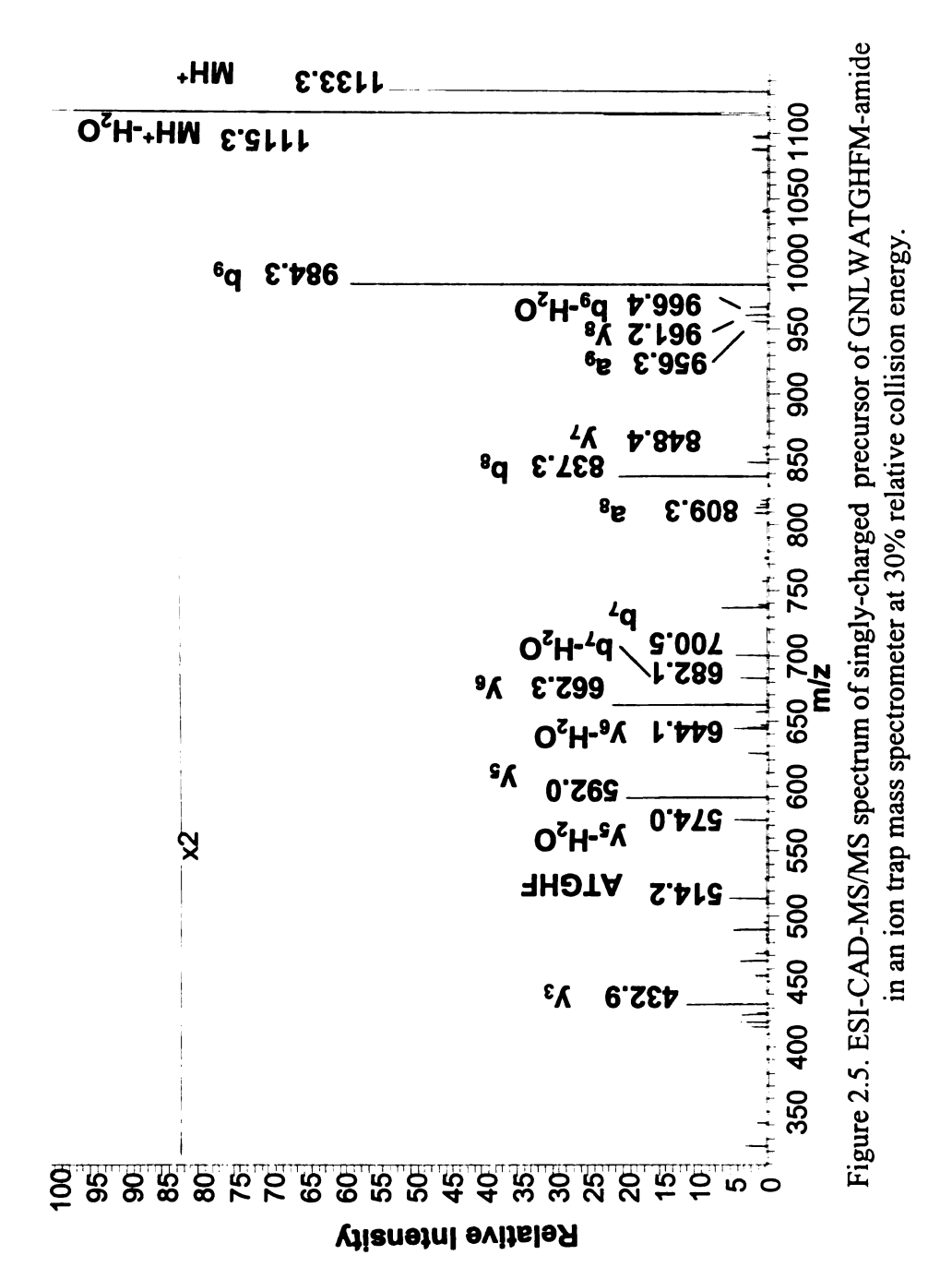
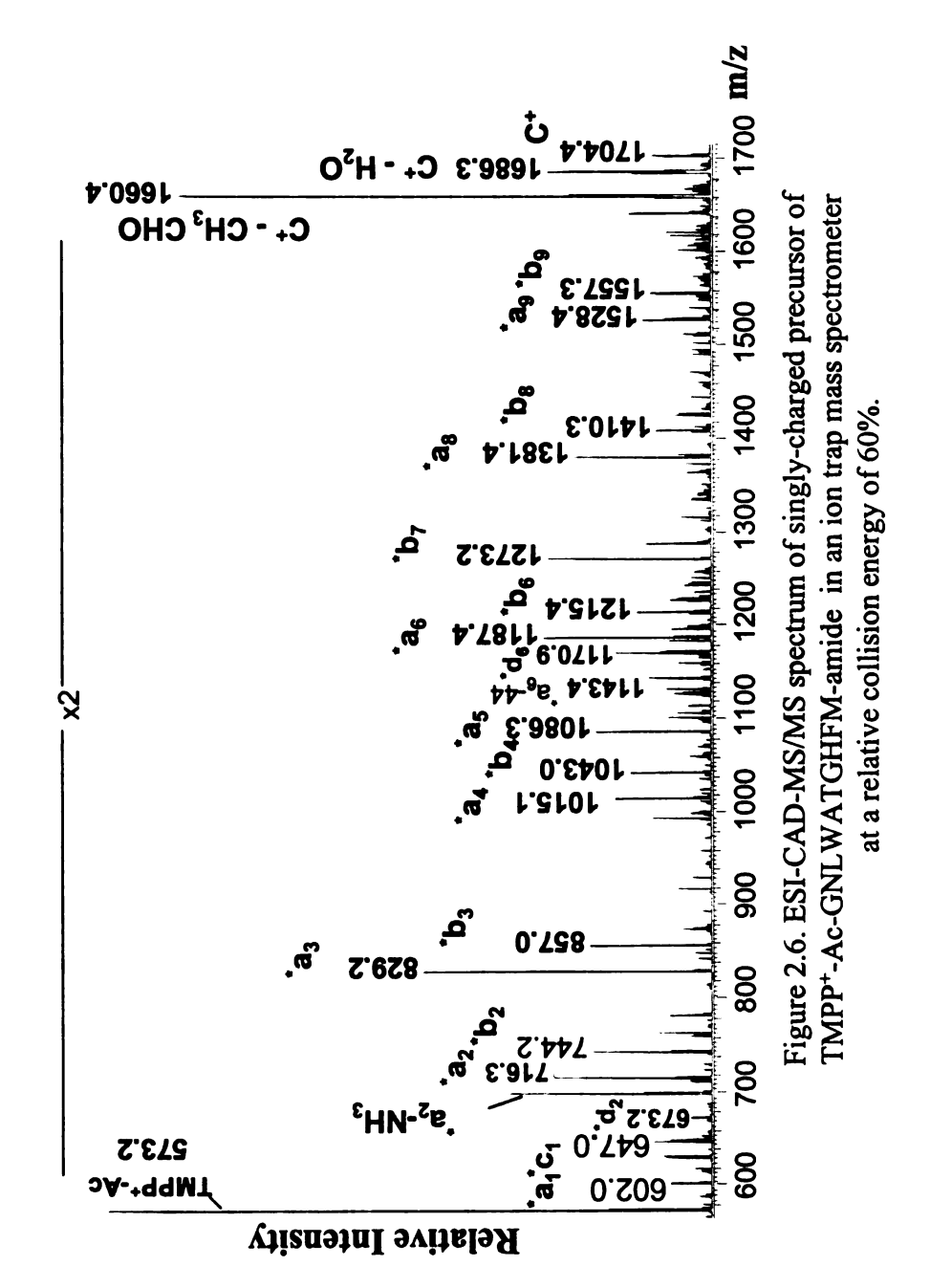


Figure 2.4. ESI-CAD-MS/MS spectrum of TMPP⁺-Ac-GGSLYSFGL-amide, doubly-charged precursor at m/z 736 in a triple quadrupole mass spectrometer at a collision energy of 65 eV.





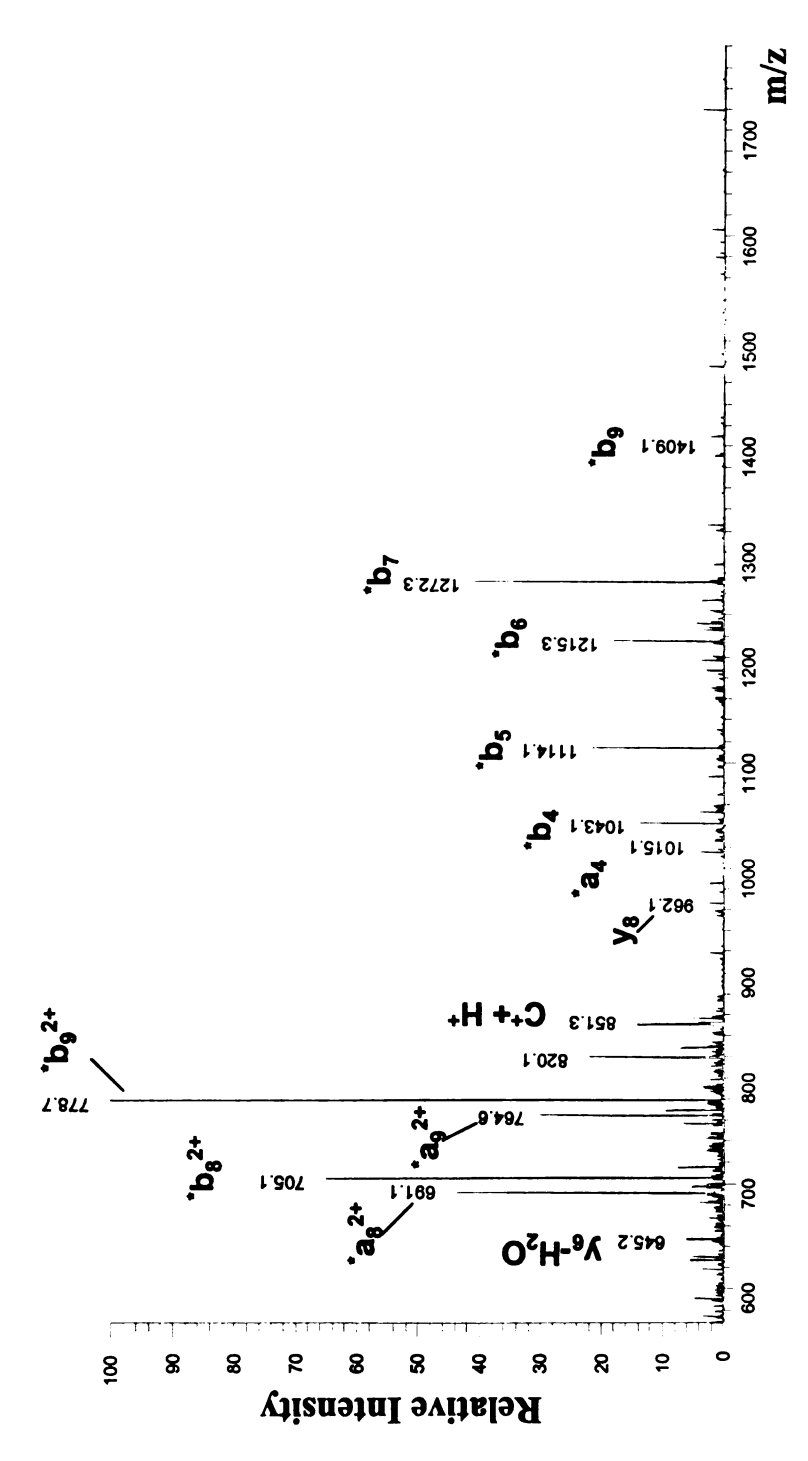


Figure 2.7. ESI-CAD-MS/MS spectrum of doubly-charged precursor of TMPP*-Ac-GNLWATGHFM-amide in an ion trap mass spectrometer at a relative collision energy of 35%.

It can be seen that fragmentation of the singly-charged precursor yields an uninterrupted series of $*a_n$ ions along with $*b_n$ ions, as opposed to the case of the fragmentation of the doubly-charged precursor, which gives a series of $*b_n$ ions, and some doubly-charged ($*b_n+H^+$) ions, along with a few C-terminal ions noticeable in the lower m/z region of the mass spectrum. It may be that the fragmentation pathways available to the doubly-charged ions are charge-mediated by the proton, which is mobile, while fragmentation of the singly-charged ion (the fixed charge) occurs by a charge-remote mechanism. It has also been reported by $Lin\ and\ Glish\ [8]$ that a series of $*a_n$ ions is observed for TMPP*-Ac derivatized peptides when a singly-charged precursor generated by FAB is fragmented in an ion trap.

C) Comparison of the Fragmentation of the TMPP⁺-Ac Derivatives of Peptides by ISF vs. MS/MS:

Although fragmentation of the TMPP⁺-Ac derivatives of peptides by MS/MS in triple quadrupole and ion trap mass spectrometers is more specific due to precursor selection, essentially the same information can be obtained from in-source fragmentation (ISF). Figure 2.8 shows the results from analyzing TMPP⁺-Ac-GGSLYSFGL-NH₂ by ISF and MS/MS. A complete series of *a_n ions is obtained in each case. Signal due to the intact molecular cation (C⁺) is not completely diminished with ISF (Figure 2.8a), indicating that this process is not as efficient for fragmentation as conventional CAD. However, MS/MS studies provided the opportunity to compare the fragmentation pattern originating from a singly-charged ion with that from a doubly-charged ion. The MS/MS technique also allowed us to observe the fragmentation of the various precursors at various collision energies.

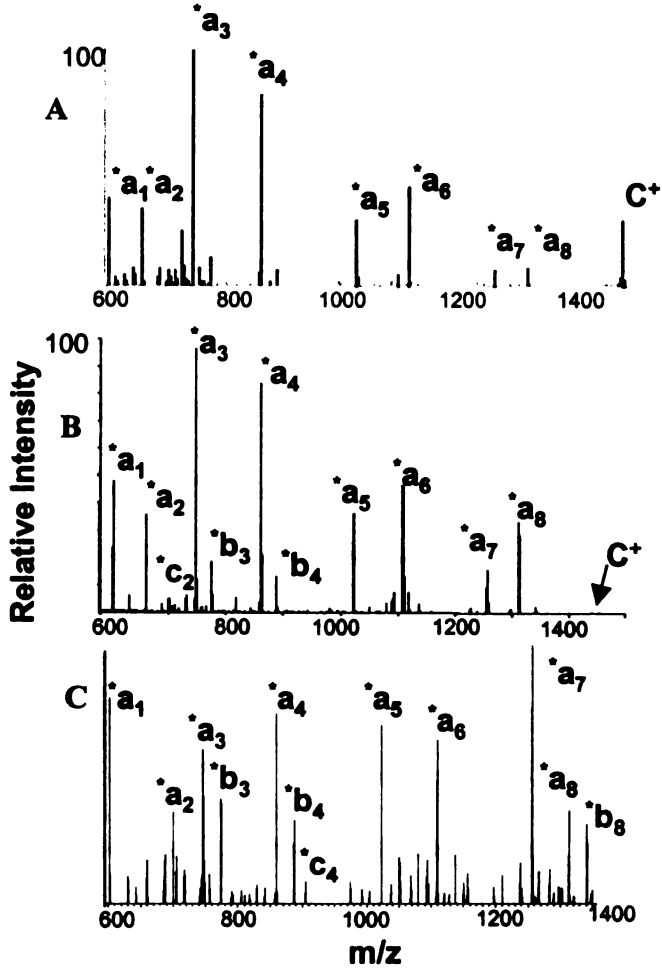


Figure 2. 8. A comparison of the fragmentation of TMPP+-Ac-GGSLYSFGL-amide by A) In-source fragmentation, B) CAD-MS/MS in a triple quadrupole (doubly-charged precursor) C) CAD-MS/MS in an ion trap (singly-charged precursor) mass spectrometers.

D) Comparison of the Fragmentation of the TMPP⁺-Ac Derivatives of Peptides in Triple Quadrupole vs. Ion Trap:

It appears that the TMPP⁺-Ac derivatives of peptides fragment through the charge-remote pathways (based on the formation of a-type ions) when subjected to CAD-MS/MS in the triple quadrupole mass spectrometer both as doubly- and singly-charged precursor, and as a singly-charged precursor in the ion trap. However, during the fragmentation of a doubly-charged precursor (one charge on the derivatized moiety, the second due to a proton along the backbone) in the trap, some C-terminal ions were detected along with the N-terminal ion types. These results suggested to us that perhaps due to the long (tens of msec) residence time in the trap, the large number of low-energy collisions allow observation of both charge-mediated and charge-remote fragmentation. During the fragmentation of the doubly-charged precursor, doubly-charged fragment ions were also commonly observed unlike fragmentation in the triple quadrupole and by ISF. Indirect evidence for these phenomena was acquired by in-source fragmentation where the trap was used only as an m/z analyzer (in which case the residence time of the ions was on the order of tens of microseconds), rather than as a CAD device with subsequent m/z analysis. The result of ISF with m/z analysis by the trap is shown in Figure 2.9, where the mass spectrum essentially represents $*a_n$ ions, since processes leading to charge-mediated fragmentation did not have sufficient time to occur. However, the doubly-charged ion did not seem to fragment by charge-mediated pathways during MS/MS in the triple quadrupole mass spectrometer. The quadrupole ion trap and transmission quadrupole mass spectrometers are distinctly different, i.e., in the transmission quadrupole, the residence time of the ions in the collision cell is short (<100 usec).

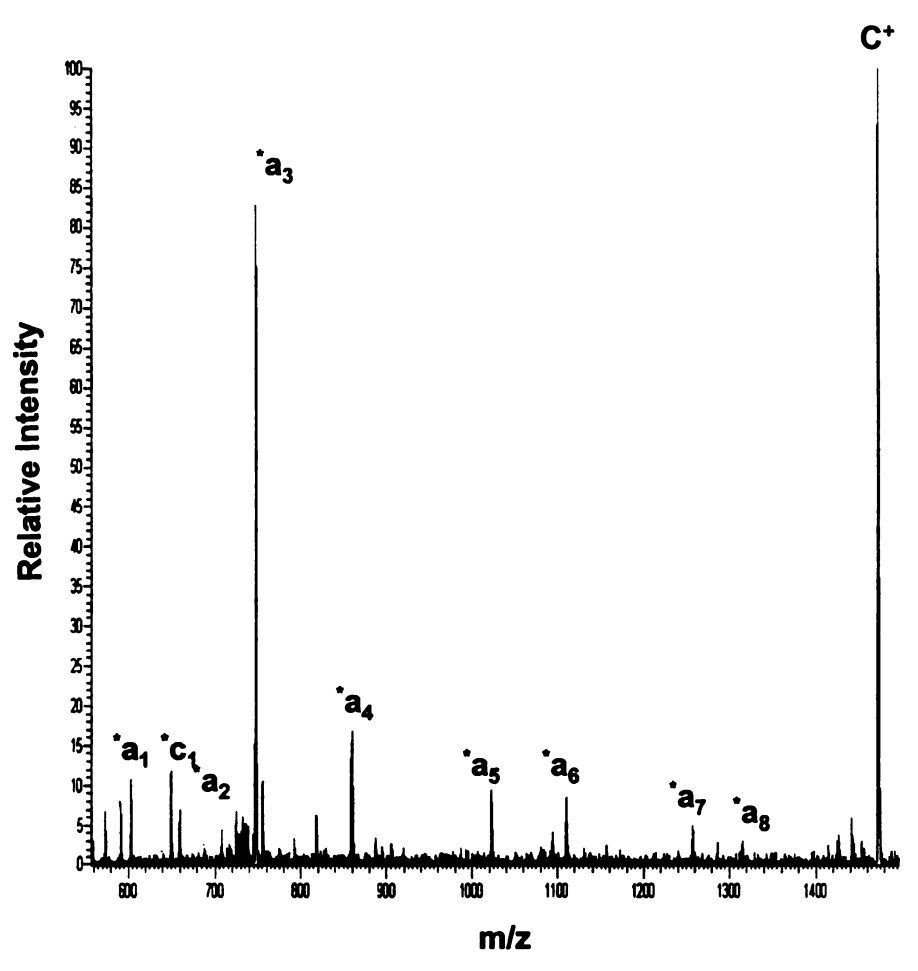


Figure 2.9. In-source fragmentation of TMPP+-Ac-GGSLYSFGL-amide followed by m/z analysis of fragment ions in an ion trap mass spectrometer.

In the ion trap considerably more collisions will occur and, in principle, higher internal energies can be deposited in an ion, but in smaller increments. In addition, due to the longer reaction times, an ion that has accumulated sufficient internal energy to decompose by a low-energy process may not survive to undergo another activating collision [32]. Thus, it is not surprising that the mass spectra for the fragmentation of doubly-charged ions in the trap have peaks corresponding to fragment ions produced from charge-mediated processes. The presence of peaks corresponding to neutral loss such as water and ammonia from both the precursor and fragment ions also suggest the predominance of lower energy pathways.

E) Speculation on the Fragmentation Pathways of TMPP⁺-Ac-Peptides:

The major pathway by which an $\mathbf{a_n}$ ion can be formed during fragmentation of the peptide backbone is by loss of CO from a $\mathbf{b_n}$ ion [13]. In the case of charged derivatives, 1,2-elimination is responsible for $\mathbf{*a_n}$ ion formation [33], which is a charge-remote mechanism. Recently, a mechanism for $\mathbf{*a_n}$ ion formation in the case of TMPP⁺-Ac derivatives of peptides has been proposed by *Liao et al.* [7], through the shift of an amide hydrogen.

Although in FAB-CAD (high-energy), * $\mathbf{b_n}$ ions were not commonly observed, they are observed during our low-energy CAD studies by ESI-MS. Higher laser powers in MALDI-PSD also produced * $\mathbf{b_n}$ ions. Charge-remote mechanisms for $\mathbf{b_n}$ ion formation in multiple-charged ions by low-energy CAD have been proposed earlier [34]. Wagner proposed charge-remote mechanisms for * $\mathbf{b_n}$ ion formation in charge-derivatized peptides when studied by FAB-CAD [35]. According to this, formation of * $\mathbf{b_n}$ ions by charge-remote mechanisms in TMPP⁺-Ac-peptides could be from α -hydrogen shifts.

During the fragmentation of doubly-charged ions of TMPP⁺-Ac-peptides (hence protonated along the backbone) by low-energy CAD (other than in the ion trap), if charge-mediated processes occur predominantly, there should be some characteristic evidence in the spectrum. For example, if a *b_n ion is formed by a charge-mediated process, it should carry a charge on its carbonyl end (C-terminus). This process will make it a doubly-charged ion (as there is already a fixed charge on the N-terminus), which would be represented by a peak in the lower m/z range. This was not observed during CAD of any of the model peptides (ranging from 5 to 15 residues) that we investigated. Further, no complementary y-ion signals were widely observed. Hence, charge-mediated pathways can be ruled out as producing the *b_n ions. Conceivably, prior to the fragmentation of the doubly-charged species, charge-stripping (removal of the additional proton) may occur yielding a species with a fixed charge (C⁺), which undergoes further fragmentation (presumably via charge-remote pathways) both in ISF and MS/MS. Since charge-stripping is the process that requires the least amount of energy, this assumption seems reasonable. However, during fragmentation of the doublycharged ions in the ion trap mass spectrometer, a mixture of N-terminal and very few Cterminal ions was observed which led us to conclude that charge-mediated pathways may also be available. Also doubly-charged fragment ions were commonly seen during fragmentation of the doubly-charged precursor. This suggests that charge-stripping may not be complete in the ion trap mass spectrometer, which allows some possibility for charge-mediated fragmentation. This does not suggest that in all cases where *b_n ions are formed there is some charge-mediated fragmentation. In fact, the predominant pathway is probably charge-remote. However, the origin of the shifting proton during

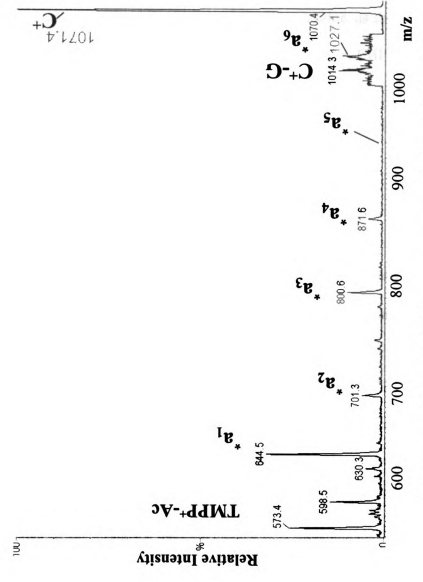
their formation is not clear at this point. Labeling studies using deuterium at various sites of the peptide would help identify this mechanism clearly.

F) Characteristic Fragmentation Behavior of Some Amino Acid Residues:

There are 20 amino acids and it is important to understand if the fragmentation of all the amino acids is the same or different when present in the sequence of the TMPP⁺-Ac derivative. For most amino acids, present in the sequence of a charge-derivatized peptide, the predominant ion formed is *a_n. In the case of the quadrupole mass spectrometers the high-mass fragment ions are less abundant than the low-mass fragment ions; and low-mass *a_n fragment ions were accompanied by *b_n and *c_n ions. However, in the ion trap such discrimination was not observed. For residues such as serine, threonine, valine, and leucine, *d_n ions were often observed. But this was not consistent. So it cannot be generalized or used as a rule in the identification of these residues. Some characteristic fragmentation patterns were observed for the following residues and an effort to generalize this observation is made in the following text, which will aid in identifying the presence of the residue in unknown sequences.

a) Proline (P):

In our study of a variety of derivatized peptides, whenever proline (P) was present in the amino acid sequence, there was no conspicuous signal due to cleavage at that position during ISF in the VG platform MS in most cases. Figure 2.10 shows the ESI-ISF mass spectrum for TMPP⁺-Ac-VGVAPG; it is clear that a series of *a_n ions is produced except for *a₅, which corresponds to cleavage at the position of the proline residue.



single-quadrupole mass spectrometer. Spectrum shows a series of *an ions, except Figure 2.10. ESI-source-CAD mass spectrum of TMPP*-Ac-VGVAPG in a for cleavage at the site of proline (*a5).

This provides a significant clue on the mechanism that is probably operative in the formation of the $*a_n$ ions during low-energy CAD. Since proline lacks an amide hydrogen when present in a peptide sequence, it is probably the amide hydrogen shift that results in the formation of the $*a_n$ ions. It has been already been proposed by Liao et al. [7] that the lack of an amide hydrogen on a proline residue, as shown in Figure 2.11, does not allow the mechanism for $*a_n$ ion formation in the TMPP⁺-Ac derivatives when analyzed by MALDI-PSD.

Figure 2.11. Structure of proline (P) residue.

However, a weak signal corresponding to cleavage at the proline residue is observed during fragmentation of certain peptides like TMPP+-Ac-FYGPV and TMPP-PHPFHFFVYK during ISF-MS. During our ESI-CAD-MS/MS study of the peptide derivative of TMPP+-Ac-VGVAPG a weak signal is observed for *a₅ and *b₅ ions. Also, a weak signal was obtained in MALDI-PSD for cleavage at proline at higher laser powers [7]. Thus, the mechanistic aspects are unclear. These observations suggest that, if during the analysis of an unknown sequence there is a large mass difference in between two peaks that cannot be filled by one amino acid residue, it probably implies the presence of proline in the corresponding portion of the sequence.

b) Threonine (T):

A threonine residue has a hydroxyl containing side chain. Loss of water from the precursor is a common observation due to the presence of such residues during CAD-MS/MS. Other noticeable features due to fragmentation at T were the formation of a *d_n ion and the formation of an *a_n-44 ion. The formation of the *a_n-44 could be due to the loss of the complete side chain as CH₃CHO. The structure of T is shown in Figure 2.12. This can be seen from the MS/MS spectrum of TMPP⁺-Ac-GNLWATGHFM-amide (Figure 2.6). This is also observed in the ISF-CAD-MS spectrum for TMPP⁺-Ac-VHLTPVEK (Figure 2.20).

Figure 2.12. Structure of threonine (T) residue.

c) Aspartic Acid (D):

Aspartic acid (D) is an amino acid with an acidic side chain, as shown in Figure 2.13.

Figure 2.13. Structure of aspartic acid (D) residue.

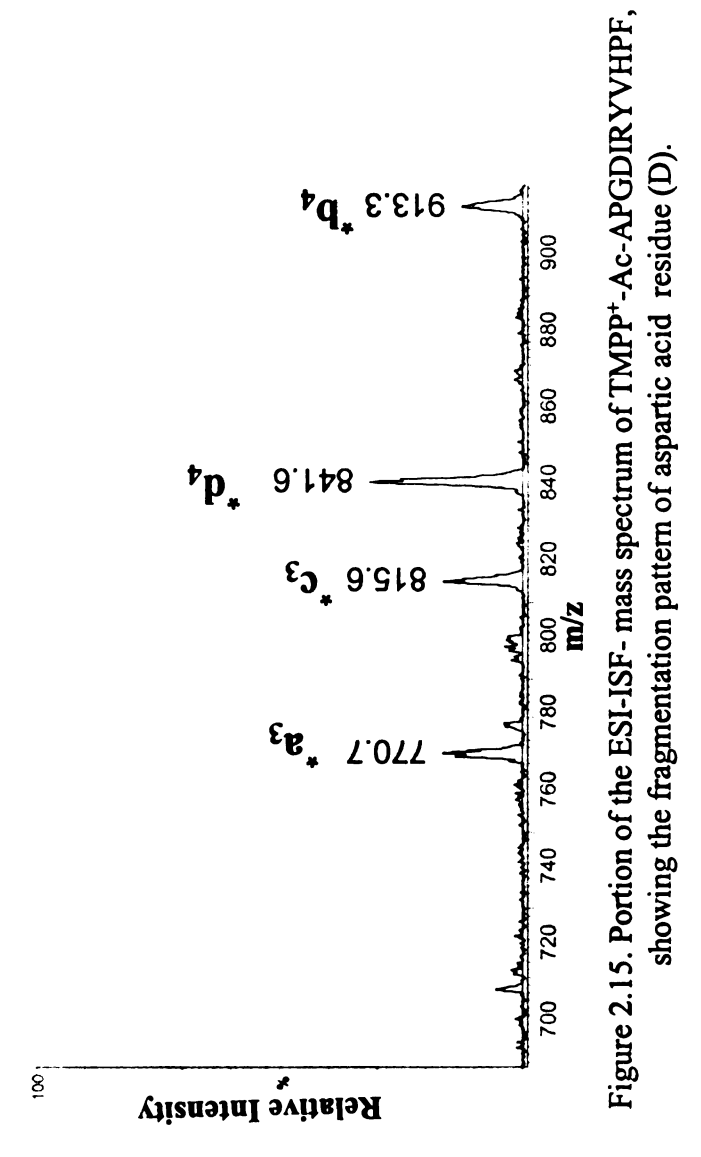
Fragmentation of a peptide derivative containing aspartic acid, does not yield an $*a_n$ ion; it yields a $*d_n$ ion, due to the loss of the side chain at the site of D. It has been proposed that the $*d_n$, $*b_n$, and $*c_{n-1}$ ions are formed via cyclic intermediates involving the side chain, and hence are formed preferentially over the $*a_n$ ion [7]. Mechanism for formation of $*b_n$, $*d_n$, and $*c_{n-1}$ ions as adopted from this reference are shown in Figures 2.14 a, b and c, respectively.

Figure 2.14a. Mechanism for the formation of *b_n ion due to fragmentation at D.

Figure 2.14b. Mechanism for the formation of $*d_n$ ion due to fragmentation at D.

Figure 2.14c. Mechanism for the formation of $\,^*c_{n-1}$ ion due to fragmentation at D.

Figure 2.15 is a portion of the ESI-ISF mass spectrum of TMPP⁺-Ac-APGDIRYVHPF. Fragmentation at D, shows a prominent peak for the $*d_3$ ion (no $*a_3$ ion) along with peaks for a $*b_3$ ion and a $*c_2$ ion. Similar observations have been made for other peptide derivatives containing D. Thus, cleavage at the site of the aspartic acid residue yields a signature pattern ($*c_{n-1}$, $*b_n$, $*d_n$), which, even though it disrupts the $*a_n$ series, should not be difficult to identify due to the characteristic presence of the three peaks as a cluster.



d) Asparagine (N):

Asparagine is the amide version of aspartic acid (residue structure shown in Figure 2.16), where the -OH on the side chain is replaced by -NH₂. Thus, a similar behavior as that of aspartic acid could be expected for asparagine.

Figure 2.16. Structure of asparagine (N) residue.

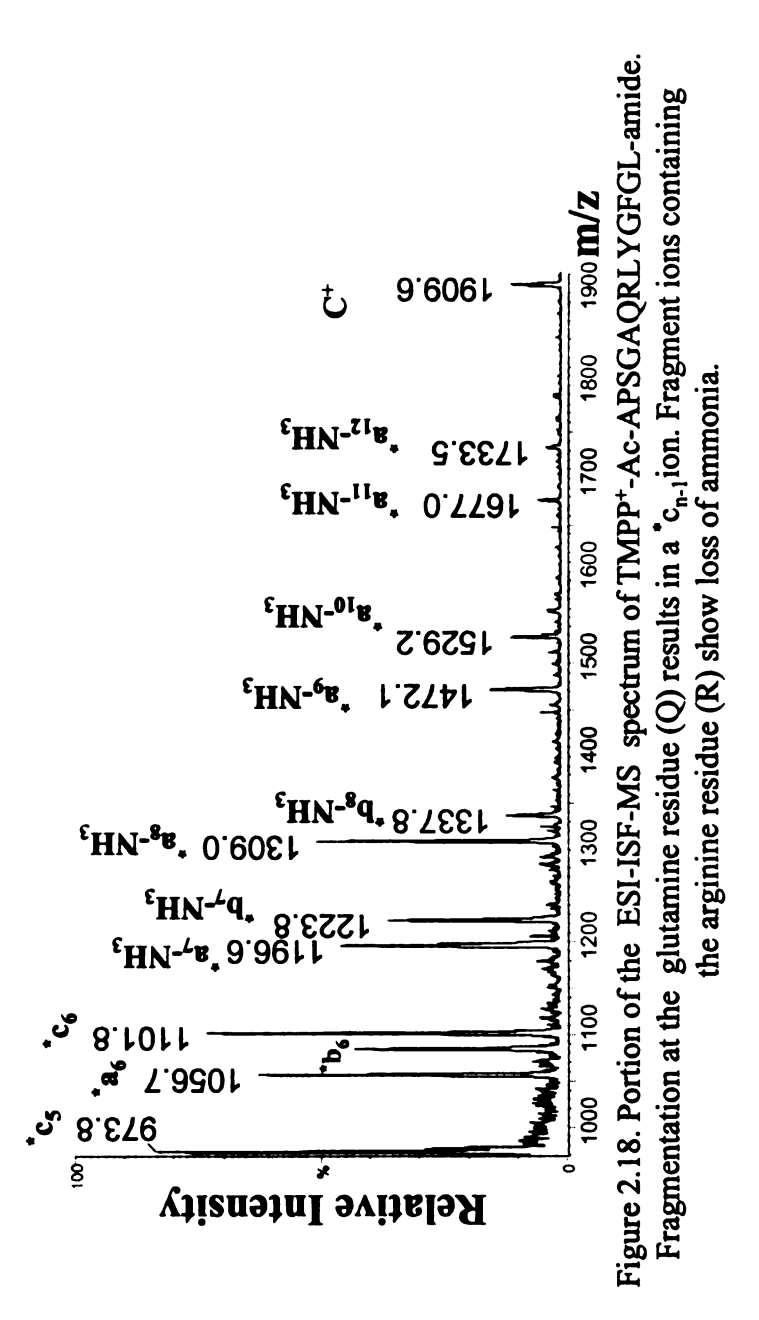
An example of a peptide containing N, TMPP*-Ac-MNYLAFPRM-amide is shown in Figure 2.3. It can be noticed that as in the case of aspartic acid, prominent peaks due to ${}^*\mathbf{c}_{n-1}, {}^*\mathbf{d}_{n}, {}^*\mathbf{b}_{n}$ ions are seen. Along with these, ${}^*\mathbf{a}_{n}$ and ${}^*\mathbf{a}_{n} - \mathrm{NH}_3$ ions are also seen. Thus a similar mechanisms as shown in Figures 2.14a, b and c can be assumed operative even for asparagine. However, the mechanism for the formation of the ${}^*\mathbf{a}_{n}$ ion is also operative as seen from the ${}^*\mathbf{a}_{2}$ peak in the spectrum along with the ${}^*\mathbf{a}_{2}$ -NH₃ peak. Although this is a cumbersome pattern of fragmentation with the appearance of 5 peaks due to one single residue, it is still characteristic and can be used as a bench mark in the case of unknowns. The presence of the two additional peaks (${}^*\mathbf{a}_{n}$ and ${}^*\mathbf{a}_{n}$ - NH₃) in the case of asparagine along with the signature as seen for D (${}^*\mathbf{c}_{n-1}, {}^*\mathbf{d}_{n}, {}^*\mathbf{b}_{n}$), will help distinguish between the aspartic acid and asparagine residues.

e) Glutamine (Q):

The structure of Glutamine is shown in Figure 2.17. Glutamine has a structure similar to asparagine with the side chain longer by one methylene unit. Hence, a similar fragmentation pattern to that of aparagine can be expected for glutamine.

Figure 2.17. Structure of glutamine (Q) residue.

However, the results from two peptides (TMPP⁺-Ac-APSGAQRLYGFGL-amide and TMPP⁺-Ac-IFVQK) containing Q suggests that fragmentation at the site of glutamine results in *c_{n-1} and *a_n ions. There is no conspicuous signal for *d_n or *b_n ions. Loss of ammonia from the *a_n ion is not observed either. Thus, the presence of one additional methylene unit drastically alters the fragmentation pattern of this residue because it disrupts the intermediates required to form the expected ions. The spectrum of TMPP⁺-Ac-APSGAQRLYGFGL-amide is shown as an example to demonstrate the fragmentation pattern of Q in Figure 2.18. Here Q is the 6th residue, and peaks for *c₅ and *a₆ ions are seen in the spectrum. Similarly, in Figure 2.23, the spectrum of TMPP⁺-Ac-IFVOK, peaks for *c₃ and *a₄ ion are observed.



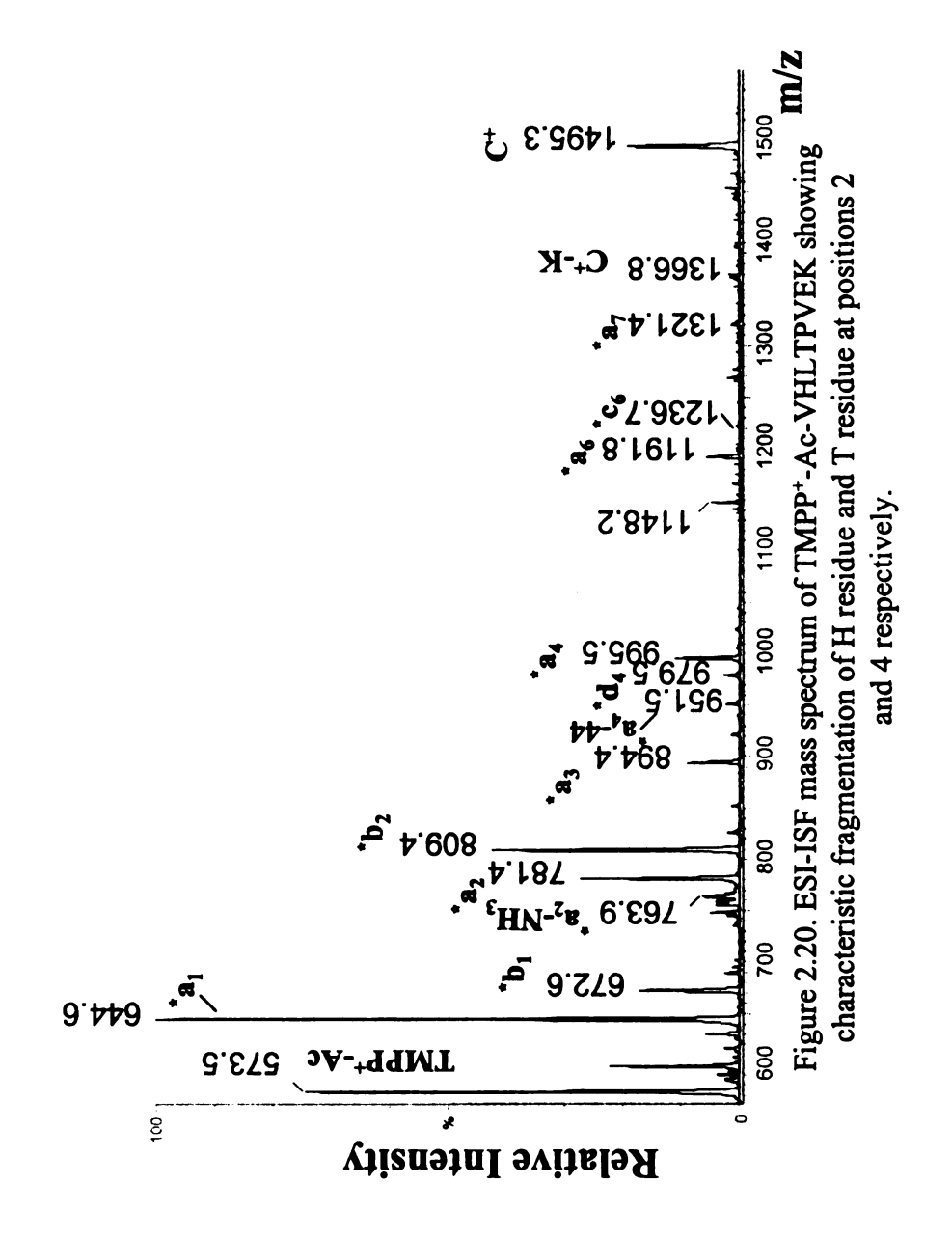
A similar result can also be expected for the residue glutamic acid, which has the acidic functionality instead of the amide functionality in glutamine. In the list of peptides studied, only one has the residue E, TMPP⁺-Ac-VHLTPVEK, and the fragmentation at E for this peptide is not very intense to draw any conclusions. However, there are weak signals observed for *c₆ and *a₇ ions (Figure 2.20). Roth has observed *d_n and *c_{n-1} ion formation for fragmentation at E during a MALDI-PSD study of the peptide TMPP⁺-Ac-AEKAA and has proposed mechanisms similar to that shown in Figure 2.14a, b and c for their formation [36].

f) Histidine (H):

Histidine is one of the three residues (Structure shown in Figure 2.19), that contains a basic side chain.

Figure 2.19. Structure of histidine (H) residue.

The fragmentation at histidine results in both $*a_n$ and $*b_n$ ions. The intensity of the peak due to the $*b_n$ ion is higher if not equal to that of the peak due to the $*a_n$ ion. An example spectrum is shown in Figure 2.20 for the peptide derivative TMPP⁺-Ac-VHLTPVEK.



The peak for *b₂ is more intense than the peak for *a₂. This observation was also made for TMPP⁺-Ac-PHPFHFFYK and TMPP⁺-Ac-HWSYGLRPG-amide. The structure of *b_n is probably stable when H is the terminal residue in the fragment and hence it is possibly formed preferentially.

g) Arginine (R):

Arginine is another amino acid (Structure shown in Figure 2.21) with a basic side chain along with histidine and lysine.

Figure 2.21. Structure of arginine (R) residue.

Cleavage at arginine for TMPP⁺-Ac-Peptides results in an $*a_n$ ion with loss of ammonia; all the fragment ions that contain arginine seem to lose ammonia, too. This behavior is demonstrated in the CAD-MS/MS spectrum (Figure 2.18) for TMPP⁺-Ac-APSGAQRLYGFGL-amide. There is a series of $*a_n - NH_3$ peaks after residue 7, which is R. The other feature noticeable is the $*c_{n-1}$ ion which is $*c_6$. A similar observation is made for TMPP⁺-Ac-YGGFLRKYPK. Formation of the $*c_{n-1}$ ion is not dependent on the residue present before R, because the residue L does not produce a characteristic $*c_n$ fragment when present in other peptide sequences. It is due to the influence of R being

the successive residue in the sequence; a mechanism similar to the one shown in Figure 2.14c can be assumed. In the case of arginine, the proton transfer for the formation of the *c_{n-1} ion probably originates from the -NH₂ group of the side chain. These patterns suggest the presence of R in the sequence. Although these characteristics are not very diagnostic, they do provide some clues to identifying the presence of R in the sequence.

G) Comparison of the Fragmentation of TMPP*-Ac-peptides by ESI-ISF vs. by MALDI-PSD and FAB-CAD:

TMPP⁺-Ac-peptides have been thoroughly studied for their fragmentation behavior by MALDI-PSD [7] and FAB-CAD [6]. Hence, it is meaningful to compare the results from ESI-ISF with those from the other two methods. The results from ESI-ISF match more closely with those from MALDI-PSD than those from FAB-CAD. For example, analysis of a derivatized peptide containing proline by FAB-CAD always yields an $*a_n$ ion due to cleavage at the site of the proline residue, while in ESI-ISF the signal for this ion is weak and, in MALDI-PSD, the signal is laser power-dependent [7]. The formation of a $*d_n$ ion from fragmentation exclusively at the position of aspartic acid is observed with both ESI-ISF and MALDI-PSD. In FAB-CAD, although a $*d_n$ ion is observed, there is also an $*a_n$ ion without the loss of side chain.

These variations in results can be attributed to the differences inherent in these methods of analysis; high-energy vs. low-energy. High-energy CAD spectra are usually the result of single collisions between precursor ions and the inert gas-phase atoms, while low-energy CAD results from multiple collisions and reflects multi-step cleavage reactions [37]. In FAB-CAD (high-energy), dissociation is induced by imparting excess energy to a selected precursor ion, promoting high-energy fragmentation. In MALDI-PSD, although a precursor can be selected, CAD is not promoted intentionally. The

fragments formed either during desorption (prompt fragmentation) or from metastable decay of the precursor during flight are identified using the reflectron. Since it is possible to control the fragmentation by adjusting the laser power, most probably fragmentation occurs during the desorption/ionization (D/I) process. Therefore, it cannot be called a true collisional process. Although the energy imparted in the process is quite enough to promote fragmentation, it is not like the high-energy CAD in FAB. Similarly, in ESI-ISF, the increase in cone voltage promotes more energetic ion/molecule collisions, but the amount of energy transferred to the fragmenting ion is unknown. However, because ISF is a low-energy process, fragmentation is not expected to be similar to that in highenergy FAB-CAD. Figure 2.22 compares the spectra of TMPP⁺-Ac-GMDSLAFSSGL-NH₂ as obtained by all the three ionization techniques. All three spectra show a complete series of *a_n ions; a few *b_n ions and *c_n ions are observed in all of them especially in the lower m/z region. Note that due to cleavage at the aspartic acid residue, *a₃ is seen in the FAB-CAD spectrum in addition to *d₃, while in MALDI-PSD and ESI-ISF spectra, only $*d_3$ is seen.

H) ESI-CAD-MS/MS Study of TMPP*-Ac Derivatized Tryptic Digests:

We have extended the study of derivatized synthetic peptides to derivatized peptide fragments produced during tryptic digestion of proteins. Advantages due to TMPP⁺-Ac derivatization are explicit during the chromatographic separation of digestion products.

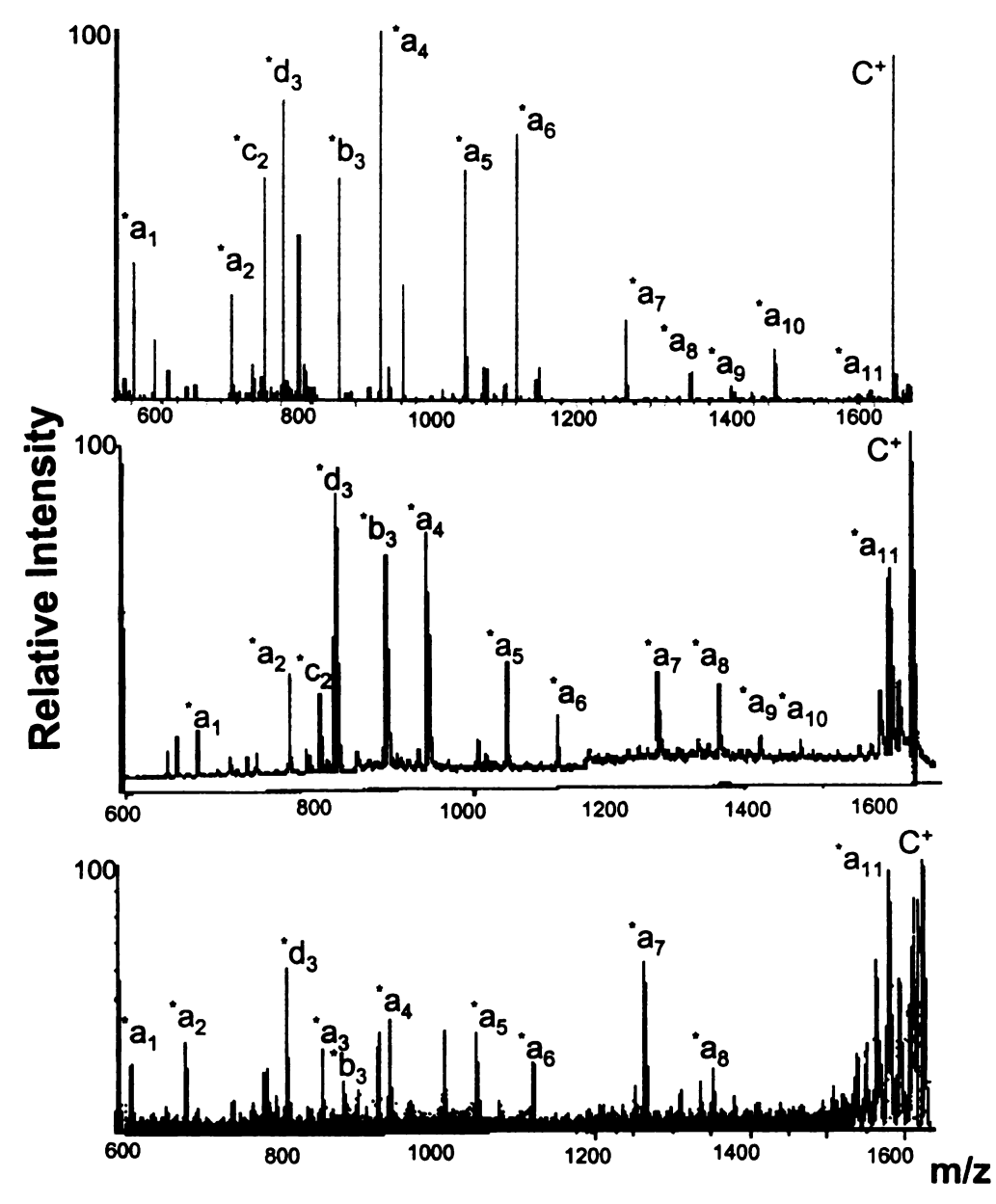


Figure 2.22. A comparison of the fragmentation of TMPP⁺-Ac-GMDSLASFGGL-amide by ESI-ISF-MS, MALDI-PSD-MS and FAB-CAD-MS respectively.

Certain peptides, which are of short length, have very short retention times; after TMPP⁺-Ac derivatization, the retention times are increased, thereby permitting better separation and detection of these species. Also, the detection limit for fragments in protein digests on a conventional reverse phase column can be increased by derivatization because the molar absorptivity of the TMPP⁺-Ac derivatized peptides is much higher than that for underivatized peptides. Hence, even if picomoles of the protein are digested, TMPP⁺-Ac derivatized tryptic peptides can be separated and detected by conventional HPLC using an absorbance detector.

It should be noted that the TMPP⁺-Ac reagent undergoes rapid hydrolysis to produce TMPP-CH₂COOH during its reaction with the peptides. TMPP itself is another by- product. These products are represented by major peaks in the chromatogram. Often a major peak for TMPP-CH₂COOH occurs amidst the peaks corresponding to derivatives of some of the peptides. Fortunately, there were no cases of co-elution of the reagent-related species and derivatives of the peptides reported in this paper. Problems due to co-elution could be overcome by LC-MS using the mass spectrometer for precursor ion selection.

a) Cytochrome-C:

The chromatogram for the HPLC separation of TMPP⁺-Ac derivatized tryptic peptides of cytochrome—c is shown in the top panel of Figure 2.23. The peak at ~35 min corresponds to TMPP-CH₂COOH. It was possible to identify 15 TMPP⁺-Ac derivatized tryptic fragments from cytochrome-c, whereas in the underivatized mixture only 13 were identified.

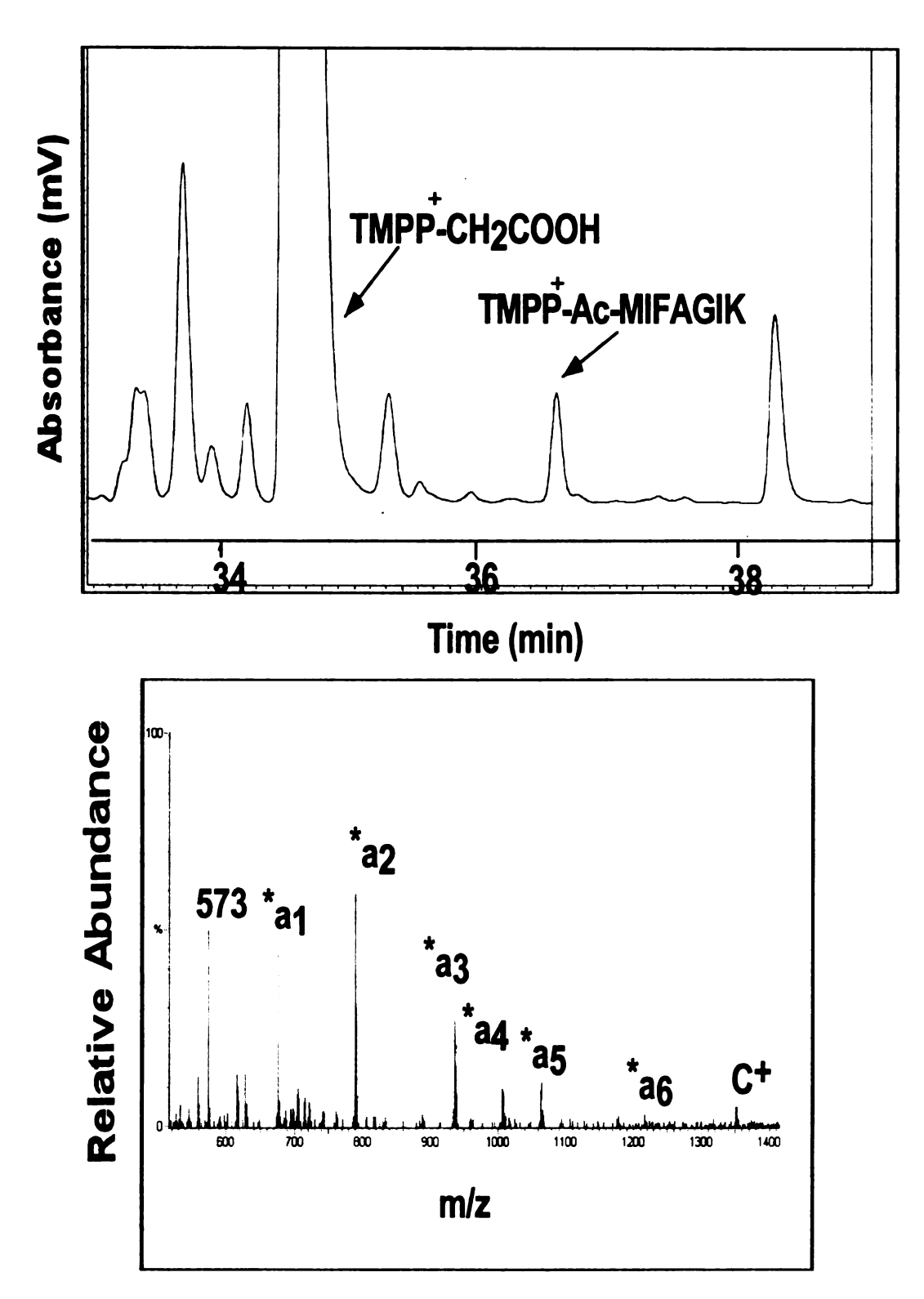


Figure 2.23. LC-MS results of the TMPP⁺-Ac-derivative mixture of the tryptic digest of cytochrome-C. Top panel shows the chromatogram for the separation of the mixture. Bottom panel shows the ESI-ISF mass spectrum of a peptide derivative (residues 80-86), TMPP⁺-Ac-MIFAGIK.

While some tryptic fragments were unidentified (by MALDI-MS or ESI-MS) before derivatization, it was possible to detect them after derivatization, especially the ones with masses less than 500 Da.

The ESI-ISF mass spectrum of TMPP $^+$ -Ac-MIFAGIK (see labeled peak in the chromatogram), representing the TMPP $^+$ -Ac derivative of the tryptic fragment containing residues 80-86, is shown in the bottom panel of Figure 2.23. A series of $*a_n$ ions, from which the sequence can be deduced, is seen. In some cases, the signal due to fragmentation of the last residue in a tryptic fragment is not detectable. However, because the C-terminal residue can only be lysine or arginine, absence of said peak should not preclude identification of the complete sequence. Note also that most of the fragments observed in bottom panel of Figure 2.23 are $*a_n$ ions, and that no $*b_n$ or $*c_n$ ions are present.

Analysis of the same sample by online LC-MS was performed using a Waters chromatographic system and LCQ mass spectrometer. During the LC-MS run, the LCQ was operated in the dual scan mode (double play). A full scan was first performed, and a subsequent MS/MS scan was performed at relative collision energy of 65% on a list of precursor ions. The ESI-CAD-MS/MS spectrum of TMPP⁺-Ac-IFVQK (residues 9-13) is shown in Figure 2.24. A series of *a_n ions is seen in the spectrum along with an intense peak at m/z 1078, corresponding to the *c₄ ion or loss of the terminal K residue from the precursor (C⁺).

The following example shows that it is possible to obtain simple and interpretable spectra from TMPP⁺-Ac derivatives of peptides whose sequences are not known a priori.

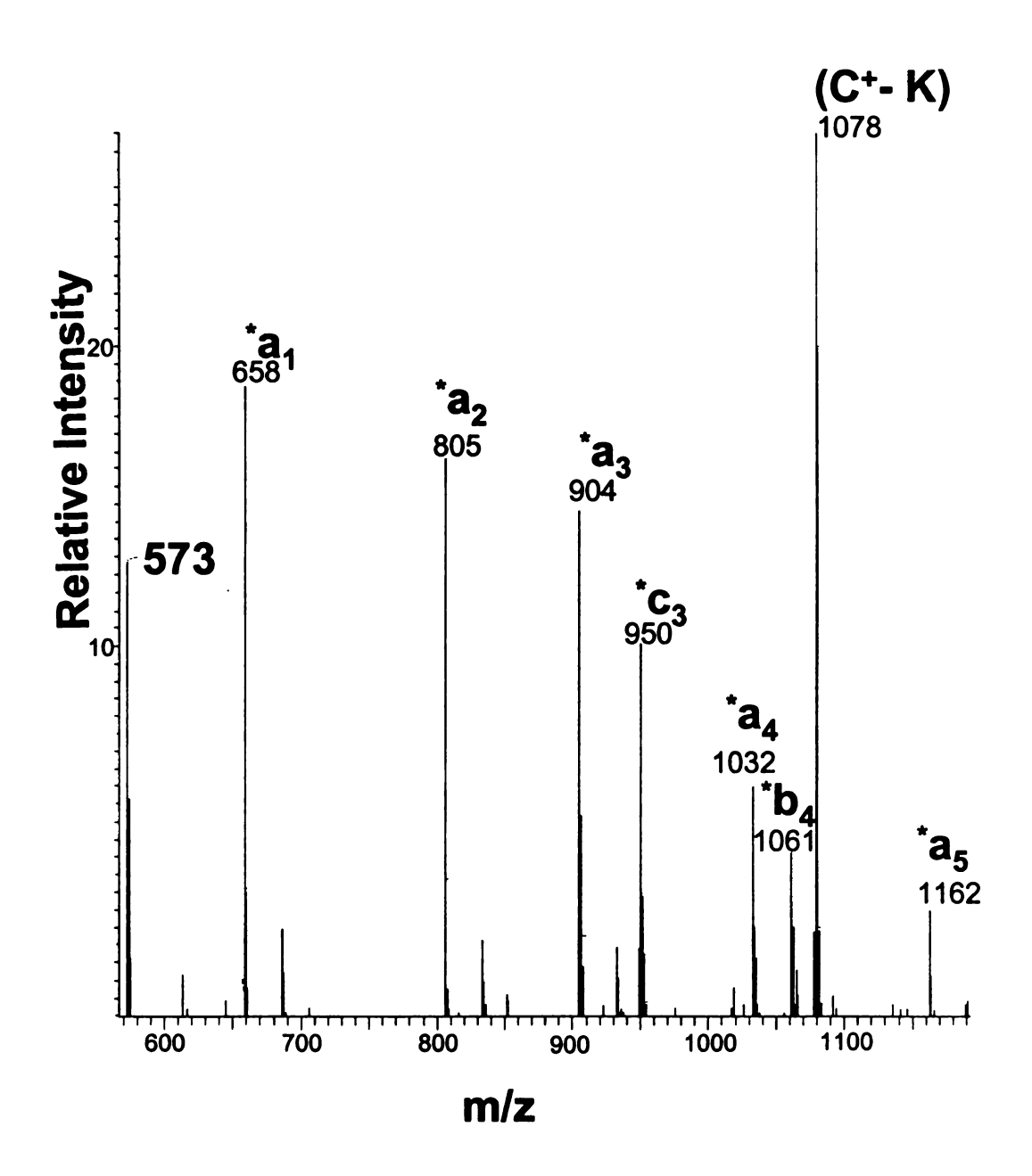


Figure 2.24. ESI-CAD-MS/MS of TMPP⁺-Ac-IFVQK, peptide derivative from tryptic digest of cytochrome-c, in an ion trap mass spectrometer at 55% relative collision energy.

While analyzing the derivatized mixture of tryptic fragments of cytochrome-c by LC-MS, MS/MS was performed on a precursor ion of m/z 1179.0. From the calculated masses of possible tryptic fragments and their derivatives, 1179.0 Da corresponds to TMPP⁺-Ac-GITWK. However, the peaks in the MS/MS spectrum did not match the m/z of any ions that would be produced from fragmenting this derivatized peptide. Upon closer examination, it was possible to deduce the sequence of the derivatized peptide as being MIFAGI, corresponding to residues 80-85; the mass of TMPP⁺-Ac derivative of MIFAGI (where the C-terminus is not an acid) is also 1179 Da. This peptide probably originated from the loss of K from the tryptic fragment MIFAGIK. Thus, this example demonstrates the applicability of correlating the MS/MS spectra of the TMPP⁺-Ac derivatives of peptides to their amino acid sequence, due to a major series of *an ions, as shown in Figure 2.25.

b) Glucagon:

Another protein studied was glucagon, HSQGTFTSDY SKYLDSRRAQ DFVQWLMNT, 29 residues in length, with three cleavage sites. Three tryptic fragments were obtained corresponding to residues 1-12, 13-17, and 18-29. The TMPP⁺-Ac derivatized fragments were prepared, and then separated by HPLC. Figure 2.26 shows the ESI-ISF MS (on the VG-Platform MS) of the TMPP⁺-Ac derivative of YLDSR (residues 13 - 17). Note that there is a series of mostly *a_n ions, corresponding to the first four residues. Cleavage at the aspartic acid residue results in a *d₃ ion rather than an *a₃ ion, along with a *b₃ ion and a *c₂ ion. This result is expected from our earlier observations.

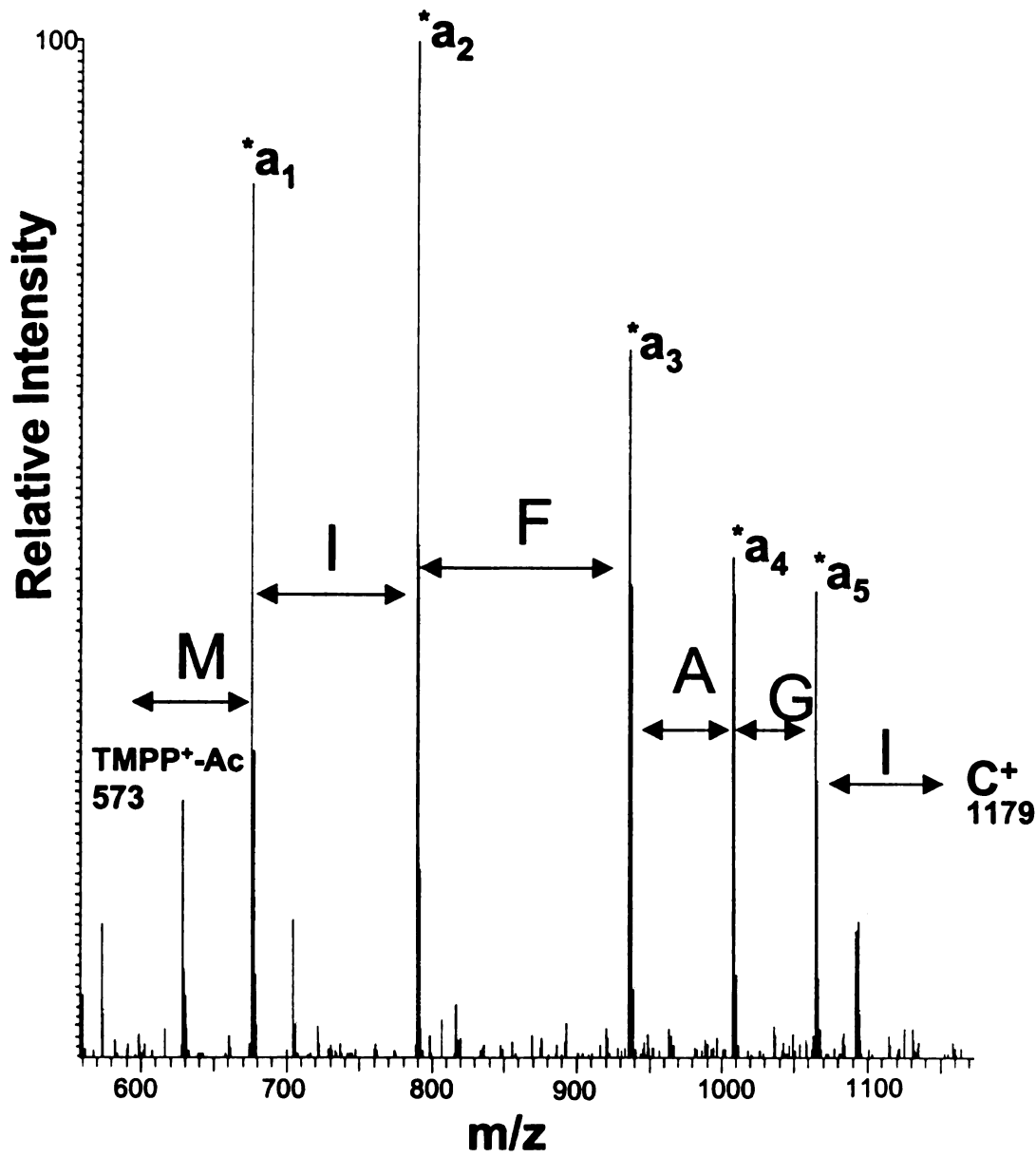


Figure 2.25. ESI-CAD-MS/MS of a peptide derivative from cytochrome-c tryptic digest with a precursor mass of 1179 Da at a relative collision energy of 60%.

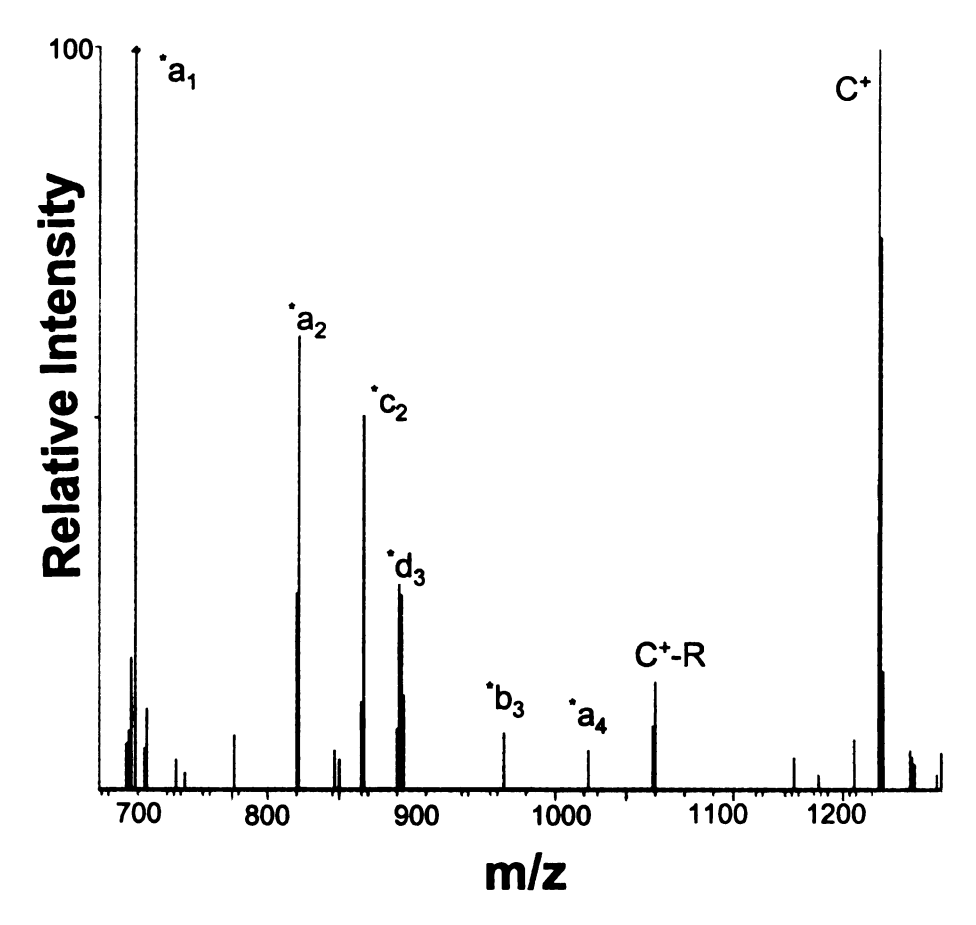


Figure 2.26. ESI-CAD-MS of TMPP⁺-Ac-YLDSR, peptide derivative from the tryptic digest of glucagon, showing the characteristic fragmentation pattern of aspartic acid residue D.

c) Insulin Chain-B:

The oxidized B-chain of insulin (30 residues and 2 cleavage sites) was digested and the resulting fragments derivatized with the TMPP⁺-Ac reagent. The ESI-ISF and MALDI-PSD spectra of one of the derivatized fragments (residues 23-29) are shown in Figure 2.27. Again, a series of *a_n ions is observed for the first five residues in the top panel. Residue 6 is proline, and the signal due to *a₆ is not discernible; this, again, is consistent with our earlier observations. The ESI-ISF spectrum in Figure 2.27 compares well with that of the MALDI-PSD spectrum of the same derivatized peptide, in that *a_n ions are observed in each. The difference is that *a₆, the ion due to cleavage at the proline residue is observable in MALDI-PSD, as is a signal due to fragmentation of the terminal lysine (*a₇). Previous studies have shown that the signal due to cleavage at proline in MALDI-PSD is laser power-dependent [7].

Although analysis of enzymatic digests of proteins by LC-MS/MS is becoming routine, preliminary TMPP⁺-Ac derivatization would help detect the smaller peptide fragments, resulting in better coverage. In addition, the relatively simple fragmentation pattern of the TMPP⁺-Ac-peptides, even under low-energy CAD, would help one to deduce the amino acid sequence without the aid of extensive computation.

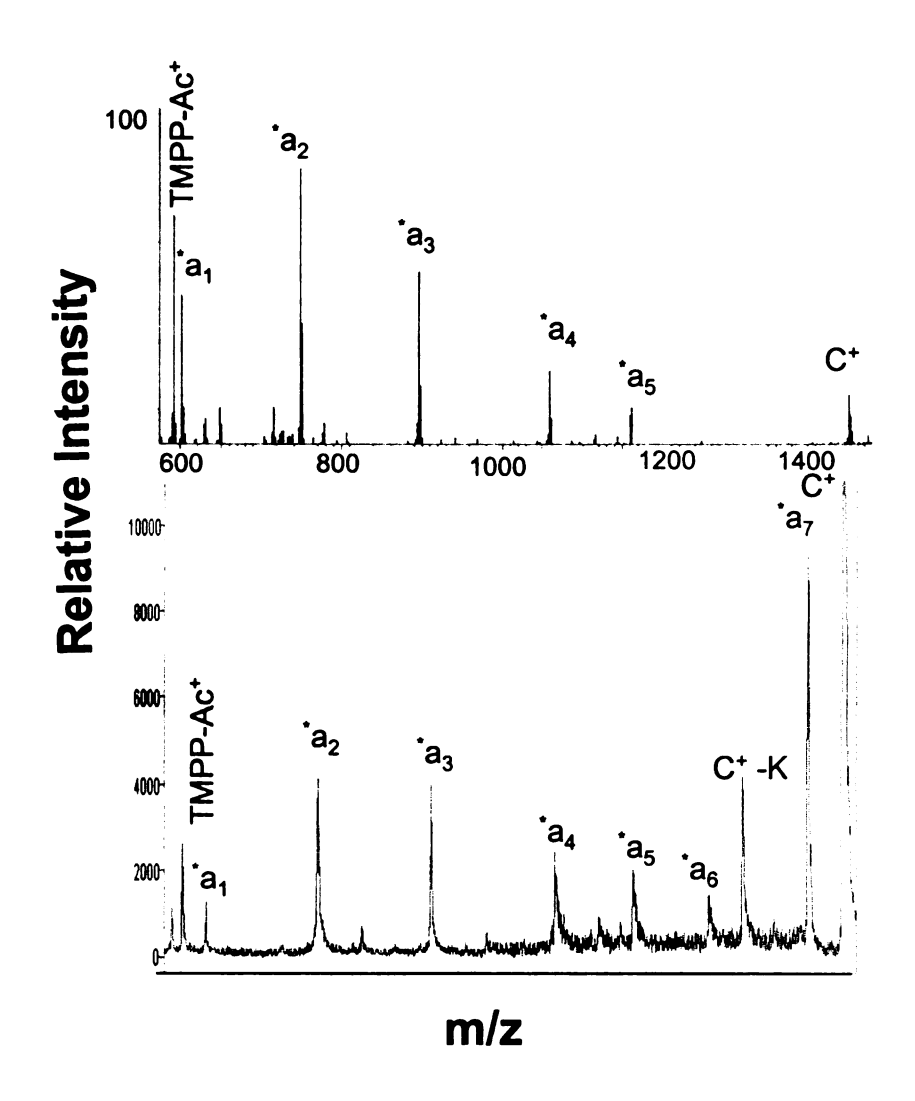


Figure 2.27. A comparison of ESI-ISF mass spectrum (top panel) with MALDI-PSD spectrum (bottom panel) of TMPP⁺-Ac-GFFYTPK, a peptide derivative from the tryptic digest of insulin chain-B.

IV. Conclusions

This ESI-ISF/CAD-MS study of the TMPP⁺-Ac derivatives of peptides shows that a series of *a_n ions is consistently produced. The fact that *a_n ions are observed suggests that the fragmentation is likely via charge-remote pathways. Our results from ESI-CAD-MS/MS are also similar to those observed in FAB-CAD-MS and MALDI-PSD-MS for TMPP⁺-Ac-peptides. Comparison of the results of the ESI-ISF-MS and the MS/MS study of the TMPP⁺-Ac-derivatives shows that precursor-selected CAD-MS/MS is similar to ISF-MS. Fragmentation of these charged derivatives differs in an ion trap depending on whether a singly- or doubly-charged precursor is selected; charge-mediated processes also seem to be present in the latter case.

The results from analyses of derivatized protein digests indicate that the behavior of individual TMPP⁺-Ac derivatives is maintained even in the case of complicated mixtures such as those derivatized from protein digests. Sequence information is readily obtainable based on the predominance of a simple series of $*a_n$ ions.

V. References

- 1. Yates, J. R. J. Mass Spectrom. 1998, 33, 1.
- 2. Carr, S.A.; Hemling, M.E.; Bean, M.F.; Roberts, G.D. Anal. Chem. 1991, 63, 2802.
- 3. Biemann, K. Biomed. Environ. Mass Spectrom. 1988, 16, 99.
- 4. Biemann, K. Methods in Enzymology, Ed. J.McCloskey, 1990, 193, 886.
- 5. Roth, K.D.W.; Huang, Z.-H.; Sadagopan, N.; Watson, J.T. Mass Spectrom. Rev. 1998, 17, 255.
- 6. Huang, Z.-H.; Wu, J.; Roth, K. D. W.; Yang, Y.; Gage, D. A.; Watson, J. T. Anal. Chem. 1997, 69, 137.
- 7. Liao, P.-C.; Huang, Z.-H.; Allison, J. J. Am. Soc. Mass Spectrom. 1997, 8, 501.
- 8. Lin, T.; Glish, G.L. Proceedings of the 45th ASMS Conference on Mass Spectrometry and Allied Topics, Palm Springs, California, June 1-5, 1997.
- 9. Huang, Z.-H.; Shen, T.S.; Wu, J.; Gage, D. A.; Watson, J. T. Analytical Biochemistry, 1999, 268, 305.
- 10. Kidwell, D. A.; Ross, M. M.; Colton, R. J. J. Am. Chem. Soc. 1984a, 106, 2219.
- 11. Renner, D.; Spiteller, G. Angew. Chem. Int. Ed. Engl. 1985, 24, 408.
- 12. Vath, J. E.; Zollinger, M.; Biemann, K. Fresenius Z. Anal. Chem. 1988, 331, 248.
- 13. Johnson, R. S.; Martin, S. A.; Biemann, K. Int. J. Mass Spectrom. Ion Processes. 1988, 86, 137.
- 14. Wetzel, R.; Halualani, R.; Stults, J.T.; Quan, C. Bioconjugate Chem. 1990, 1, 114.
- 15. Vath, J. E.; Biemann, K. Int. J. Mass Spectrom. Ion Processes. 1990, 100, 287.
- 16. Wagner, D. S.; Salari, A.; Gage, D. A.; Leykam, J.; Fetter, J.; Hollingsworth, R.; Watson, J. T. Biol. Mass Spectrom. 1991, 20, 419.
- 17. Burlet,O.; Orkiszewski, R.S.; Ballard, K.D.; Gaskell,S.J. Rapid Commun. Mass Spectrom. 1992, 6, 658.
- 18. Stults, J. T.; Lai, J.; McCune, S.; Wetzel, R. Anal. Chem. 1993, 65, 1703.

- 19. Jeffery, W.A.; Bartlett-Jones, M.; Pappin, J.C. Proceedings of the 43rd ASMS Conference on Mass Spectrometry and Allied Topics, Atlanta, Georgia, May 21-26, 1995.
- 20. Spengler, B.; Luetzenkirchen, F.; Metzger, S.; Chaurand, P.; Kaufmann, R.; Jeffery, W.; Bartlet-Jones, M.; Pappin, D. J. C. *Int. J. Mass Spectrom. Ion Processes.* 1997, 169/170, 127.
- 21. Hines, W.; Peltier, J.; Hsieh, F.; Martin, S.A. Proceedings of the 43rd ASMS Conference on Mass Spectrometry and Allied Topics, Atlanta, Georgia, May 21-26, 1995.
- 22. Naven, T. J. P.; Jeffery, W. A.; Bartlet-Jones, M.; Rahman, D.; Pappin, D. J. C. *Proceedings of the 45th ASMS Conference on Mass Spectrometry and Allied Topics*, Palm Springs, California, June 1-5, 1997.
- 23. Liao, P.-C.; Allison, J. J. Mass Spectrom. 1995, 30, 511.
- 24. Stults, J. T. Proceedings of the 40th ASMS Conference on Mass Spectrometry and Allied Topics, Washington, DC, May 31-June 5, 1992.
- 25. Cárdenas, M. S.; van der Heeft, E.; de Jong, A. P. J. M. Rapid Commun. Mass Spectrom. 1997, 11, 1271.
- 26. Griffiths, W.J.; Lindh, I.; Bergman, T.; Sjovall, J. Rapid Commun. Mass Spectrom. 1995, 9, 667.
- 27. Lindh, I.; Griffiths, W.J.; Bergman, T.; Sjovall, J. Int. J. Mass Spectrom. Ion Processes, 1997, 164, 71.
- 28. Lindh, I.; Sjovall, J.; Bergman, T.; Griffiths, W.J. J. Mass Spectrom. 1998, 33, 988.
- 29. Downward, K.M.; Biemann, K. J. Am. Soc. Mass. Spec. 1994, 5, 966.
- 30. Dongre, A.R.; Jones, J.L.; Somoygi, A.; Wysocki, V.H. J. Am. Chem. Soc. 1996, 118, 8365.
- 31. Van Dongen, W.D.; van Wijk, J.I.T.; Green, B.N.; Heerma, W.; Haverkamp, J. Rapid Commun. Mass Spectrom. 1999, 13, 1712.
- 32. Hayes, R.N.; Gross, M.L. Methods in Enzymology, J. McCloskey, Ed. 1990, 193, 886.
- 33. Watson, J.T.; Wagner, D.S.; Chang, Y.S.; Strahler, J.R.; Hanash, S.M.; Gage, D.A. Int. J. Mass Spectrom. Ion Processes, 1991, 111, 191.
- 34. Tang, X.-J.; Thibault, P.; Boyd, R.K. Anal. Chem, 1993, 65, 2824.

- 35. Wagner, D. S. Ph.D. Dissertation, Michigan State University, East Lansing, MI (1992).
- 36. Roth, K.D.W. Ph.D. Dissertation, Michigan State University, East Lansing, MI (1999).
- 37. Papayannopoulos, I. A. Mass Spectrom. Rev. 1995, 14, 49.

Chapter 3

EFFECT OF CHARGE-DERIVATIZATION IN THE DETERMINATION OF PHOSPHORYLATION SITES IN PEPTIDES BY ESI-CAD-MS/MS

I. Introduction

Phosphorylation is a post-translational modification of proteins important for signal transduction and enzyme activity. Proteins are phosphorylated in the post-transcriptional stage by enzymes known as kinases using adenosine-tri-phosphate (ATP). Of the twenty essential amino acids, only the amino acids tyrosine, serine and threonine can be phosphorylated; these contain hydroxyl groups in their side chain. The structures of these three amino acid residues are given in Figure 3.1.

Figure 3.1. Structures of amino Acid residues serine (S), threonine (T), and tyrosine (Y) respectively.

Enzymes called phosphatases are usually involved in dephosphorylation of a protein. Many proteins have multiple phosphorylation sites, which are phosphorylated by different kinases. A cascade of processes eventually results in an active protein. For example, receptor tyrosine kinases phosphorylate specific tyrosine residues on intracellular signaling proteins (receptors). On the other hand, receptor tyrosine phosphatases remove phosphate groups from tyrosine residues of specific intracellular signaling proteins. Signaling through tyrosine kinase domains of such receptor proteins is involved in a variety of diverse biological processes such as cell growth, transcription and apoptosis. The cytosolic region of the receptors has a tyrosine kinase domain of 250-300 amino acid residues, which bind to different proteins when phosphorylated [1]. Thus, in order to understand the activity of proteins, in many cases it becomes vital to locate the sites of phosphorylation.

The conventional technique used for amino acid sequencing, Edman sequencing, uses harsh chemical conditions under which the phophoester bonds in serine and threonine are unstable [2,3]. The phosphoester bond is usually hydrolyzed or the moiety is eliminated as inorganic phosphate. However, phosphotyrosine can be converted to the phenylthiohydantoin derivative without degradation, and can be analyzed by HPLC. But very low recovery continues to be a problem. The other techniques for determining sites of phosphorylation include, radiolabeling with the ³²P isotope [4]. The cells are incubated with inorganic radiolabeled phosphate until a steady state is achieved in cells, at which point the radiolabel is incorporated into the proteins. Further enzymatic digestions of the protein and HPLC fractionation followed by Cherenkov counting of the radioactivity in the HPLC fractions help identify the site of phosphorylation. However,

the validity of the assumption of achieving a true steady state has never been tested, and this poses a problem in estimating the stoichiometry of phosphorylation at a particular site.

Mass spectrometry has been used as a tool for determination of the site of phosphorylation since fast atom bombardment (FAB) or liquid secondary ionization (LSI) was adopted as a desorption/ionization (D/I) technique. Theoretically. phosphorylation of a single site on a peptide increases the mass by 80 Da. This increase in mass can be used as a method of determining if a particular peptide is phosphorylated. Also, if a peptide is originally phosphorylated it can be dephosphorylated using alkaline phosphatase and a consequent decrease in mass by 80 Da will indicate the presence of a single site of phosphorylation. If a protein contains phosphate and if the sequence of the protein is known a priori, the mass mapping approach is used. The protein is proteolytically digested and the smaller pieces are analyzed. Thus, if there is a mass increase of 80 Da for a peptide containing a phosphorylatable site, then it is concluded that the peptide sequence derived from the given protein is phosphorylated. However, if there is more than one possible site for phosphorylation, direct sequencing of the peptide by collisionally activated dissociation (CAD) alone can exactly locate the site, provided the phosphate remains bound and intact. During CAD, loss of H₃PO₄ from the precursor results in a peak that is 98 Da lower than the precursor and loss of HPO₃ results in a peak 80 Da lower than the precursor. Loss of 80 Da is common when the phosphotyrosine is present, and loss of 98 Da is commom for phosphoserine and phosphothreonine. Biemann and Scoble have reported the determination of phosphorylation at the Nterminal serine residue of troponin T, a regulatory muscle protein by FAB-CAD-MS [5].

The presence of an ion 98 Da less than the precursor ion, in the positive ion mode, for one of the peptides from the protein, due to the loss of H₃PO₄, helped determine phosphorylation. The sequence of the peptide contained only one such phosphorylatable residue (S) at the N-terminus. In the case of FAB, a peptide containing a phosphate moiety, and thus charged, would have a reduced surface activity [6]. Surface activity of a peptide is important for its desorption and ionization in FAB. However this is not a serious problem. For example, proteins such as glycogen synthase have been studied by continuous-flow LSIMS and sequenced by CAD-MS [7]. There are several other examples where FAB-CAD-MS has been used for determination of phosphorylation sites such as in riboflavin binding protein, spinach chloroplasts, and MAP kinase [8,9,10].

MALDI-MS has also been used in such determination of sites of phosphorylation in proteins from biological sources using picomolar quantities by mass mapping approaches [11-14]. Wang et al. used ³²P labeling of Jurkat leukemic T-cells. The phosphoprotein OP18 isolated by preparative 2D electrophoresis was eluted from the nitrocellulose membrane. Its tryptic digest after HPLC fractionation was analyzed by MALDI-MS. Although there were three isomass peptides present in the mixture analysis that would correspond to the phosphopeptide, use of phosphatase decreased the mass of one of the peptides (15-27) by 80 Da, proving that it was phosphorylated. Further enzymatic digestions with chymotrypsin and endoproteinase Glu-C helped exactly determine the site of phosphorylation, serine-25. Annan and Carr (1996) have shown the use of MALDI-PSD-TOF in the determination of sequence as well as phosphorylation information using α- casein and calmodulin as examples [15]. Qin and Chait have also shown the use of MALDI combined with an ion trap as an analytical tool for

determination of posttranslational modifications including phosphorylation in model proteins [16]. Following these, the MALDI-trap instrument has been used to obtain phosphorylation information on biological samples such as myosin kinase and Sendai virus protein [17,18]. MALDI-MS has been used in combination with ESI-MS in certain cases as a complementary tool [19,20]. *Burlingame* and coworkers have presented a study using IR-MALDI on α-casein [21]. They find that the elimination of labile phosphate groups is minimized in IR-MALDI as opposed to using a UV laser, and thus the signal is improved. Recently, a matrix additive, diammonium citrate, has been shown to enhance the detectability of phosphate containing peptides in the positive ionization mode in MALDI-MS [22].

Electrospray ionization (ESI) mass spectrometry has served as an important tool in the identification of phosphorylation sites in many proteins as well. Several studies using this technique are reported because it can be interfaced with separation techniques. Enzymatic-digestion/peptide mass mapping has been routinely used for this purpose [23,24], and MS/MS with CAD has been employed to obtain unambiguous results [25-30]. In order to improve the sensitivity of the technique, neutral loss monitoring with orifice-potential stepping in a triple quadrupole was developed by *Carr* and coworkers in 1993 [31]. The loss of HPO₃ or H₃PO₄ moieties from phosphopeptides, due to increasing cone voltage, is monitored by scanning the first stage of the triple quadrupole mass spectrometer. This helps selectively identify the phosphopeptides. This procedure has been used by *Hunter et al.* (1994) in studying α-casein [32]. Similarly, orifice potential stepping and detection of negative ions was simultaneously developed by *Kassel* and coworkers for phosphopeptide monitoring [33]. *Knapp* and coworkers studied the effect

of various charge states on peptides during MS/MS in a triple quadrupole instrument [34]. Carr and coworkers also developed a reaction monitoring method, in which the peptide was collisionally activated in the second stage of a triple quadrupole mass spectrometer and the m/z difference between the first and third stage was used for monitoring the neutral loss originating from a phosphopeptide [35]. This enabled obtaining information selectively on phosphopeptides. Lehmann and coworkers have systematically studied the fragmentation mechanisms of various phosphopeptides and their analogues [36]. Almost all of the studies mentioned above are based on the use of triple quadrupole instruments. However, recently there is a growing interest in investigating phosphopeptides by ion trap mass spectrometers equipped with an ESI source [37]. Degnore and Qin have reported detailed study on the behavior of phosphopeptides in an ion trap mass spectrometer and the effects of charge state of a phosphopeptide on its fragmentation during CAD [38]. Although the loss of H₃PO₄ or HPO₃ has been used as a signature to determine the presence of phosphorylation in most studies, they show that phosphorylation on S, T, or Y cannot generally be distinguished based solely on the observed loss of H₃PO₄ in an ion trap mass spectrometer. In addition. they have shown that this loss is charge-state dependent, and is not observed when higher charge-states of the same peptide are subjected to MS/MS in most cases.

CAD-MS/MS of a peptide often yields a variety of fragment ions retaining either the N- or C-terminus, which can make spectral interpretation tedious and sometimes uncertain. Another complication relates to dephosphorylated fragment ions obtained during CAD-MS/MS of a phosphorylated peptide [8]. Thus the ion current is distributed over multiple channels of information and hence the sensitivity is diminished. In some

cases, peptides do not fragment completely during CAD; charge-derivatization of peptides often produces better fragmentation yielding a series of ions and simpler spectra during CAD-MS/MS. In the case of underivatized peptides and those lacking basic side chains where charge fixation is not possible, fragmentation is explained by the "mobile-proton model" [39]. Here, the amide bonds are protonated preferentially and localization of charge at one particular site is minimal. A recent approach to minimizing charge-localization involves addition of a sulfonic acid group to the N-terminus [40]; this is an alternative to the fixed charge-derivatization approach. Conversion of the N-terminus to a sulfonic acid derivative has been used in the determination of phosphorylation in a model peptide by MALDI-PSD. However, in the case of charge-derivatized peptides, the charge is fixed on either terminus and charge-remote fragmentation pathways enable the production of a series of either only N-terminal or only C-terminal fragment ions, thereby simplifying the spectrum. There are very few studies describing the impact of charge-derivatization on the CAD-MS/MS of phosphopeptides [41].

The advantage of tris-[(2,4,6-trimethoxyphenyl)phosphonium]-acetyl (TMPP⁺-Ac) charge-derivatization of peptides prior to analysis by FAB-CAD-MS and MALDI-PSD has been demonstrated [42-44]. The previous chapter describes a detailed ESI-CAD-MS/MS study of TMPP⁺-Ac-peptides and their behavior in various mass spectrometers [45]. This chapter focuses on the utility of TMPP⁺-Ac derivatization, for preparation of an N-terminal charge-derivative, in facilitating the determination of the site(s) of phosphorylation in a peptide by CAD-MS/MS (using an ion trap).

II.Experimental

Phosphopeptides are purchased from the University of Michigan Peptide Synthesis Facility, Ann Arbor, MI. The following is a list of phosphopeptides used in this study:

Table 3.1. List of Phosphopeptides Used in the Study:

Peptide	Mass of Peptide	Mass of TMPP ⁺ -Ac
		Derivative
KRtIRR	908.5	1481.5
LKRAyLG-amide	899.5	1471.7
LKRAsLG-amide	823.5	1396.6
LKRAtLG-amide	837.4	1409.5
KRPsQRHGSKY-amide	1423.5	1996.2
KIGEGtyGVVYK	1474.5	2047.3

TMPP⁺-Ac derivatization of the peptides was performed by adding a 5-fold molar excess of the derivatizing reagent to the peptide (1 nmol) in the presence of a 10-fold excess of the base (dimethylaminopyridine) at room temperature. The reaction was allowed to proceed for 15 min. The reaction mixture was separated by HPLC, and the fraction corresponding to the TMPP⁺-Ac-peptide (diluted to 10 pmol/µL) was infused into the mass spectrometer at a rate of 3 µL/min.

In order to obtain the phosphopeptide containing multiple phosphorylation sites from a biological sample, tryptic digestion was attempted on the milk protein β-casein. The protein (100 μg) (purchased from Fluka) was digested with trypsin (5% w/w) in 0.05 M tris hydrochloride (pH 8.6) for 4 h at 35°C. The resultant digestion mixture was analyzed by MALDI-MS. An aliquot of the digest mixture was reacted with a 10-fold molar excess of the TMPP⁺-Ac reagent with the resultant number of moles of peptide from the digest. The mixture was allowed to react for 30 min at room temperature. The products were then separated by reverse-phase HPLC. An Immobilized metal affinity column (IMAC), made from FeCl₃ in sodium acetate, was used to enhance recovery of the phosphopeptide from the digestion mixture prior to HPLC [46].

Mass spectrometry was performed in a Finnigan-LCQ instrument; CAD was performed using MS/MS in the trap with helium as the collision gas. The spectra were collected at 3 µscans/sec. Similarly, CAD-MS/MS of underivatized phosphopeptides was also performed in the trap. The collision energy for the phosphopeptides was about 30% (of a total scale of 5V) while it was 60% for the derivatized phosphopeptides.

In-source fragmentation of the phosphopeptides was performed by elevating the capillary voltage to 90 V from a regular value of 25 V. This causes an increase in the kinetic energy of the ionic species travelling between the capillary and the counter-electrode. Consecutive collisions with the gas and other species in that region result in fragmentation of the ions.

III. RESULTS

A) Fragmentation of Phosphorylated Tyrosine Residue Containing Peptide Derivatives by CAD-MS/MS:

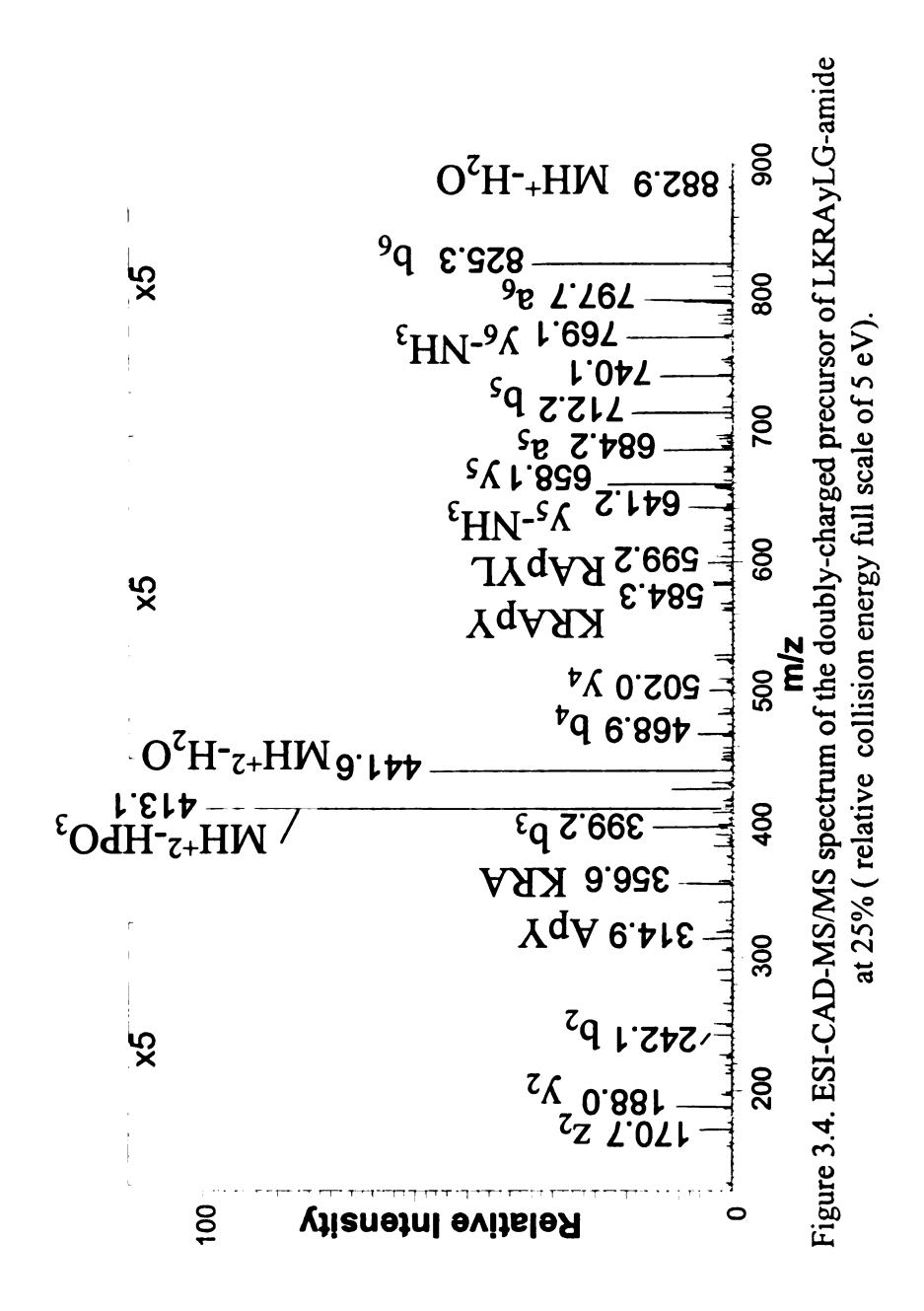
Of the three phosphorylated residues, phosphorylated tyrosine (Y) is distinguished from phosphorylated serine (S) and threonine (T) by a signature loss of just 80 Da as opposed to the loss of 98 Da from the latter residues during CAD-MS/MS. The recent article on the study of mechanisms of fragmentation of phosphopeptide, as studied in a triple quadrupole mass spectrometer, suggests a reasonable mechanism explaining this observation as shown in Figure 3.2 [36].

Figure 3.2. Loss of phosphoric acid via a six-membered transition state in peptides containing phosphorylated serine, and threonine residues.

The presence of a bulkier aromatic group in tyrosine prevents the formation of a six-centered transition state required for the loss of H₃PO₄ (98 Da). The mechanism as proposed by Lehmann and coworkers is shown in Figure 3.2. The authors suggest that the C-O bond in tyrosine phosphate is stronger than the corresponding C-O bond in serine phosphate due to the direct neighborhood of the aromatic ring. This also results in a weaker O-P bond in the phosphotyrosine. Formation of H₃PO₄ requires cleavage of the C-O bond whereas formation of HPO₃ requires fission of the P-O bond. Thus tyrosine phosphate preferentially eliminates HPO₃. Although this is a reasonable mechanism, loss of H₃PO₄ from tyrosine phosphate residue is possible since the hydrogen from the phenyl ring could be involved via a six-membered transition state as shown in Figure 3.3a. However, the ΔH for this reaction is probably higher than elimination of H₃PO₄ from an alipahtic system. This can be assumed to be similar to a dehydration reaction. A simple comparison between dehydration in an aliphatic and aromatic alcohol is shown in Figure 3.3b. The ΔH for the formation of benzyne is 80.2 kcal/mol, whereas it is only 10.8 kcal/mol for ethene [47]. Therefore, benzyne is formed less preferentially over ethene. A similar extension can be made for the elimination of phosphoric acid. Thus, the loss of HPO₃ rather than H₃PO₄ is preferred in the tyrosine phosphate containing peptides.

Similar observations have been made during studies in an ion trap as well [38,48]. The same results are als true for TMPP⁺-Ac-derivatized peptides. Figure 3.4 shows the ESI-CAD-MS/MS spectrum of doubly-charged precursor of LKRAyG-amide (m/z 450) (the phosphorylated residues are denoted as y, s and t while the non-phosphorylated residues are denoted as Y,S and T).

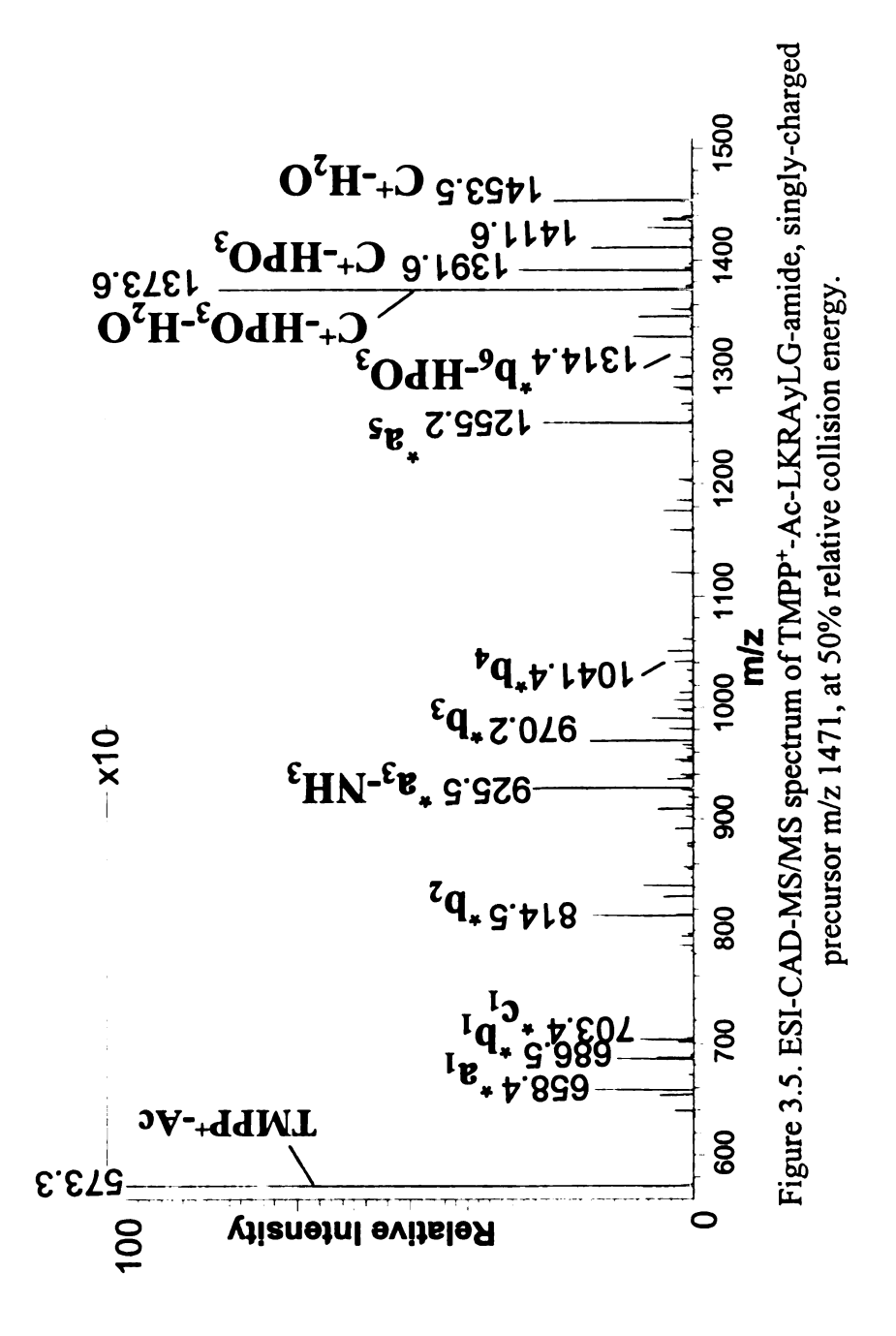
Figure 3.3. a) Possible elimination of H₃PO₄ from tyrosine phosphate. b) Dehydration of an aromatic alcohol vs. an aliphatic alcohol.



The precursor loses 80 Da, which corresponds to loss of HPO₃ (peak at m/z 413). Fragmentation of the singly-charged precursor of the same peptide, show peaks corresponding to loss of both 80 Da and 98 Da. Figure 3.5 shows the ESI-CAD-MS/MS of the TMPP⁺-Ac derivatized version of the same peptide (C⁺ peak at m/z 1471). There is a peak corresponding to the loss of PO₃ at m/z 1391. There is also a peak corresponding to loss of 98 Da (m/z 1373), which can be assigned as loss of water along with loss of HPO₃. This is similar to what is observed for the single-charged precursor of the underivatized peptide. These observations are consistent to those observed by *Qin and DeGnore*, that the charge state of a phosphopeptide dictates its fragmentation pattern.

In charge-derivatized peptides more information is obtained from backbone. However, elimination of the phosphate moiety seems to be preferred whether the peptide is derivatized or not. Minimization of the loss of the phosphate group in the charged derivative might be due to a salt-bridge type of interaction between the positively-charged moiety and the phosphate group to some extent. A similar hypothesis is proposed for larger peptides that get multiply protonated and undergo more backbone cleavages than phosphate loss [38]. It is suggested in these cases that probably the charged amino acid residue (a basic residue) interacts with the phosphate group.

Figure 3.5, the CAD-MS/MS spectrum for TMPP⁺-Ac-LKRAyLG-amide, shows peaks corresponding to N-terminal ions corresponding to cleavage at residues 1-5. The peak at m/z 1314 corresponds to loss of HPO₃ from the *b₆ fragment. Thus the spectrum gives evidence for the presence of a tyrosine residue, due to the occurence of -80 Da peaks both from the precursor and the fragment ions. Also a series of peaks is evident which aids in better spectral interpretation.

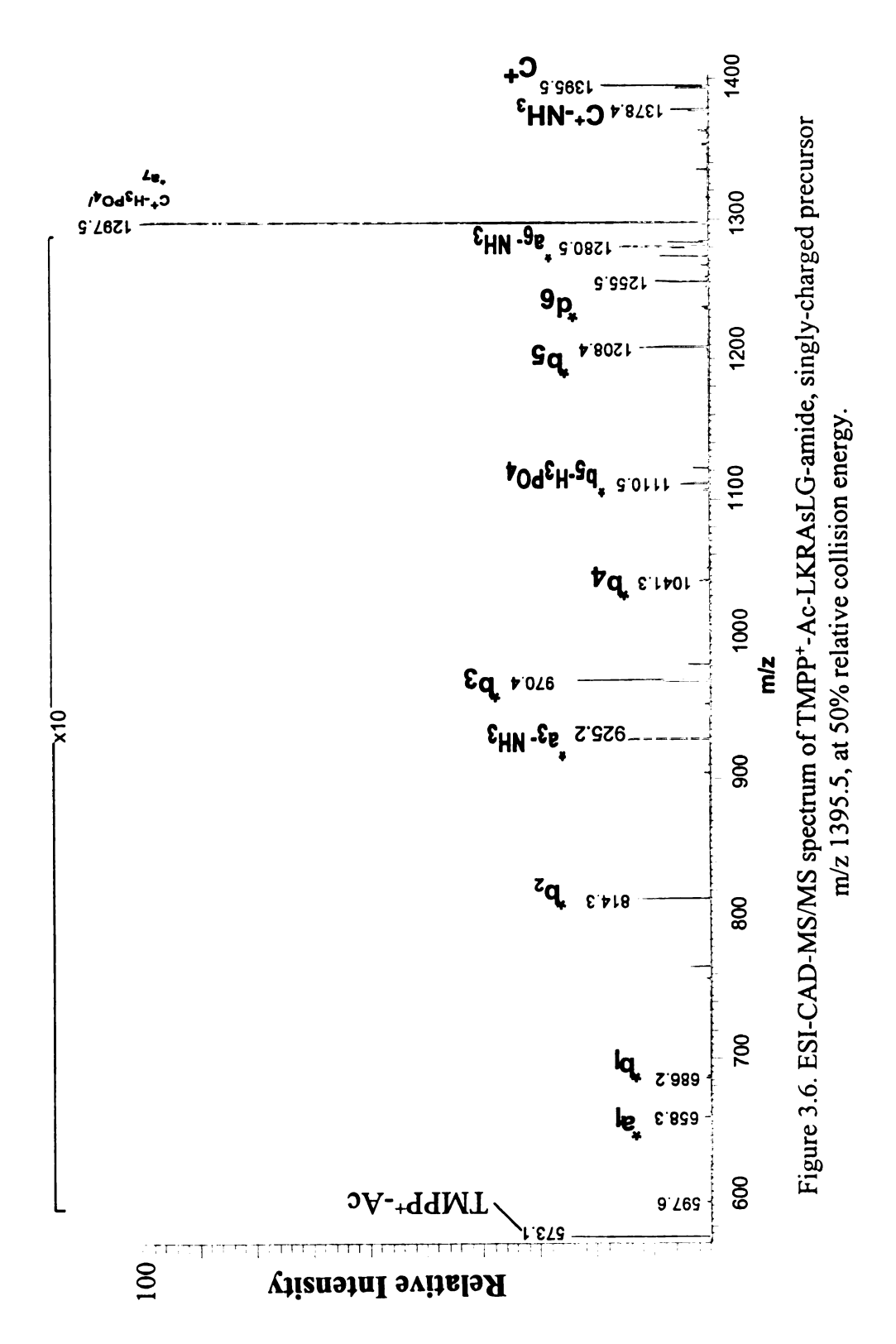


The spectrum is shown for CAD-MS/MS at a relative collision energy of 50%. Higher collision energies up to 70% result in the same pattern of fragmentation, but the S/N is poor.

B) Fragmentation of Phosphorylated Serine Residue Containing Peptide Derivative by CAD-MS/MS:

Derivatized peptides containing phosphorylated serine expel H₃PO₄ from the intact cation (C⁺), resulting in a dehydroalanine residue in place of the phosphorylated residue, when analyzed by CAD-MS/MS. This can be seen in Figure 3.6, the CAD-MS/MS mass spectrum for TMPP⁺-Ac-LKRAsLG-amide, as represented by the peak labeled as C⁺-98 in the mass spectrum. In the case of phosphotyrosine containing peptide, there is loss of HPO₃, followed by loss of water from C⁺.

CAD-MS/MS of the derivatized phosphopeptides in the trap yield N-terminal fragment ions such as 'b_n from which the sequence of the peptide could be deduced; these included fragment ions providing information on the site of phosphorylation. Predominantly 'b_n ions are formed with occasional 'a_n ions, as seen in Figure 3.6. This is also seen in Figure 3.5, the CAD-MS/MS spectrum of TMPP⁺-Ac-LKRAyLG-amide. However, CAD-MS/MS of derivatives of peptides without phosphorylation yield abundant 'a_n ions along with 'b_n ions. These observations imply that the presence of phosphorylation in the peptide seems to favor the formation of 'b_n ions. It may be that the structure of the 'b_n ions with a phosphate group is more stable, or the conformation of the derivatized peptides with phosphogroups in the gas-phase has a greater feasibility for the formation of the 'b_n ions. The mass difference between 'b₄ and 'b₅ is 167 Da, which confirms the presence of a phosphorylated serine residue.



The peptide KRPsQRHGSKY-amide, which also contains a phosphorylated serine residue, could not be TMPP+-Ac derivatized. The reaction procedure was attempted multiple times, and neither the HPLC separation nor the MALDI-MS analysis of the mixture showed the formation of the derivative. The presence of more than one residue with bulky side chains in the peptide could be inhibiting the reaction of the N-terminus with the TMPP+-Ac reagent.

C) Fragmentation of Phosphorylated Threonine Residue Containing Peptide Derivative by CAD-MS/MS:

Figure 3.7a shows the ESI-CAD-MS/MS of the peptide LKRAtLG-NH₂ (underivatized). Upon comparison with Figure 3.7b, the ESI-CAD-MS/MS spectrum of TMPP⁺-Ac-LKRAtLG-NH₂ (derivatized), it is apparent that the latter is a simpler spectrum than the mass spectrum of the underivatized peptide (Figure 3.7a). Fragments such as *d₆, *a₆ - NH₃, *b₆, and *c₆ also contain the phosphate group intact. The same information could be obtained from Figure 3.7a, but it is relatively complicated. There are several other peaks between those representing b₄ and b₅ in Figure 3.7a, some of which correspond to C-terminal fragments and their dephosphorylated variants. If the sequence of this model peptide were unknown, it appears that it would be easier to derive the sequence information from the MS/MS spectrum of the derivatized peptide (Figure 3.7b) than from that of the underivatized peptide (Figure 3.7a).

Similar information regarding phosphorylation is obtained for the peptide KPtIRR after TMPP⁺-Ac derivatization. The difference between this peptide and LKRAtLG-amide is the position of the phosphorylated residue. However, the results do not seem to have a large impact due to the position of the phosphate moiety,

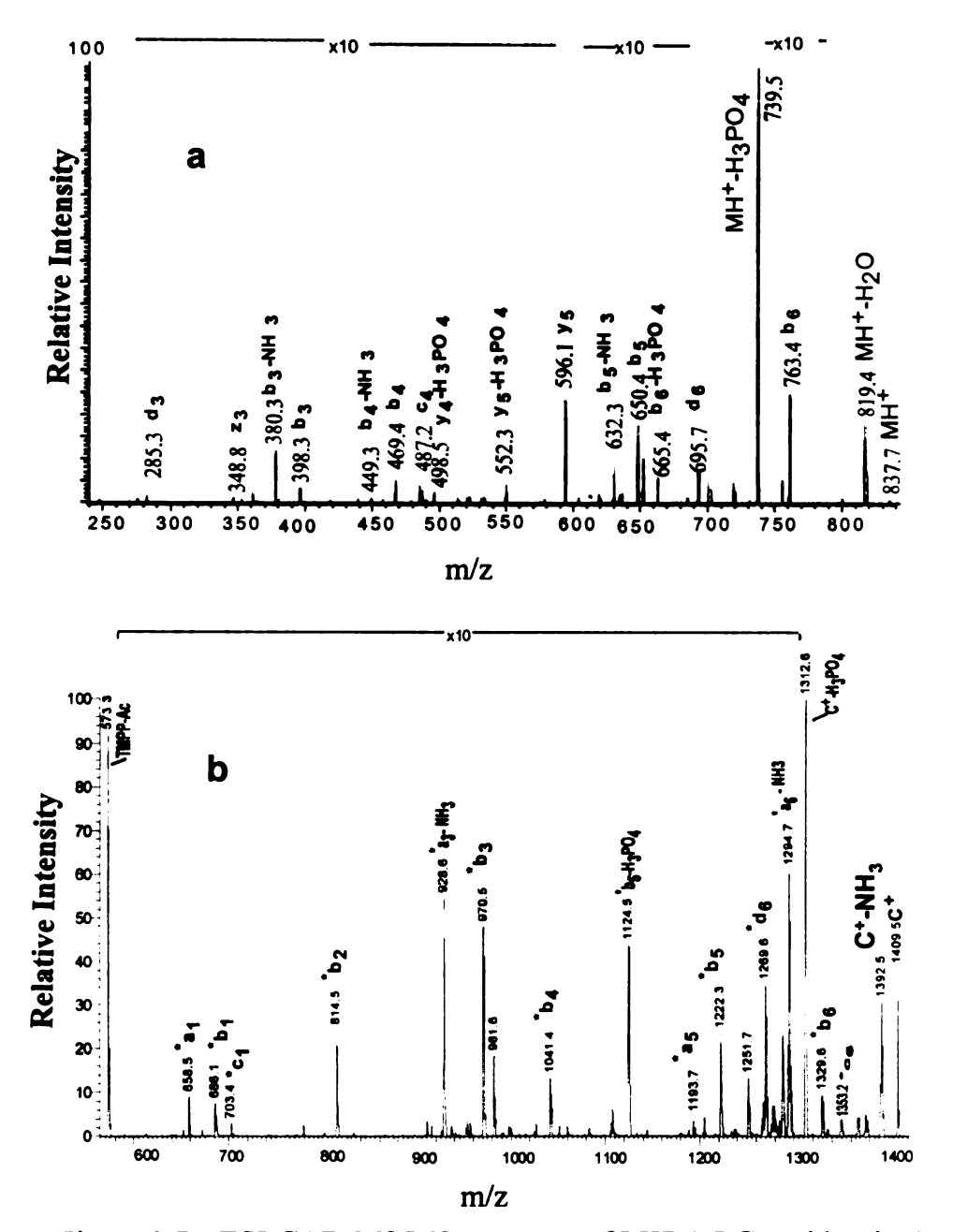


Figure 3.7a. ESI-CAD-MS/MS spectrum of LKRAtLG-amide, singly-charged precursor m/z 837, 30% relative collision energy.

Figure 3.7b. ESI-CAD-MS/MS spectrum of TMPP+-Ac-LKRAtLG- amide, singly-charged precursor m/z 1409.5, 50% relative collision energy.

D) Fragmentation of Doubly Phosphorylated Peptide Derivative Containing Threonine and Tyrosine Residues by CAD-MS/MS:

Figure 3.8 shows the CAD-MS/MS spectrum of TMPP⁺-Ac-KIGEGtyGVVYK. Note that there are two phosphorylated sites in this case. The doubly-charged ion of the above species was fragmented at 35% relative collision energy, which produced a nearly complete series of b_n fragment ions. The fragment ions b₇ through b₁₀ contain both phosphate groups; some of these also appear as doubly-charged ions, as seen in the lower m/z range of the spectrum. There are a few peaks that represent loss of the phosphate moiety from these fragment ions. Some of the fragment ions lose 80 Da, which implies that the loss of the phosphate group is from the tyrosine residue rather than from the A few very weak C-terminal fragments (y_n ions) and their threonine residue. dephosphorylated variants are observed in this spectrum, possibly because the doublycharged precursor is fragmented, which has a mobile proton in addition to the fixedcharge moiety. In this context, it should be mentioned that fragmentation of a doublycharged precursor of a TMPP⁺-Ac-peptide usually results in less abundant C-terminal fragment ions. This has been discussed in Chapter 2 of this dissertation. Thus, it is preferable to use the singly-charged precursor to obtain CAD-MS/MS data. Use of the singly-charged precursor does require higher collision energy, but it does not result in Cterminal ions. In this particular case the mass (2047 Da) of the singly-charged precursor is higher than the mass range of the mass spectrometer and hence the doubly-charged precursor is chosen for CAD-MS/MS.

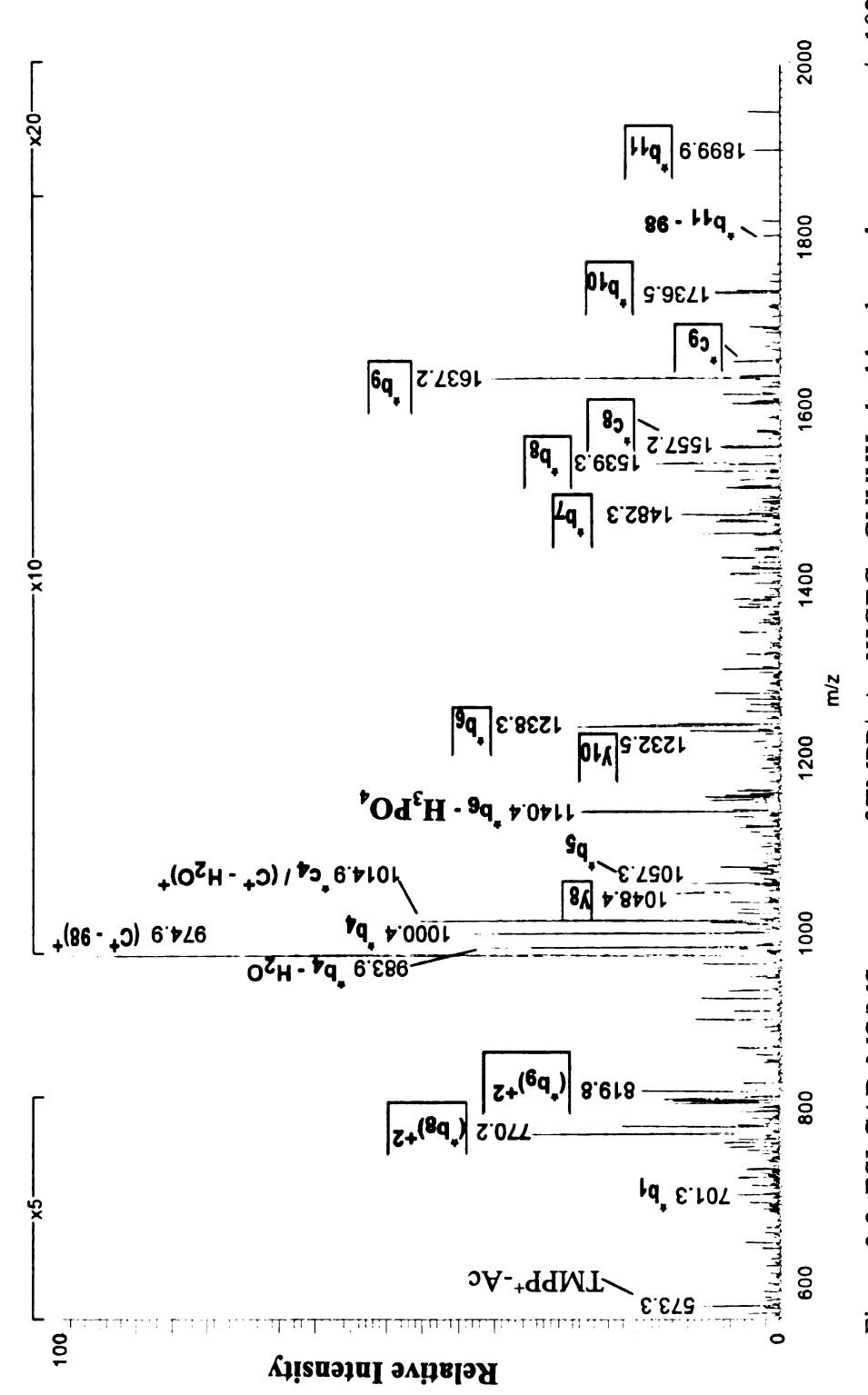
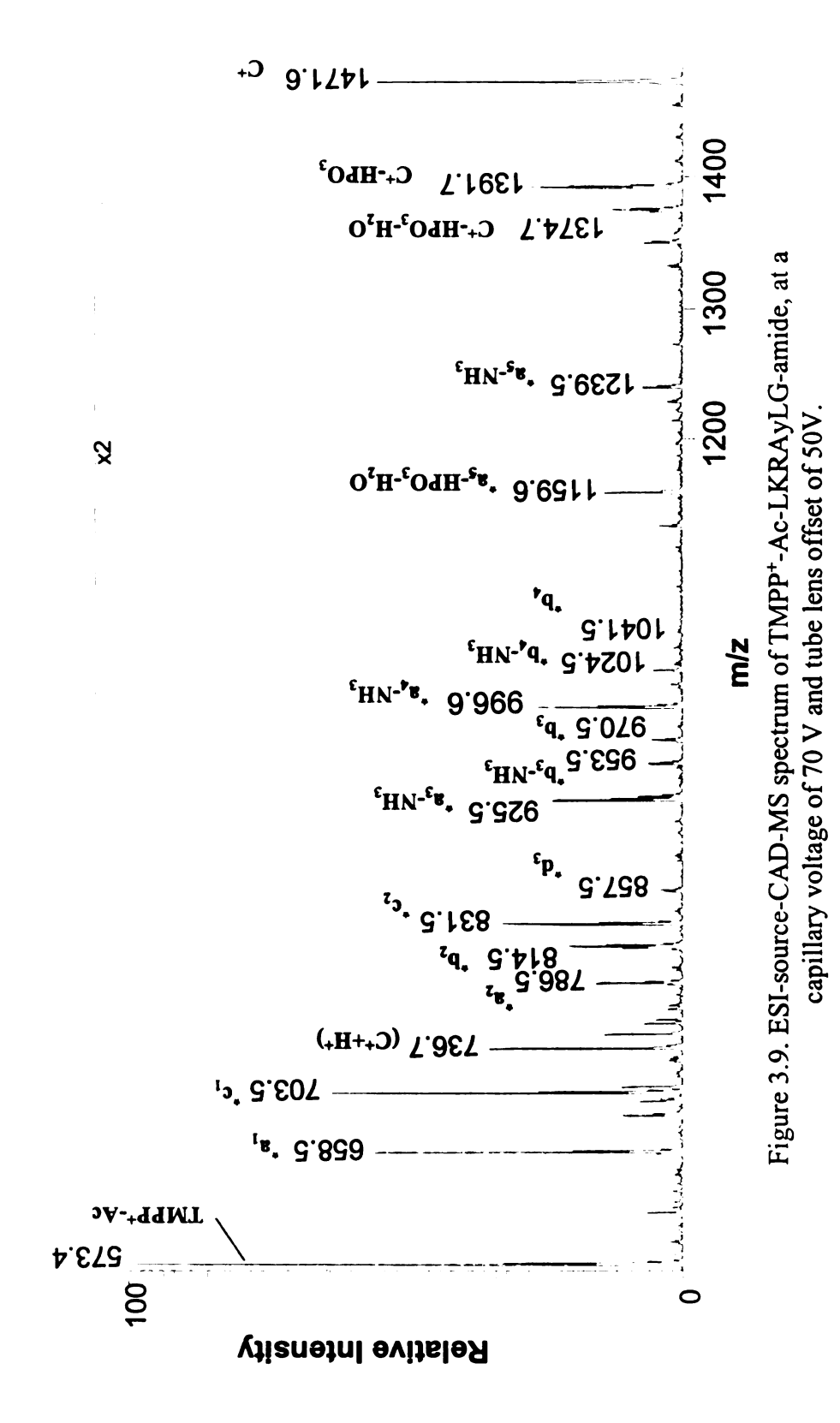


Figure 3.8. ESI-CAD-MS/MS spectrum of TMPP+-Ac-KIGEGtyGVVYK, doubly-charged precursor m/z 1024, 35% relative collision energy. The boxed notations indicate the fragments retaining the phosphate moiety.

E) In-Source-CAD-MS of Phosphopetide Derivatives in an Ion Trap Mass Spectrometer:

In-source-CAD of the phosphopeptide derivatives were performed by elevating the voltages of the capillary and the skimmer in the ion source of the instrument. Figure 3.9 shows the in-source-CAD-MS spectrum for TMPP*-Ac-LKRAyLG-amide. This and in-source-CAD-MS spectra for other peptide derivatives show that the fragment ion abundances are higher than those derived from MS/MS. The graph represented by Figure 3.10 compares the peak intensities due to the fragment ions derived from source-CAD-MS. The intensity of the fragment ion peaks at high m/z is lower than of the fragment ion peaks at low m/z, when produced by source-CAD-MS. Efficiency of fragmentation of the precursor is less during in-source-CAD, since the signal of the intact precursor is still significant (Figure 3.9). There is considerable dephosphorylation of the precursor, but backbone cleavage is equally observed which produces the fragment ions. The fragment ions include *c_n ions that are predominant (Figure 3.10). Typically, the *c_n ion requires higher energy for formation than the *a_n or *b_n ions [49]. The energy imparted during source-CAD is high enough to result in the formation of these ions.

The graph shown in Figure 3.11 compares the abundances of the fragment ions derived from MS/MS. In MS/MS, at least one type of ion (*a_n or *b_n) is abundant at both high and low m/z values. This is helpful in obtaining complete sequence information. The other major feature in the case of MS/MS is that the intensity of the *c_n ions is very low throughout the spectrum. These types of ions are not predominantly observed during MS/MS.



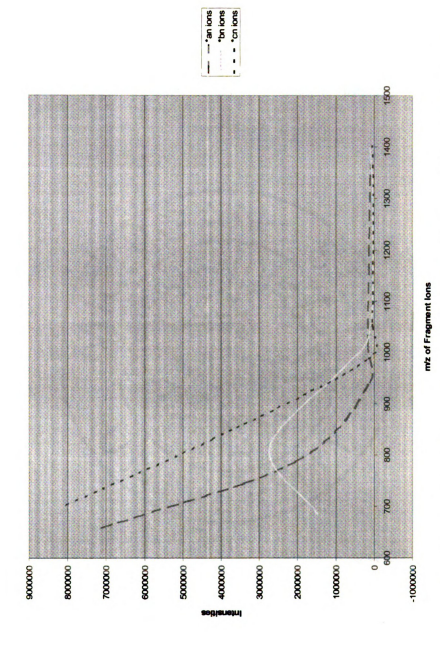


Figure 3.10. Abundance of fragment ions formed from TMPP*-Ac-LKRAyLG-amide by source-CAD-MS.

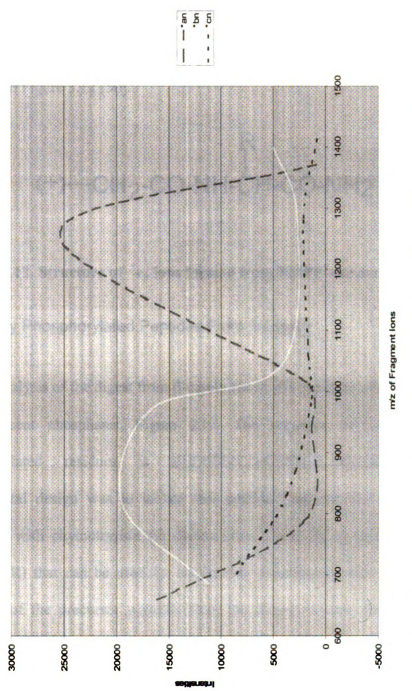


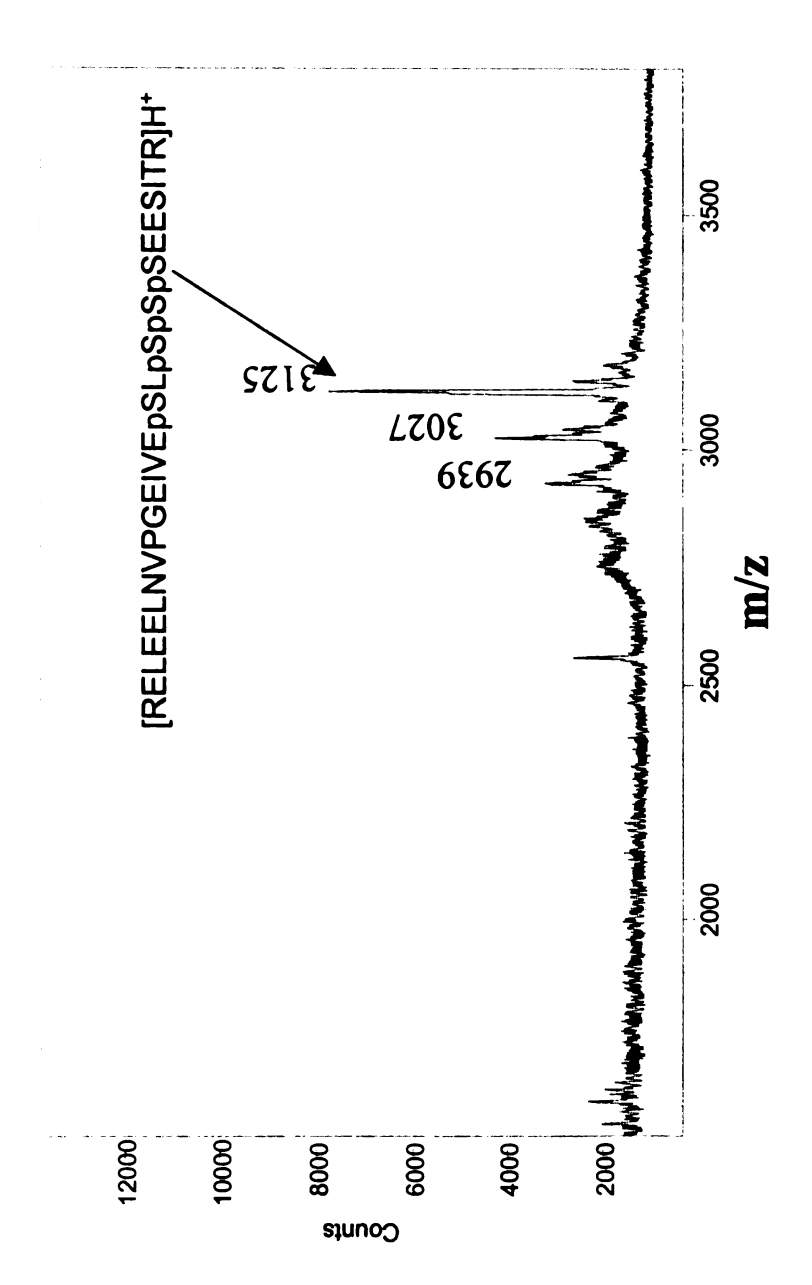
Figure 3.11. Abundance of fragment ions formed from TMPP*-Ac-LKRAyLG-amide by CAD-MS/MS.

These observations once again imply that phosphorylation of the peptide seems to favor the formation of ${}^*\mathbf{c}_n$ ions during in-source-CAD-MS. This may be attributed to the stability of these ions or the conformation of the derivatized phosphopeptides in the gasphase that may aid in their formation preferentially. Additionally, the energetics involved during in-source-CAD is higher than during MS/MS. The proposed structure of a ${}^*\mathbf{c}_n$ ion is shown in Figure 3.12 [50].

Figure 3.12. Structure of *c_n ions formed from TMPP*-Ac derivatives of peptides.

F) Multiply Phosphorylated Peptides From β -casein:

Analysis of the digest from β-casein shows the presence of a phosphopeptide with four adjacent phosphates, Figure 3.13. The sequence of the peptide with four phosphorylated residues is RELEELNVPGEIVESLsssEESITR. The original experimental design was to isolate this peptide fragment and further enzymatically process it with chymotrypsin (to cleave after L and F), to yield a peptide fragment (sssEESITR) that can be used for sequencing experiments. However, due to recovery problems of the precursor peptides from the digest mixture, this could not be done. Attempts to derivatize the mixture with the TMPP⁺-Ac reagent failed. Although there were signals due to TMPP⁺-Ac derivatives of other tryptic peptides of the protein, no signal is observed for the derivatized version of this precursor peptide.



peak at m/z 3125 represents a protonated phosphopeptide with four phosphates. The peaks at Figure 3.13. MALDI-TOF mass spectrum of the tryptic digestion mixture of β-casein. The m/z 3027 and 2939 represent the protonated singly and doubly dephosphorylated forms of the peptide RELEELNVPGEIVESLSSSEESITR respectively.

Arginine (R) is the N-terminal residue of this peptide; the bulky side chain of arginine probably offers steric hindrance to the reactive amino terminus which prevents it from reacting with the incoming TMPP⁺-Ac group. Additionally, several attempts to try to separate the phosphopeptide before derivatization failed. Although, an IMAC column was used as a precolumn to help improve the recovery of the multiply phosphopeptide, the results were not reproducible. Thus, it was not possible to pursue further experiments using the multiply phosphorylated peptide from β-casein.

IV. Conclusions

TMPP⁺-Ac derivatives of phosphopeptides predominantly lose the phosphate moiety during CAD-MS/MS along with other fragments due to weaker backbone cleavage. The fragment ions formed in the examples shown are useful in predicting the sequence as well as the phosphorylation information. Loss of HPO₃ is preferred from the singly-charged precursor for tyrosine phosphorylated peptides, whereas loss of H₃PO₄ is preferred from serine and threonine phosphorylated peptides. This is similar to what has been reported by other researchers for underivatized peptides. However, there are no distinguishing features in terms of the fragment ion formation when any one of the three phosphorylated residues is present. Usually a series of *b_n ions is observed. The *b_n ions seem to be preferentially formed over *a_n ions in the case of phosphorylated peptides. During in-source-CAD-MS of the same peptide derivatives, the fragment ion abundances (at the low m/z range) are higher and more backbone cleavage is observed. However, fragment ions with intact phosphate moieties are not clearly observed. Thus one should use CAD-MS/MS if the sequence is known a priori and the goal is to obtain phosphorylation information. However, if the sequence is unknown, source-CAD-MS can also be used in conjunction with CAD-MS/MS to obtain complementary information on sequence, as the backbone cleavage is higher in the former method. Additionally, *c_n ions are formed in the case of the in-source-CAD-MS of phosphopeptide derivatives. These ions are usually not observed as predominantly in non-phosphorylated peptide derivatives during source-CAD-MS. This suggests that the TMPP⁺-Ac head group of phosphorylated peptide derivatives allows for special conformation of these gas phase precursors, enabling the formation of the *c_n type ions.

These results show promise that the TMPP⁺-Ac derivatives of phosphorylated peptides, when subjected to CAD, provide direct evidence for the site of phosphorylation. The type and abundance of fragment ions appear to depend on the sequence of the peptide. Another encouraging feature of these preliminary data is the presence of a nearly complete series of peaks corresponding to N-terminal fragment ions; such a feature is important to confirm the sequence in cases of isomass peptides and in the analysis of unknowns.

V. References

- 1. L.N. Johnson, M.E.M. Noble, D.J. Owen Cell, 85, 149 (1996).
- 2. D.B.Rylatt, P.Cohen FEBS Lett., 98, 71 (1979).
- 3. C.G.Proud, D.B. Rylatt, S.J.Yeaman, P.Cohen *FEBS Lett.*, **80**, 435 (1977).
- 4. J.C. Garrison Methods in Enzymology, 99, 20 (1991).
- 5. K.Biemann, H.A.Scoble *Science*, **237**, 992 (1987).
- 6. B.W. Gibson, P.Cohen *Methods in Enzymology*, **193**, 488 (1991).
- 7. L.Poulter, S.-G. Ang, B.W.Gibson, D.H.Williams, C.F.B.Holmes, F.B.Caudwell, J.Pitcher, P.Cohen *Eur. J. Biochem.*, **175**, 497 (1988).
- 8. C.Fenselau, D.Heller, M.S.Miller, H.B.White Anal. Biochem., 150, 74 (1994).
- 9. M. Hanspeter, D. F. Hunt, J. Shabanowitz, J.Bennet J.Biol. Chem., 263, 309 (1985).
- 10. A.K.Erickson, D.M. Payne, P.A.Martino, A.Rossomando, J. Shabanowitz, M. Weber, D. F. Hunt, and T. W. Sturgill *J.Biol. Chem.*, **265**, 19728 (1990).
- 11. Y.K.Wang, P.-C.Liao, J. Allison, D.A. Gage, P.C.Andrews, D.M. Lubman, S.M. Hanash, J.R. Strahler *J.Biol. Chem.*, **268**, 14269 (1993).
- 12. P.-C.Liao, J. Leykam, P.C.Andrews, D.A. Gage, J. Allison Anal. Biochem., 219, 9 (1994).
- 13. W.Zhang, A.J. Czernik, T.Yungwirth, R.Abersold, B.T. Chait *Prot. Sci.*, 3, 677 (1994).
- 14. T.-T.Yip, T.W. Hutchens FEBS Lett, 308, 149 (1992).
- 15. R.S. Annan, S.A.Carr Anal. Chem., 68, 3413 (1996).
- 16. J.Qin, B.T.Chait Anal. Chem., 69, 4002 (1997).
- 17. J. Szczepanowska, X. Zhang, C. J. Herring, J. Qin, E. D. Korn, H. Brzeska *Proc. Natl. Acad. Sci. USA*, **94**, 8503 (1997).
- 18. K.R. Jonscher, J.R. Yates J. Biol. Chem., 272, 1735 (1997).
- 19. R. S. Annan, and S. A. Carr J. Prot. Chem., 16, 391 (1997).

- 20. X. Zhang, C.J. Herring, P.R. Romano, J. Szczepanowska, H. Brzeska, A.G. Hinnebusch, J. Qin *Anal.*. Chem., 70, 2050, (1998).
- 21. R.Cramer, N.J.Richter, E.Stimson, A.L. Burlingame Anal. Chem., 70, 4939 (1998).
- 22. J.M.Asara, J.Allison *J.Am.Soc. Mass. Spectrom.*, 10, 35 (1999).
- 23. A. Rossomando, J. Wu, M. Hanspeter, J. Shabanowitz, D. F. Hunt, M. Weber, T. W. Sturgill *Proc. Natl. Acad. Sci. USA*, **89**, 5779 (1992).
- 24. K. Palczewski, J. Buczylko, P. Van Hooser, S. A. Carr, M. J. Huddleston, J. W. Crabb J. Biol. Chem., 267, 18991 (1992).
- 25. H. Taniguchi, M. Suzuki, S. Manenti, K. Titani J. Biol. Chem., 269, 22481 (1994).
- 26. M. Affolter, J. D. Watts, D. L. Krebs, R. Aebersold Anal. Biochem., 223, 74 (1994).
- 27. C. R. Lombardo, T. G. Consler, D. B. Kassel Biochem., 34, 16456 (1995).
- 28. K. A. Resing, R. S. Johnson, K. A. Walsh Biochem., 34, 9477 (1995).
- 29. R. D. Ladner, S. A. Carr, M. J. Huddleston, D. E. McNulty, S. J. Caradonna J. Biol. Chem., 271, 7752 (1996).
- 30. A. Weijland, G. Neubauer, S. A. Courtneidge, M. Mann, R. K. Wieranga, G. Superti-Furga *Eur. J. Biochem.*, **240**, 756 (1996).
- 31. M. J. Huddleston, R. S. Annan, M. F. Bean, S. A. Carr J. Am. Soc. Mass Spectrom., 4, 710 (1993).
- 32. A.P.Hunter, D.E. Games Rapid Commun. Mass Spectrom., 8, 559 (1994).
- 33. J. Ding, W. Burkhart, D. B. Kassel Rapid Commun. Mass Spectrom., 8, 94 (1994).
- 34. M. Busmann, K.L. Schey, J.E. Oatis Jr., D.R. Knapp J. Am. Chem. Soc., 7, 243 (1996).
- 35. S.A.Carr, M.J.Huddleston, R.S. Annan Anal. Biochem., 239, 180 (1996).
- 36. A. Tholey, J. Reed, and W. D. Lehmann J. Mass Spectrom., 34, 117 (1999).
- 37. Y.V.Lyubraska, S.A.Carr, D. Dunnington, W.P. Pritchett, S.M. Fischer, E.R. Applebaum, C.S.Jones, B.L. Karger *Anal. Chem.*, 70, 4761 (1998).
- 38. J. P. DeGnore, J. Qin J. Am. Soc. Mass Spectrom., 9, 1175 (1998).

- 39. A.R. Dongre, J.L. Jones, A.Somoygi, V.H. Wysocki J. Am. Chem. Soc., 118, 8365. (1996).
- 40. T.Keough, R.S. Youngquist, M.P. Lacey Proc. Natl. Acad. Sci., 96, 7131, (1999).
- 41. Wagner, D.S. *Ph.D. Dissertation*, Michigan State University, East Lansing, MI, (1992).
- 42. Z. -H. Huang, J. Wu, K. D. W. Roth, Y. Yang, D. A. Gage, J. T. Watson *Anal. Chem.*, **69**, 137 (1997).
- 43. P. -C. Liao, Z. -H. Huang, J. Allison J. Am. Soc. Mass Spectrom., 8, 501 (1997).
- 44. Z. -H. Huang, T. L. Shen, J. Wu, D. A. Gage, J. T. Watson *Anal. Biochem.*, 268, 305-317 (1999).
- 45. N. Sadagopan, J. T. Watson J. Am. Soc. Mass. Spectrom., 11, (2000).
- 46. L.M. Nuwaysir, J.T. Stults J. Am. Soc. Mass Spectrom., 4, 662 (1993).
- 47. S.G.Lias, J.F.Bartmess, J.F.Liebman, J.L.Holmes, R.D.Levin, W.G.Mallard J. Phys. Chem. Ref. Data, 17 (1), (1988).
- 48. N.Sadagopan, M.Malone, J.T. Watson J. Mass Spectrom., 34, 1279 (1999).
- 49. I. A. Papayannopoulos Mass Spectrom. Rev., 14, 49 (1995).
- 50. K.D.W. Roth, Z.-H. Huang, N. Sadagopan, J.T. Watson, Mass Spectrom. Rev., 17, 255 (1998).

Chapter 4

MECHANISMS OF FRAGMENTATION OF PEPTIDES AFTER CHARGE-DERIVATIZATION BY ESI-CAD-MS/MS AND MALDI-PSD-MS

I. Introduction

A) Collisionally Activated Dissociation of Protonated Peptides:

Structural information for a molecule after ionization and desorption into the gas phase by electrospray is typically obtained by m/z analysis of fragments following collisionally activated dissociation. In the case of peptides, the protonated molecule fragments by charge-mediated pathways. There are several mechanisms proposed explaining these pathways, and the "mobile-proton model" is widely accepted [1]. The random localization of the proton has been supported by deuterium exchange studies performed by Johnson et al. [2]. Proton transfers occur very fast, in the nanosecond time scale, and since the lifetime of the ions in the mass spectrometer is considerably larger than this, the ionizing proton gets randomly distributed throughout the peptide. In solution, the pK_a values of the N-terminus and the basic side-chains (lysine, arginine and histidine) are significantly higher than those of the intervening amides, however the gasphase proton affinites are comparable [3]. During electrospray ionization, the singly- or multiply-charged ions are ejected with the protons initially located on the same position as in solution, the amino terminus or the basic side chain. However, in the gas phase this proton is free to transfer to the amides where it may induce cleavage [4]. Also, in the gas phase, solvent molecules are absent and charge delocalization can occur by internal

solvation, a folding process that brings one or more of the amide linkages in close proximity to the protonated amino terminus [5]. Since the proton affinity of a single peptide amide linkage (217 kcal/mol [6]) is comparable to that of a three-carbon primary amine in the gas phase (218 kcal/mol [7]), internal solvation provides a convenient pathway for proton-transfer reactions that distribute the charge onto the various amide linkages of the peptide backbone. Intramolecular hydrogen bond formation involving other amide linkages in the peptide liberates at least 7 kcal/mol and provides the additional driving force for preferential charge localization on the various amide bonds in the gas phase [5]. In cases where there is no basic side chain, protonation occurs at the amino terminus and it has been shown that fragmentation of peptides with the free amino terminus requires more energy than those with an acetylated N-terminus [8].

When the collection of peptides protonated at various amide locations is subjected to CAD, kinetic energy is converted to vibrational energy and many of the ions suffer fragmentation at one of the amide bonds. During CAD, the proton transfers from the more basic sites to less basic sites and initiates cleavage. The *Ab initio* and MNDO bond order calculations have indicated that the amide N-protonated form can cleave readily [9]. High energy pathways involve cleavage of single bonds whereas low-energy pathways involve mechanisms of simultaneous bond breaking and bond making.

When proline is present in any of the protonated peptides, fragmentation is highly favored at that site. This is called the "proline effect" [5]. This is because the secondary amine functionality, the imino group of proline, is part of a five-membered ring and in an amide linkage, it is devoid of hydrogen. The imino group has a higher gas phase basicity,

several kcal/mol higher than the other amide bonds in the peptide backbone, and is preferentially protonated [10].

The nomenclature of ions formed from protonated peptide fragmentation was first defined by Roepstorff and Fohlmann in 1984 [11]. CAD studies were originally performed by FAB-MS. In 1986, Hunt et al. proposed mechanisms and structures for various fragment ions formed from protonated peptides based on their FAB-low energy CAD MS studies [5]. They suggested that the $Y_n + 2$ ion receives one of the hydrogens whose origin is from the FAB matrix, while the other hydrogen is the one shifting from the α -carbon of the amino acid residue (β with respect to the protonated amide nitrogen). Biemann proposed modified structures for various ions formed during these studies in 1987, and hence the $Y_n + 2$ ion is termed the y_n ion [12]. In order to verify the structure of the y_n ion, Mueller et al. performed the first deuterium labeling studies in 1988, by FAB-CAD-MS (low-energy CAD in a triple quadrupole) to pinpoint the origin of the shifting protons resulting in the formation of the y_n ions [13]. This is a hydrogen/ deuterium exchange study in which only the hydrogens on the amide nitrogen and the terminal groups are labeled. The results prove that the exchangeable amide hydrogen rather than the hydrogen from the α -carbon is transferred to the y_n fragment. Kenny et al. (1992) performed labeling studies that involved labeling of the α -carbon using FAB-high-energy CAD-MS [14]. Results from their studies show that it is migration of the hydrogen from the amide nitrogen, rather than from the α -carbon, that results in the formation of the y_n ion. Tang and Boyd in 1992 proposed a mechanism for formation of the y_n ion that involves the shift of an amide hydrogen, not necessarily to the protonated amide hydrogen but to the amide nitrogen at the site of cleavage is proposed by [15]. Formation of the b_n ion, the N-terminal counterpart of the y_n ion, resulting from cleavage of the amide bond is described as a charge-site induced α -cleavage mechanism [5].

Figure 4.1a. Mechanism of fragmentation of protonated peptides to form \boldsymbol{y}_{n} ions.

Figures 4.1a and 4.1b depict the previously proposed mechanisms for the formation of the y_n and the b_n ions, respectively.

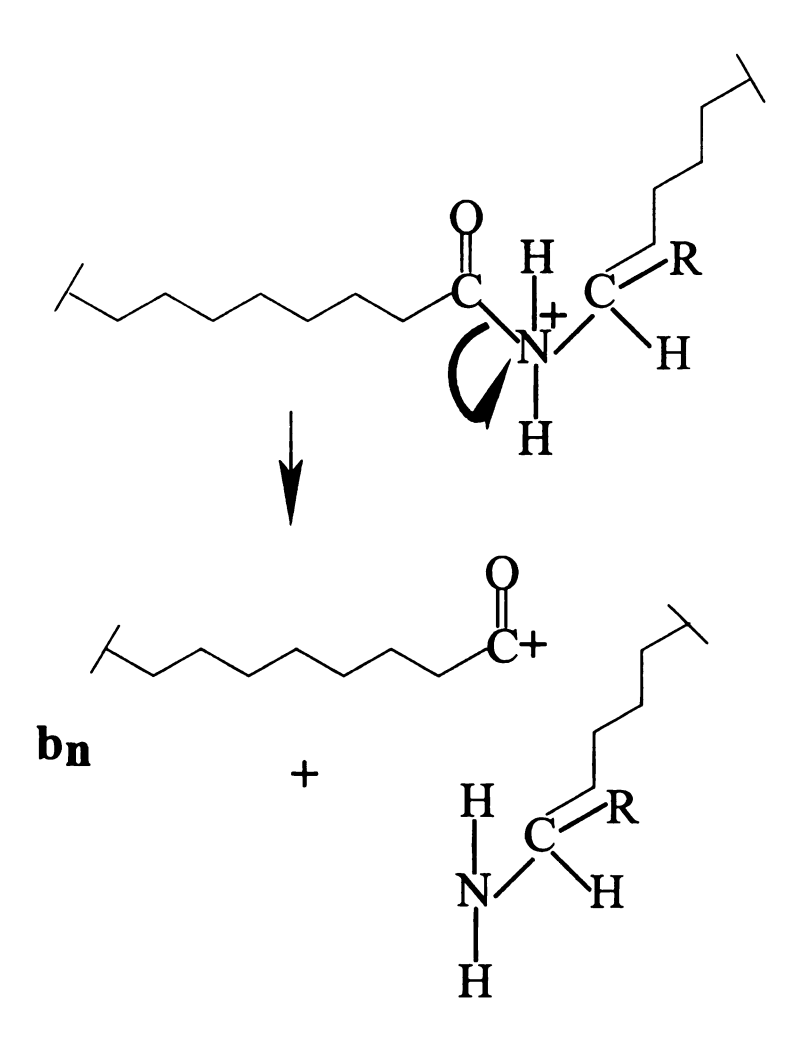


Figure 4.1b. Mechanism of fragmentation of protonated peptides to form b_n ions.

These mechanisms suggest that the localization of the proton is random and since the location of the proton dictates the fragmentation, a complete series of fragment ions necessary for sequence interpretation cannot be guaranteed. In order to overcome this problem of not being able to obtain a complete series of ions, two approaches have been developed. One approach is to fix the charge on one end of the peptide, so that the

fragmentation will not depend on an incoming proton, but rather will be due to intramolecular hydrogen shifts within the precursor ion. The result is often termed "chargeremote fragmentation" because the cleavage of the peptide bond occurs remote from the
charge-site [16]. This type of fragmentation mechanism also seems to be operative in
tryptic peptides where the C-terminal residue is a lysine or arginine. Because of the
increased basicity of their side-chains, these residues are preferentially protonated in the
gas-phase.

The second approach intentionally randomizes the charge among the various amide bonds thus resulting in a population of protonated species in which any one of the amide bonds could be charged. Recently, *Keough et al.* reported the sulfonation of the N-terminal end to aid in increased mobility of the proton [17]. This follows from similar approaches where the cysteine in the peptide, which also contains a basic side chain containing a histidine residue, is oxidized to form cysteic acid. This results in the specific interaction between the acidic and basic sites. Hence, fixation of the charge at a basic site is minimized, which results in the formation of a precursor population with a heterogeneous charge distribution [18].

B) Fragmentation of Charged Derivatives:

Fixed-charge derivatives were initially developed for FAB studies for purposes of increasing the hydrophobicity of the analyte [19]. Studies of these charged derivatives continue by MALDI-PSD and ESI-CAD-MS/MS for purposes of facilitating the formation of a complete series of ions and simplifying spectral interpretation, because fragment ions retaining just one terminus are formed. Recent reports of the [tris (2,4,6-trimethoxyphenyl) phosphonium] acetyl (TMPP⁺-Ac) N-terminal derivatives of peptides

show that charge-remote fragmentation is indeed responsible for formation of a series of a_n ions in FAB-CAD [20], MALDI-PSD [21] and ESI-CAD [22]. The fragmentation mechanisms of a related charge derivative the triphenylphosphonium (TPP) derivatives have been studied by deuterium labeling [23]. Although typically it is deemed that only FAB-CAD is suitable for studying such charged derivatives because higher energy (kV) is deposited in the precursor ion, MALDI-PSD and ESI-CAD studies which are not highenergy techniques have also been successful in obtaining fragmentation of these charged In ESI-CAD, the charged derivatives require higher energy for derivatives. fragmentation than their underivatized counterparts, but still can be fragmented well within 120 eV. This is fortunate from the peptide sequencing standpoint because MALDI-PSD and ESI-CAD-MS/MS techniques are increasingly applied for the sequencing of proteins/peptides. The energetic requirements in MALDI-PSD are still not very clear, but our studies indicate that it is intermediate between the high-energy and low-energy techniques.

During fragmentation of the charge-derivatized peptide there are three protons (α, β) or the amide (η) hydrogen as seen in Figure 4.2) that could undergo intramolecular migration to yield the fragment ions.

$$(R')_2-C-H$$

$$\sim NH-CH-CO$$

Figure 4.2. Protons that could possibly shift during charge-remote fragmentation of a peptide bond.

The FAB-CAD studies of TPP⁺-Ac derivatives of peptides suggest that the β hydrogen migrates resulting in fragmentation [23]. However, if this were the case, fragmentation at the site of glycine should not be observed. This is true for the TPP⁺-Acpeptides or TMPP⁺-Ac-peptides when studied by FAB-CAD. However, when the TMPP⁺-Ac-peptides are studied by MALDI-PSD or ESI-CAD fragmentation at glycine is not observed [21,22]. Plausible structures of *a_n, *b_n ions and related ions are given in Figure 4.3 (R, R', R_n correspond to the different side chains in the amino acid residue, and 'n' is the number of residues in the peptide).

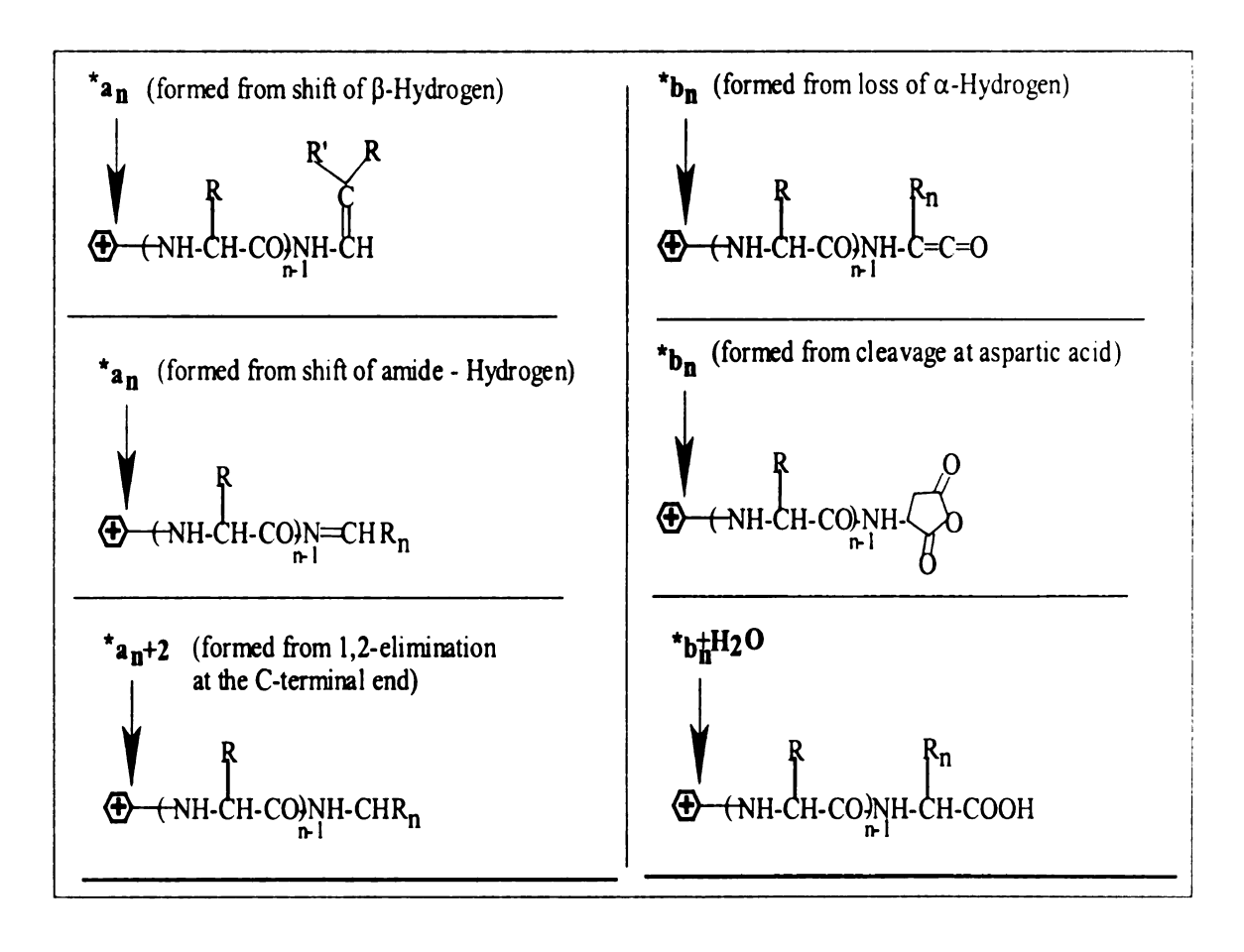


Figure 4.3. Plausible structures of fragment ions formed from fixed-charged derivatives.

There are signals observed due to fragmentation at the glycine residue (MALDI-PSD and ESI-CAD-MS/MS). Hence, the previously proposed mechanism (β-hydrogen migration) is seemingly not responsible for fragmentation in MALDI-PSD and ESI-CAD. These observations imply that the mechanisms of fragmentation are different for highenergy and low-energy CAD. Also important is the observation that there is not a noticeable signal due to cleavage at the site of proline. This is not the case in FAB-CAD studies where there is a signal due to cleavage at proline. This observation suggests that in the case of MALDI-PSD and ESI-CAD the amide proton shifts and causes fragmentation, because proline is a residue that lacks an amide hydrogen. In some cases under MALDI-PSD fragmentation at proline was dependent on laser power [21]. Also in the CAD-MS/MS studies of the TMPP⁺-Ac peptides in the ion trap, there is a very weak signal due to cleavage at the site of proline. The previously proposed mechanism involving an amide hydrogen shift for fragmentation is shown in Figure 4.4 [21]. The validity of these previously proposed mechanisms was tested in deuterium-labeling studies performed on a model peptide.

Figure 4.4. Mechanism of *a_n ion formation by amide hydrogen shift in TMPP⁺-Ac-peptides.

C) Current Studies:

The following is a report based on the ESI-CAD and MALDI-PSD studies of the peptides with deuterium labeling at various sites (α -, β -, and η -) and also with the fixed charge due to the TMPP⁺-Ac moiety at the N-terminus. The peptide chosen for this study is VGVAPG. This is a chemotactic peptide with no acidic or basic side chains. Hence fragmentation is simple. It contains proline, a residue without an amide hydrogen when present in a peptide bond, which would provide us with additional insight regarding the mechanisms of fragmentation. The following figure shows the structure of proline, Figure 4.5. In order to label the amide hydrogens deuterium exchange studies need to be performed, and the efficiency of deuterium incorporation decreases with increasing size of the peptide. Hence this relatively smaller peptide, a hexamer (VGVAPG), which will allow for complete exchange of the acidic hydrogens with deuterium is our choice.

Figure 4.5. Structure of the proline residue.

II. Experimental

A) Peptides Synthesis:

The following are the deuterium-labeled peptides used in the study:

Table 4.1. List of Labeled Petides:

Name	Position of the Deuterium Label	Peptide
A	No label	VGVAPG
В	α- Carbon (Glycine)	$VG^{\alpha}VAPG$
C	α- Carbon (Valine)	$V^{\alpha}GV^{\alpha}APG$
D	β- Carbon (Valine)	$V^{\beta}GV^{\beta}APG$
E	β- Carbon (Alanine)	$VGVA^{\beta}PG$
F	Amide Nitrogen	$^{\eta}V^{\eta}G^{\eta}V^{\eta}AP^{\eta}G$

The non-labeled species, α - and the β - labeled peptides were synthesized using solid-phase peptide synthesis. The amino acids with deuterium labels were purchased from CDN isotopes (Canada). The solid-phase peptide synthesis [24] involves three steps: chain assembly, cleavage from resin and purification. These steps are briefly described in the following text. The peptide is synthesized from the C-terminal end to the N-terminal end. The C-terminal amino acid of the desired peptide, in this case glycine, linked to the resin (a polymer of 4-(oxymethyl)-phenylacetoamidomethyl) via a benzyl ester, is used as the starting point. The amino acids have their N-terminal

protected by the FMOC (Fluorenylmethoxycarbonyl) group before they are assembled on the peptide chain, thereby minimizing interaction with the resin. The custom amino acids with the deuterium label are FMOC protected 'in house' and the product characterized by NMR. All the other amino acids were purchased with the FMOC protection. The first cycle is to deprotect the amino acid, to remove the FMOC group, using a base (ususally piperidine). The next cycle involves activation of the carboxy terminus of the incoming amino acid (proline in our case), to ensure better reactivity of the carboxy terminus. HBTU (2-(1H-benzotriazol-1-yl)-1,1,3,3tetramethyluroniumhexafluoro phosphate) is used as the activating reagent. The activated amino acid is now coupled to the deprotected amino terminus of the amino acid linked to the resin. Four equivalents of the activated amino acid are added per one equivalent of the growing peptide chain. The efficiency of coupling is over 99%. Coupling is the time consuming step of the automated synthesis. About 2 hours are allowed for each coupling step. It is usually performed in polar, aprotic solvent like dimethylformamide (DMF), to minimize peptide-peptide hydrogen bonding. After each step the resin is usually washed with dichloromethane (DCM) and N-methylpyrrolidine (NMP). A similar repetition of deprotection and coupling results in the desired peptide, which is still attached to the resin. This is an automated synthesis where the FMOC-protected amino acids are used in the synthesis of the peptide using the Fastmoc cycles (HOBt/DCC) in the AP-Biosystems peptide synthesizer. The peptide is cleaved from the resin using a TFA/water (95/5, v/v) mixture and purified by preparative HPLC. The mass of the product peptide is checked by MALDI-MS.

The peptide with deuterium labels at the amide nitrogen is prepared by incubating in D₂O/deuterated acetonitrile (1:1 v/v) for 30 min and allowing for free exchange of hydrogen with deuterium. In the case of the derivatized peptide, the peptide derivative is incubated using a D₂O/deuterated acetonitrile mixture. In other cases, the labeled synthetic peptide is first derivatized with the TMPP⁺-Ac reagent and HPLC purified to obtain the TMPP⁺-Ac derivative of the labeled peptide.

B) Derivative Synthesis:

The TMPP⁺-Ac derivatives of peptides are prepared by reacting 1 nmol of the peptide with 5-fold molar excess of the derivatizing reagent (TMPP⁺-Ac-SC₆F₅; synthesized as described in ref. 20) in the presence of dimethylaminopyridine at room temperature for 15 min. The peptide derivative is separated from the byproducts and reagents using HPLC.

C) MALDI-MS:

MALDI spectra are obtained with a Voyager Elite reflectron time-of-flight mass spectrometer (Perseptive Biosystems) using an accelerating voltage of 22 kV. The mass spectrometer is equipped with a 337-nm nitrogen laser. A saturated solution of α-cyano-4-hydroxycinnamic acid, prepared in acetonitrile/water (1:1,v/v), is used as the matrix. A 1-μL aliquot of the sample (picomoles/μL) was mixed with an equal volume of the matrix solution on the sample plate, and the mixture dried in air. PSD data are obtained with the mass spectrometer operated in the reflectron mode. Several PSD spectra, each optimized for a different range of m/z values for the fragment ions, are obtained and "stitched" together to yield the composite spectrum.

D) ESI-CAD-MS/MS:

A Finnigan LCQ, an ESI-ion trap mass spectrometer, is used to obtain CAD information on the TMPP⁺-Ac derivatives of the peptides (acetonitrile/water/1%acetic acid,10 pmol/μL) by infusion of the sample (3 μL/min). The source is held at 4.3 kV, and helium is used as the CAD gas, for MS/MS. Fragmentation of singly-charged TMPP⁺-Ac derivatives occurred at relative collision energies of 60-70% of a maximum of 5 V. For insource CAD, the source CAD option is turned on, and typically 50% is used for fragmentation. The fragmentation occurs in the source in the octapole region. This is still part of the source which is used to focus the ions into the mass spectrometer. The voltages at the entrance and exit of the octapole are varied to increase the kinetic energy of the incoming ions, which results in fragmentation.

III. Results

A) Analysis of the unlabeled TMPP⁺-Ac-VGVAPG:

The spectral results of CAD-MS of TMPP⁺-Ac-VGVAPG as analyzed by ESI (insource CAD), MALDI-PSD and FAB are shown in Figures 4.6a, 4.6b, and 4.6c respectively. It can be seen that in the case of the FAB spectrum (adopted from Ref. 22) a signal is present for cleavage at proline, whereas in MALDI and ESI there is no peak representing *a₅. This suggests that different mechanisms are operative for the genesis of these ions from these charged derivatives under high-energy and low-energy conditions.

The ESI-CAD-MS/MS spectrum of TMPP⁺-Ac-VGVPAG, in an ion trap, is shown in Figure 4.7. This spectrum is different from the spectrum in Figure 4.4a, obtained from source-CAD-MS. Here ${}^*\mathbf{b_n}$ ions are also seen along with the ${}^*\mathbf{a_n}$ ions. The most abundant ions are the ${}^*\mathbf{a_n}$ and ${}^*\mathbf{b_n}$ ions, except for cleavage at proline where the signal is very weak compared to the signal due to other ions. There is a signal due to ${}^*\mathbf{a_6}$ +2 (m/z 1028). The other ions observed are those that are 18 Da higher in mass from the ${}^*\mathbf{b_n}$ ions, which are denoted as (${}^*\mathbf{b_n}$ + $\mathbf{H_2O}$) ions.

In the following sections, results such as these, obtained from labeled derivatives will be summarized in the tables for both *a_n and *b_n ions, along with MALDI-PSD results.

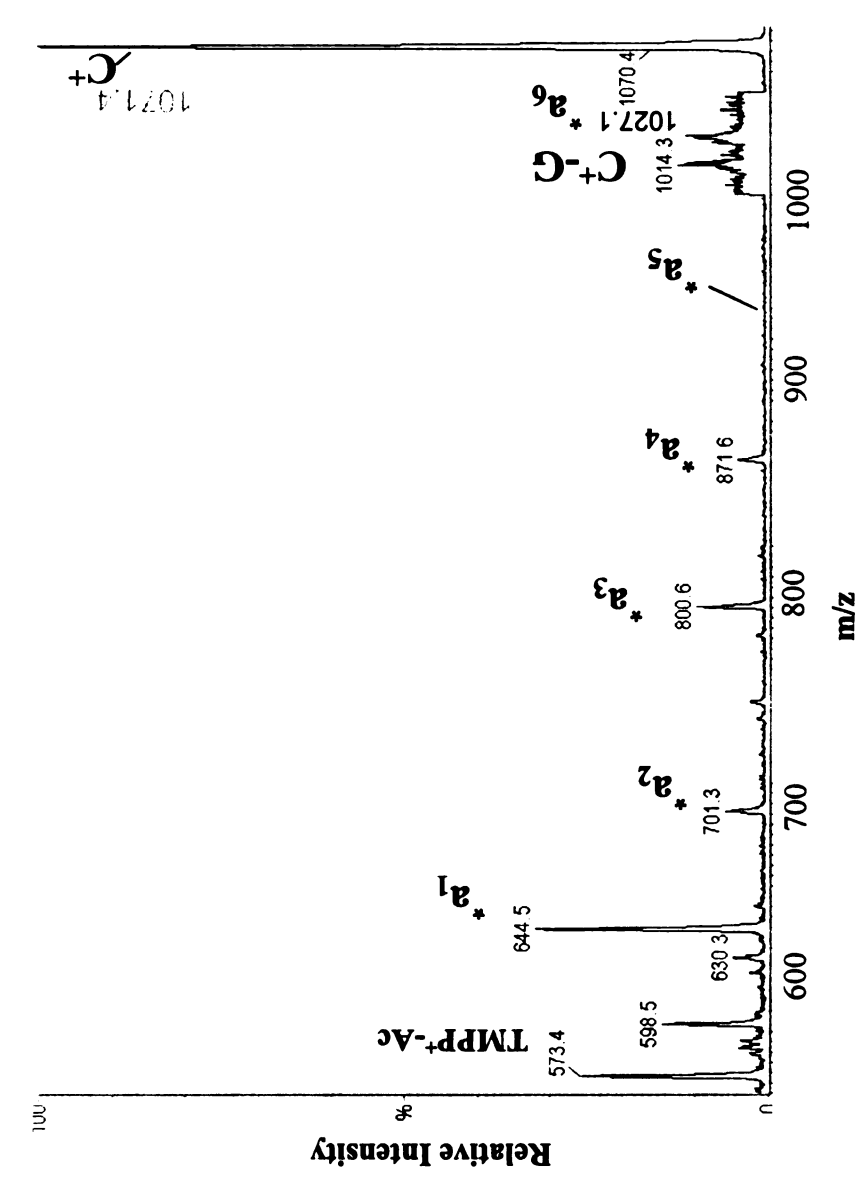


Figure 4.6a. ESI-source-CAD mass spectrum of TMPP*-Ac-VGVAPG in a single-quadrupole mass spectrometer. Spectrum shows a series of "an ions, except for cleavage at the site of proline ("a₅).

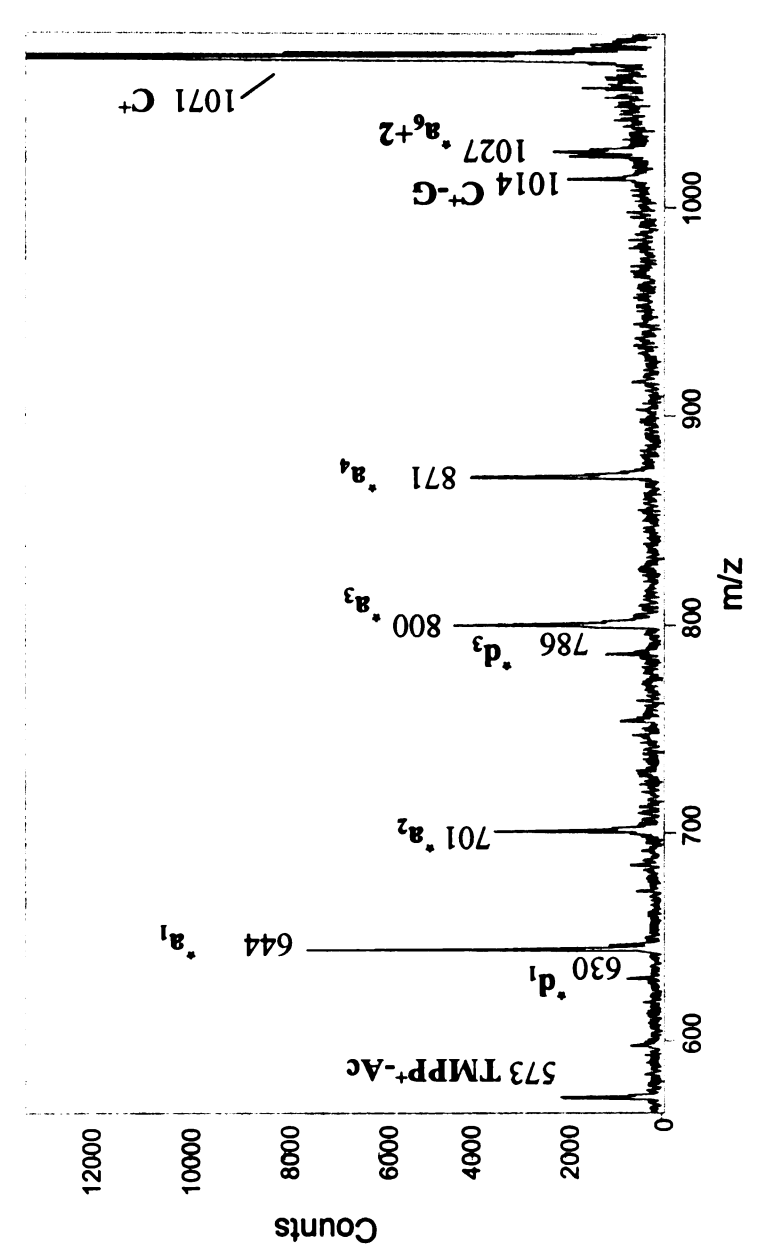
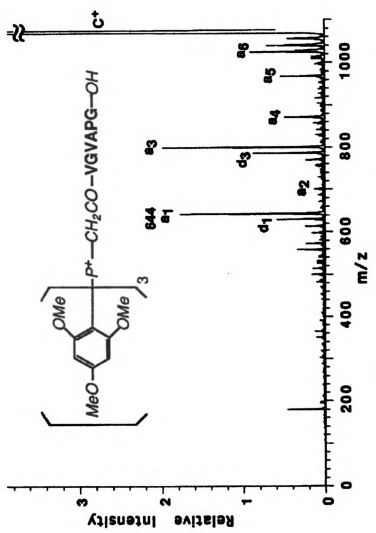
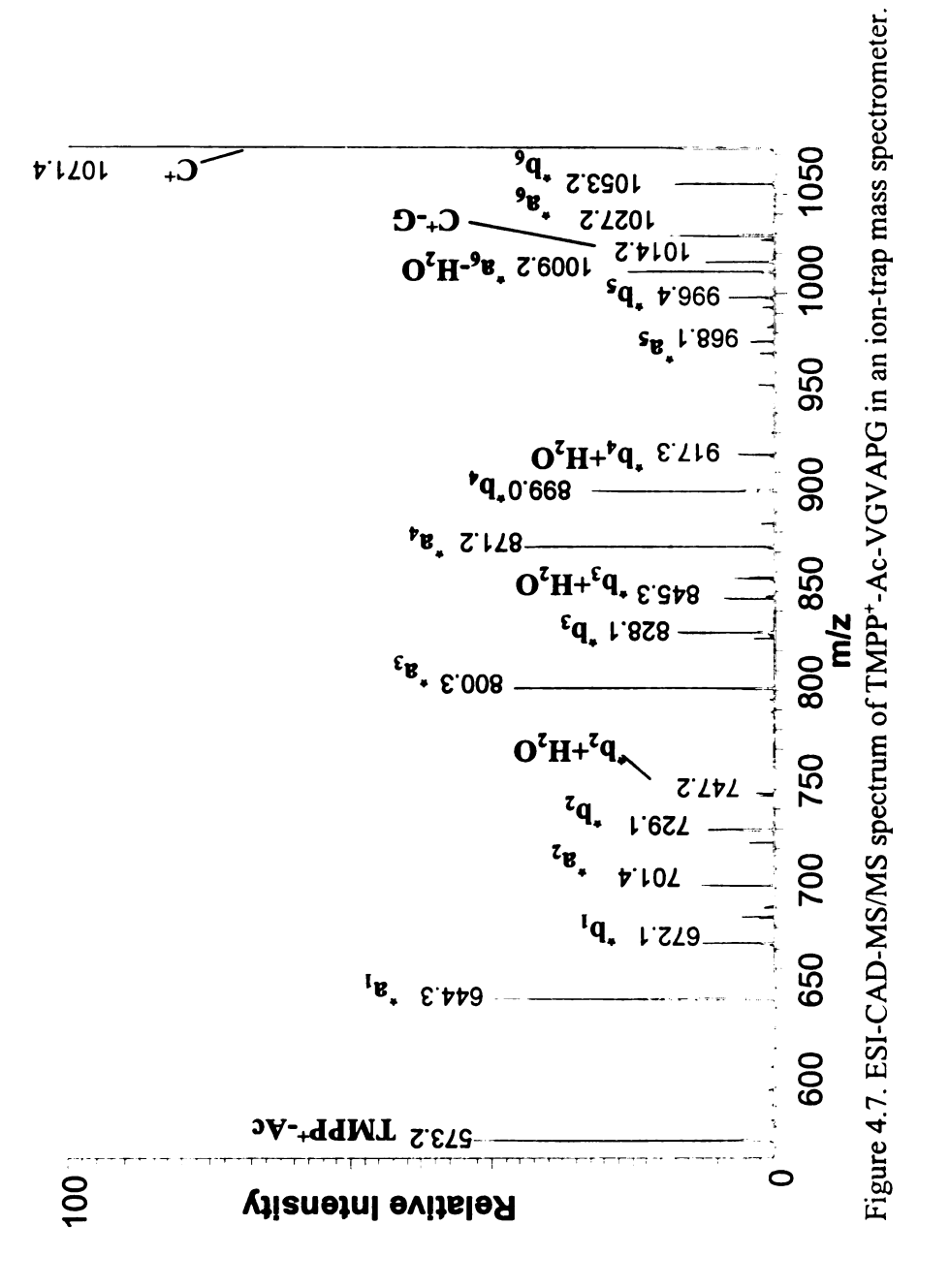


Figure 4.6b. MALDI-PSD mass spectrum of TMPP+-Ac-VGVAPG. The spectrum shows a series of an ions except for cleavage at the site of the proline residue (as).



reference 21). Peak represented by a₅ corresponds to cleavage at the proline residue. Figure 4.6c. FAB-CAD-MS/MS spectrum of TMPP*-Ac-VGVAPG (Adapted from

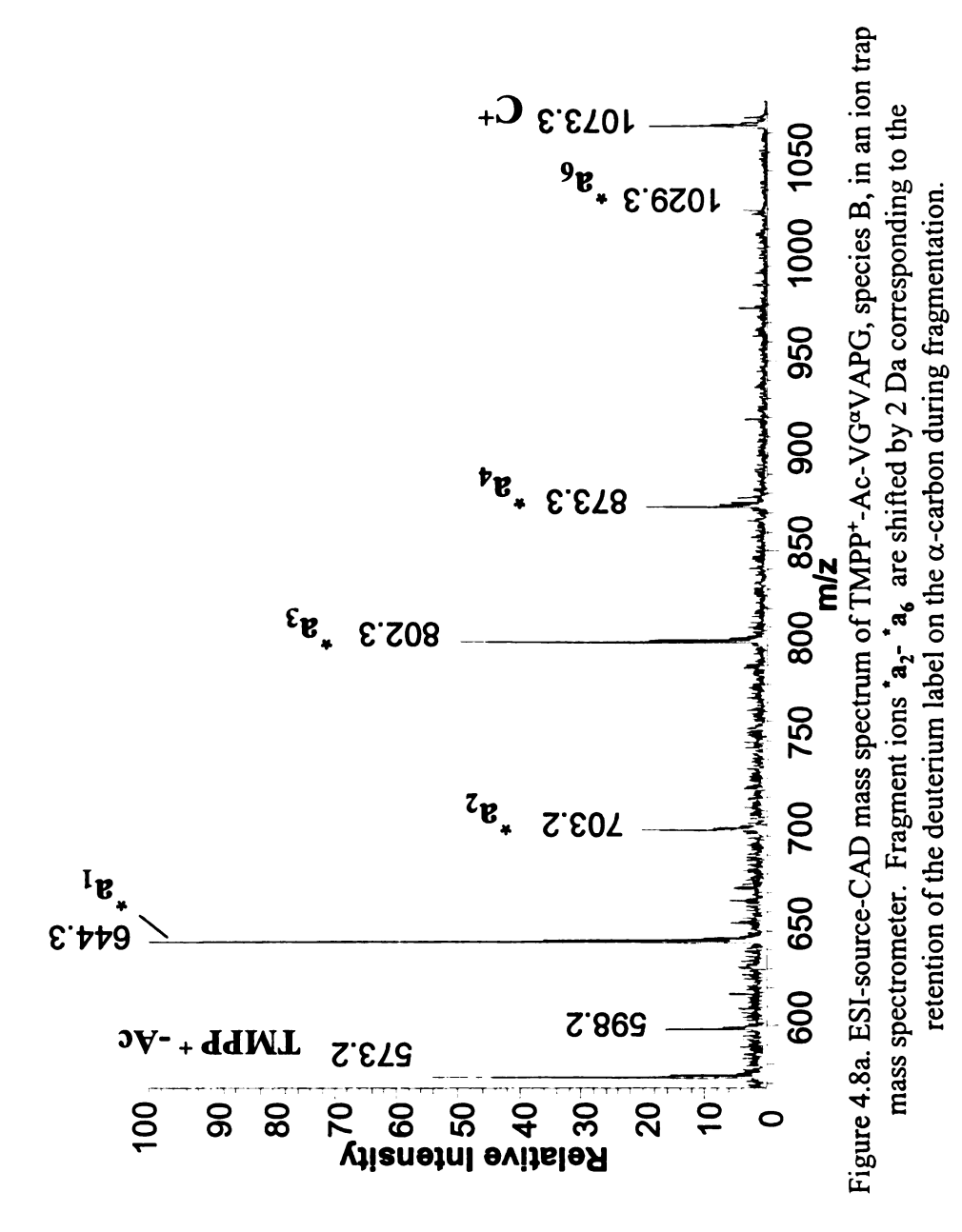


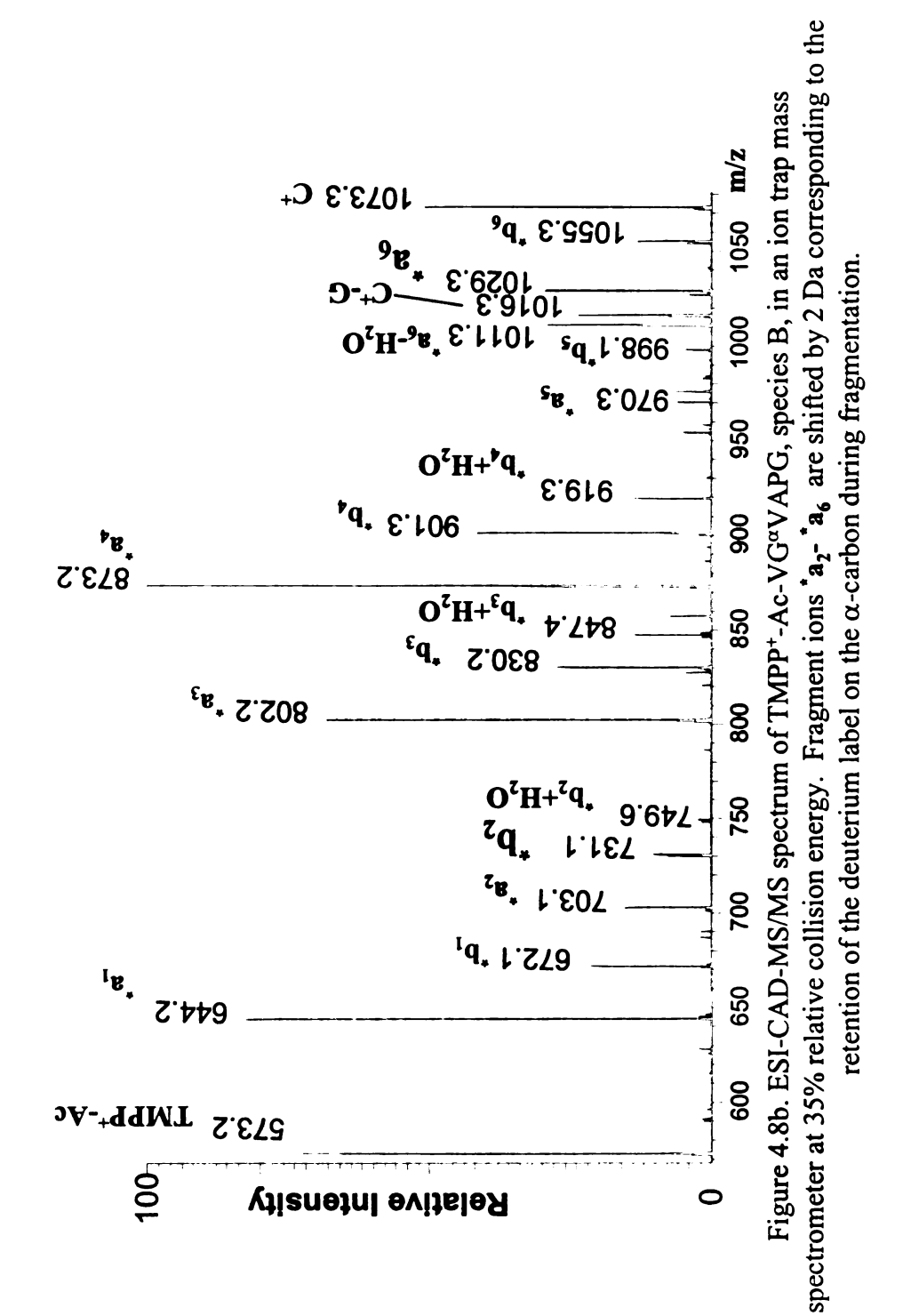
B) Results From Peptides with Deuterium Label at the α -Carbon:

a) Deuterium Label at the α -Carbon of Glycine:

Table 4.2 compares the m/z of the ions observed from the TMPP⁺-Ac-VGVAPG (A) (the unlabeled species) with TMPP⁺-Ac-VG^αVAPG (B) (the α-labeled species) by insource CAD, MS/MS in the trap and MALDI-PSD-MS. Figures 4.8a, 4.8b and 4.8c show the spectra for the fragmentation of species B by source-CAD-MS/MS, trap-CAD-MS/MS and MALDI-PSD-MS, respectively.

In species **B**, only one of the glycines (only α -hydrogens) is labeled and hence the precursor mass shifts by 2 Da (The C-terminal G is not labeled as the resin was commercially available only with the unlabeled residue). Thus, a mass shift of 2 Da will be observed for fragment ions 2-6, when compared to the fragments from the unlabeled species **A**, if the label is retained during the fragmentation. A summary of peaks observed for *a_n and *b_n ions are listed in Table 4.2 for each of three different conditions. In the MALDI-PSD spectrum very weak peaks due to *d_n ions for value are observed. From the standpoint of fragmentation, these are formed from *a_n ions. To focus more on the aspects of the formation of the major ions, the *d_n ions are not listed in Table 4.2.





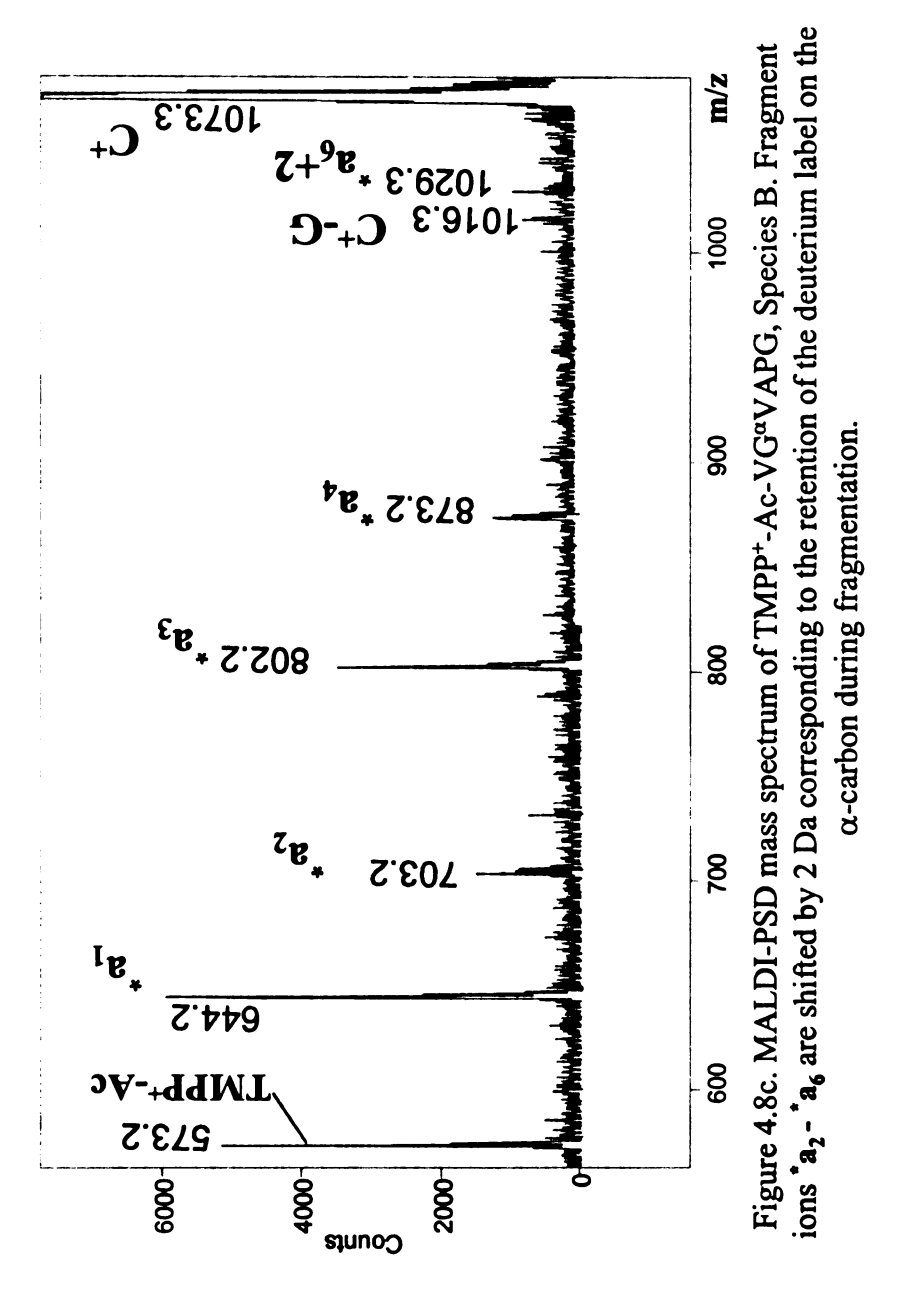


Table 4.2. Ions Observed for d₂-TMPP⁺-Ac-VG^αVAPG (B):

Ion Type	Unlabeled	α-G-labeled	α-G-labeled (B)	α-G-labeled (B)
	(A)	(B)	(Source-CAD-	(MALDI-PSD-
		(CAD-	MS)	MS)
		MS/MS)		
\mathbf{a}_1	644	644	644	644
*b ₁	672	672	none	none
a_2	701	703	703	703
$^{\bullet}b_2$	729	731	none	none
a_3	800	802	802	802
*b ₃	828	830	none	none
*a ₄	871	873	873	873
*b ₄	899	901	none	none
a _{5(#)}	968	970	none	none
*b _{5(#)}	996	998	none	none
$a_6 + 2$	1027	1029	1029	1029
*b ₆	1053	1055	none	none

#- Only observed during CAD-MS/MS in the ion trap mass spectrometer.

In the above table it can be seen that the expected mass shifts are observed corresponding to the retention of the hydrogen on the α -carbon. These results indicate that the mechanism of ${}^{\star}a_n$ ion and ${}^{\star}b_n$ ion formation does not involve the shift of hydrogen away from the α -carbon.

There is a significant difference in fragmentation of species B during in-source CAD or MALDI-PSD from that observed during MS/MS in the trap. In MALDI-PSD, only *a_n ions are observed, as opposed to fragmentation in the trap (MS/MS) where *b_n

ions are also observed. This is in agreement with what has been reported in Chapter 2, that fragmentation in the trap is different than fragmentation in the source.

In the case of source-CAD and MALDI-PSD there is no evident signal representing the *a₅ ion, whereas a very weak signal (<10% relative intensity) is observed during MS/MS in the trap. This suggests that there may be other mechanisms (not significant) that are operative along with the major pathways that lead to this type of ions.

In the MS/MS spectrum of TMPP⁺-Ac-VGVAPG in the trap, ions that are 18 Da higher than the *b_n ions are observed, which is consistent with the structure for (*b_n + H_20); as shown in Figure 4.3. The corresponding mass shifts are observed for those ions formed from the deuterium-containing peptide derivatives. This suggests that the proton on the α -carbon is retained in these fragment ions. Such ions (*b_n + H_20) have also been observed by Lin et al. during the study of TMPP⁺-Ac-peptides by FAB-ion trap-MS, which they refer to as (b_{n-1} +OH) ions [25]. This type of ion is only observed for fragmentation of peptides with a free C-terminus.

b) Deuterium label at α -Carbon of Valine:

In species C, TMPP⁺-Ac- $V^{\alpha}GV^{\alpha}APG$, both valines are labeled at the α -carbon and hence the precursor mass shifts by 2 Da. Fragment ions 1 and 2 will have a mass shift of 1 Da, whereas ios 3-6 will have a mass shift of 2 Da if the deuterium is retained on the α -carbon during fragmentation.

Table 4.3. Ions Observed for d_2 -TMPP⁺-Ac-V^{α}GV^{α}APG (C):

Ion Type	Unlabeled	α-V-labeled	α-V-labeled
••	(A)	(C)	(C)
		(CAD-	(MALDI-
		MS/MS)	PSD-MS)
\mathbf{a}_1	644	645	645
*b ₁	672	673	none
*a ₂	701	702	702
*b ₂	729	730	none
*a ₃	800	802	802
*b ₃	828	830	none
*a ₄	871	873	873
*b ₄	899	901	none
*a_5	968	970	none
*b ₅	996	998	none
•a ₆₊₂	1027	1029	1029
*b ₆	1053	1055	none

The mass shifts for all the ions are observed as expected. Also, as observed in Table 4.1, during MALDI-PSD only *a_n ions are observed. These results support the conclusions obtained from analyses of species B (Table 4.2), that the α -hydrogen does not shift during the fragmentation and formation of the *a_n and *b_n ions.

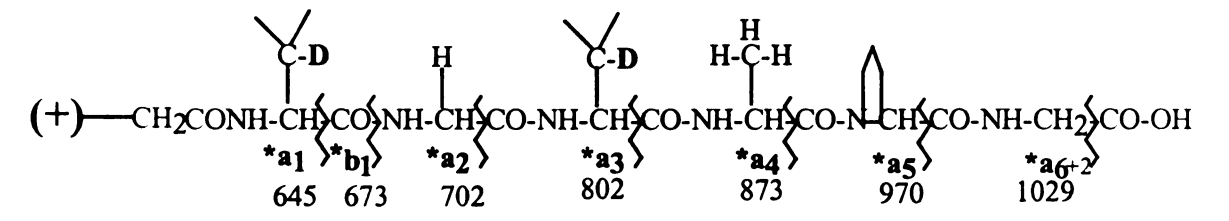
On the other hand, one need not consider all possible protons that can shift. For example, one would not consider breaking two bonds to the same carbon as this would leave a carbone as a resultant product. Such a consideration must be given to the α -carbon where migration of the hydrogen in question and cleavage of the backbone at that site would involve breaking two bonds attached to the same carbon.

C) Results From Peptides With Deuterium Labels at β-Carbons:

a) Deuterium Label at the β -Carbon of Valine:

In order to investigate the fate of hydrogen on a β -carbon atom in the TMPP⁺-Ac derivatized peptide, a variant of the peptide with deuterium on the β -carbon of valine was synthesized and studied by MALDI-MS and ESI-CAD-MS. Although our observations suggest that the migration of this β -hydrogen is not the most plausible mechanism (since signal due to cleavage at G which lacks a β -hydrogen is observed), it is yet to be proven.

Table 4.4. Ions Observed for d_2 -TMPP⁺-Ac-V^{β}GV^{β}APG (D):



Ion Type	Unlabeled	β-V-labeled	β-V-labeled
	(A)	(D)	(D)
		(CAD-	(MALDI-
		MS/MS)	PSD-MS)
$\mathbf{a_1}$	644	645	645
*b ₁	672	673	none
*a ₂	701	702	702
*b ₂	729	730	none
•a ₃	800	802	802
*b ₃	828	830	none
*a ₄	871	873	873
*b ₄	899	901	none
*a ₅	968	970	none
*b ₅	996	998	none
$^{*}a_{6} + 2$	1027	1029	1029
*b ₆	1053	1055	none

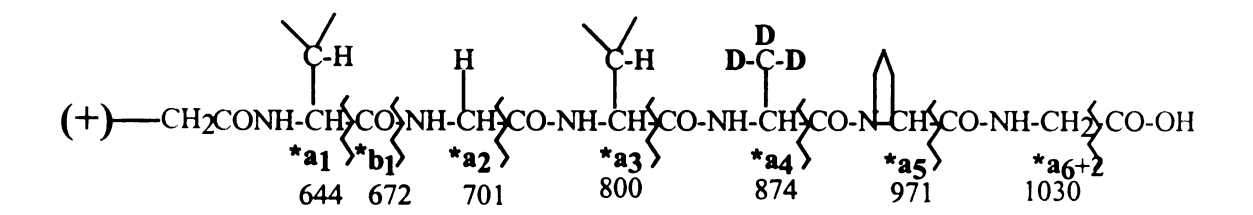
The glycine residue, which lacks a β-hydrogen, does undergo fragmentation and a signal is observed for cleavage at glycine during analysis by MALDI-PSD and ESI-CAD. However only a very weak signal is observed during FAB-CAD.

In this case, since the β -hydrogen is labeled in both the valines, the fragment ions 1-2 are expected to have a shift of 1 Da, while the fragment ions 3-6 are expected to have a shift of 2 Da, if the deuterium label is retained on the β -carbon. As listed above in Table 4.4, the mass shifts indicate retention of the deuterium label on the β -carbon.

b) Deuterium label at the β -Carbon of Alanine:

Similarly, d₃-analogue of VGAVPG containing three deuterons on the methyl group of alanine was synthesized and its TMPP⁺-Ac derivative analyzed by MALDI-PSD and ESI-CAD-MS/MS. The precursor is increased in mass by 3 Da, but the fragment ions 1-3, do not have shift whereas the fragment ions 4-6 shift in mass by 3 Da, provided the label is retained. The results (Table 4.5) show that the fragment ions do retain the deuterium label on the β -carbon of the alanine residue. These results corroborate those obtained from the study of the derivative where the β -carbon of valine is labeled. Thus, the major fragmentation pathway does not involve a β - hydrogen shift when the TMPP⁺-Ac-peptides are analyzed by MALDI-PSD and ESI-CAD-MS/MS.

Table 4.5. Ions Observed for d₃-TMPP⁺-Ac-VGVA^βPG (E):



Ion Type	Unlabeled	β-A-labeled	β-A-labeled
2011 2 7 7 7	(A)	(E)	(E)
	()	(CAD-	(MALDI-
		MS/MS)	PSD-MS)
a_1	644	644	644
$^{\bullet}$ b ₁	672	672	none
*a ₂	701	701	701
*b ₂	729	729	none
*a ₃	800	800	800
*b ₃	828	828	none
*a ₄	871	874	874
*b ₄	899	902	none
*a ₅	968	971	none
*b ₅	996	999	none
*a ₆₊₂	1027	1030	1030
*b ₆	1053	1056	none

D) Results For Peptides with Deuterium Label on the Amide - Nitrogens:

The acidic hydrogens of a peptide (-CONH, COOH, and NH₂) are readily exchangeable with those of the surrounding solvent molecules; similarly, these hydrogens can be exchanged for deuterons in a deuterated solvent. For this experiment, the TMPP⁺-Ac-VGVAPG is synthesized and dried under vacuum to remove any solvent. The residue is reconstituted with a mixture of deuterated water and deuterated acetonitrile. The mixture is allowed to equilibrate for 30 mins to ensure complete exchange of all six acidic hydrogens (five amides plus one carboxylic hydrogens).

The infusion/ sample delivery line in the ESI mass spectrometer is flushed with the deuterated solvents to ensure that the exchanged deuterium on the peptide remains intact. During MS/MS one can select ions of m/z 1077.4 +/- 0.2 for the deuterated precursor. Figure 4.7 shows the full scan mass spectrum of the d₆-TMPP⁺-Ac-VGVAPG or species **F**. The overall deuterium incorporation at all six expected sites is relatively high (relative intensities (%) of the other species d⁵,d⁴ are only 30% and 10% respectively).

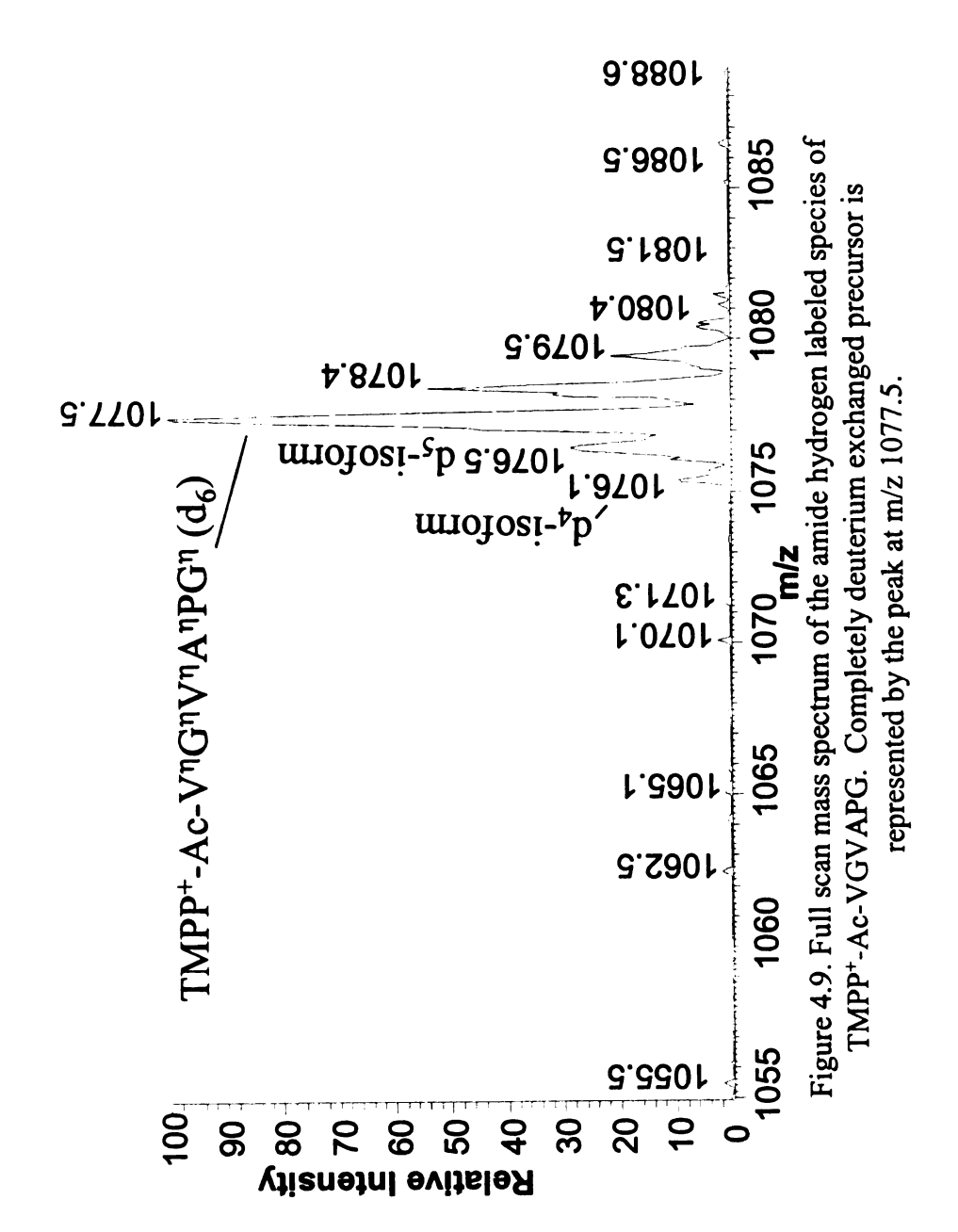


Table 4.6. Ions Observed for d₆-TMPP⁺-Ac-V^{η}G^{η}V^{η}A^{η}PG^{η} (F):

Ion Type	Unlabeled (A)	Amide hydrogen labeled (F)	Amide hydrogen labeled (F)
	(* -)	(CAD-MS/MS)	(MALDI-PSD-MS)
a_1	644	644	644
*b ₁	672	672	none
a_2	701	702	702
*b_2	729	730	none
a_3	800	802	802
*b ₃	828	830	none
*a ₄	871	874	874
*b_4	899	902	none
*a_5	968	972	none
*b ₅	996	999	none
a_{6+2}	1027	1033	1033
*b ₆	1053	1057	none

The tabulated results differ from those indicated in the structure diagram at the top of the Table 4.6 which shows the expected mass of the fragments if the deuterium label on the amide hydrogen is retained. But the actual results (Table 4.6) show fragment ions one mass unit less than the expected value for ions *a_1 through *a_4 . These results suggest that in the formation of these ions, there is a shift of the amide hydrogen. If there were no shift of the amide hydrogen, a peak at the m/z values as shown in the structure should have been observed. Also, the results from analysis of the peptides labeled at the α - and β - carbon complement this information indirectly.

a) Mechanism of Formation of the an ion due to the Shift of an Amide Hydrogen:

As mentioned at the outset, there are only three local protons that could shift. The proton located on the α -carbon, β -carbon or the η -nitrogen. The results shown earlier in this chapter suggest that there is no observed shift of the former two protons. The results from analyses of the species \mathbf{F} , where the amide nitrogen is labeled with deuterium suggest that it is the amide hydrogen that is involved in the formation of the ${}^*\mathbf{a}_n$ fragment ions when the TMPP⁺-Ac analogs of a peptide are analyzed by MALDI-PSD or ESI-CAD-MS/MS. These observations serve as experimental evidence for the plausible mechanism proposed by *Liao et al.* for the fragmentation of the TMPP⁺-Ac-peptides by MALDI-PSD [23]. The pathway involving the shift of the amide hydrogen was shown in the Figure 4.4. Evidently, the same mechanism is also responsible for fragmenation by ESI-CAD-MS/MS for most situations.

b) Mechanism for Formation of the (*a₆+2) Ion Due to the Shift of C-terminal Hydrogen Atom:

During the fragmentation of the TMPP⁺-Ac-VGVAPG, a peak appears corresponding to the mass of an ${}^*a_6 + 2$ ion instead of just an *a_6 ion. A mechanism that migh be responsible for the origin of the ${}^*a_6 + 2$ ion has been proposed earlier [23]. The results from our studies serve as evidence for such a mechanism as explained in the follosing paragraph.

For the ${}^*a_6 + 2$ ion the expected mass is (1027 + 5) 1032 Da, but the peak appears at m/z 1033. The structure of the ${}^*a_6 + 2$ ion is given in Figure 4.2. These types of ions are formed only in cases where there is a free carboxy terminus. The fact that there is a larger than expected mass shift (1033 Da instead of 1032 Da) suggests that one of the two additional protons on the $({}^*a_6 + 2)$ is not a hydrogen, but a deuterium which has its origin from the carboxy terminus.

(+) NH-CH C=0

NH-CH + C=0

*
$$a_{6}+2$$

Figure 4.10. Mechanism for formation of the terminal ${}^{\dagger}a_6 + 2$ ion.

c) Mechanism for Formation of the bn Ion Due to the Shift of an Amide Hydrogen:

The results from this study suggests that *b_n ions are formed from the shift of amide hydrogens as well because the mass of the *b_n ions is 28 Da higher than that of the *a_n ion. The previously proposed structure for a *b_n ion is a ketone as shown in Figure 4.8 (The structure proposed for the *b_n ion due to cleavage at the aspartic acid residue is different from this [18]).

(formed from loss of α -hydrogen)

Figure 4.11. Structure of a *b_n ion.

If this structure is accurate, then the results from the current studies should show that the deuterium label on the nitrogen is retained and the mass shift of the *b_n ion from an *a_n ion would be 29 Da. Also, the results from the labeling on α -carbon (Tables 4.1 and 4.2) suggest that the α -hydrogen is retained during the formation of *b_n ion, which according to Figure 4.8 is lost. Thus the structure of a *b_n ion is possibly an aziridinone, formed through a mechanism as shown in Figure 4.12, and not a ketone as proposed in Figure 4.8.

Figure 4.12. Mechanism for formation of the ${}^\star b_n$ ion during ESI-CAD-MS/MS in an ion trap mass spectrometer.

The mechanism in Figure 4.12 shows that the *b_n could be formed with the loss of an amide hydrogen. An alternate structure, as in Figure 4.16, is reasonable only if there is a rearrangement in the gas phase following fragmentation involving the loss of the amide hydrogen, but later shifting the hydrogen from the α -carbon to the amide nitrogen. However, this multi-step process seems less plausible from the mechanistic point of view.

d) Mechanism for Formation of the (*b_n+H₂O) Ion From the *b_n Ion:

The ${}^*b_n+H_2O$ ions observed in all of the CAD-MS/MS spectra from the ion trap correspond to a mass shift of 18 Da from their corresponding *b_n ions. However, these are observed at a mass shift of 20 Da from the *b_n ions in the case of the amide deuterium labeled species (F). This can be explained as the addition of D_2O , instead of H_2O since there are no external water molecules available in this case. This may be merely hydrolysis of the bond between the N and CO of the *b_n ion as shown in Figure 4.13.

Figure 4.13. Mechanism for formation of the b_n+D₂O ions from the deuterated TMPP⁺-Ac-peptide during CAD-MS/MS in an ion trap mass spectrometer.

e) Mechanism for Loss of the C-terminal Residue:

Loss of the terminal glycine residue is observed in data obtained by both MALDI-PSD and ESI-CAD-MS/MS. This has been typically observed in cases where the C-terminus is a free carboxy functionality [26], from which the authors suggest that the -OH group shifts to the neighboring amide carbonyl, resulting in the loss of the terminal residue. If this mechanism were true, the resulting fragment from the amide deuterium labeled species would be shifted by 5 Da, correspondingly.

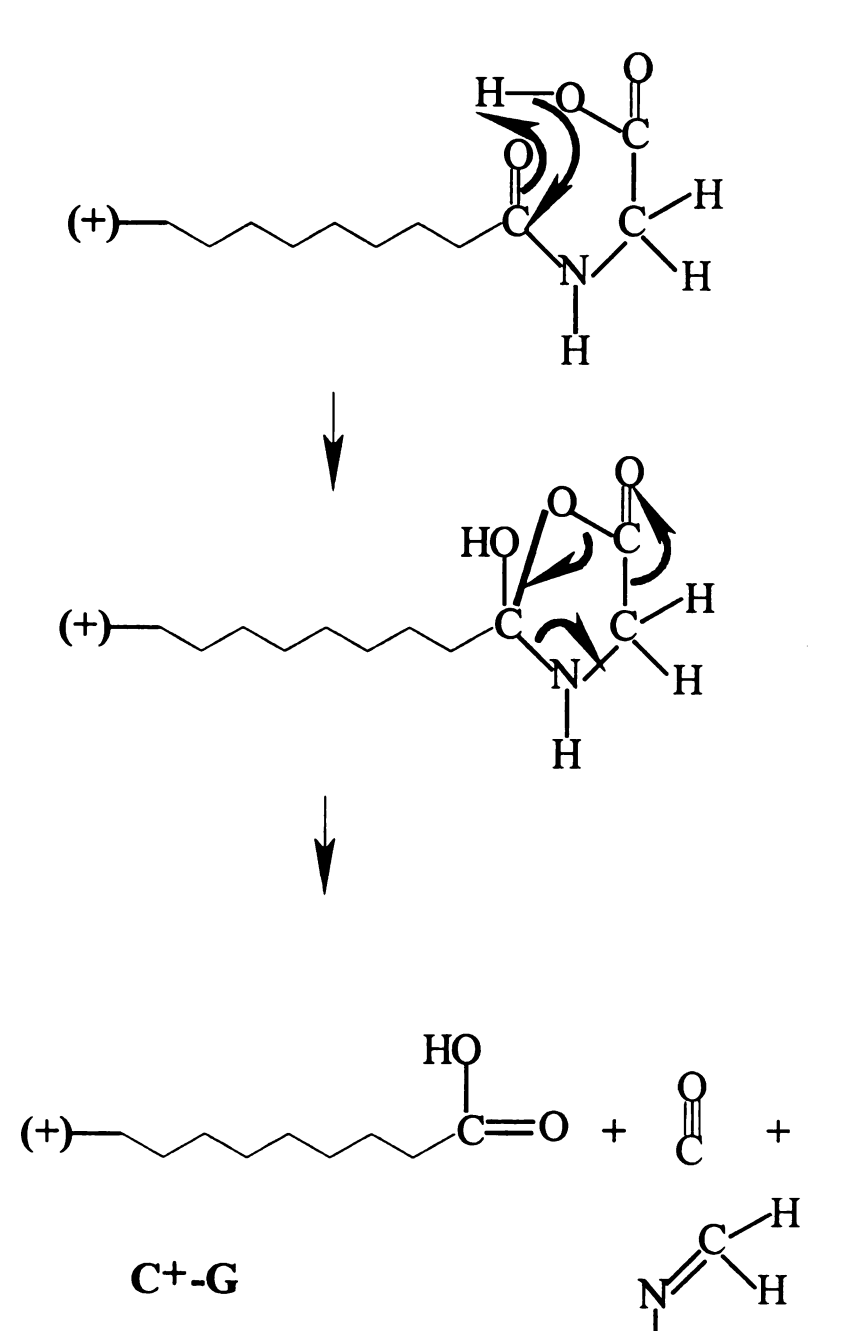


Figure 4.14. Mechanism for formation of the C⁺-G fragment from TMPP⁺-Ac-VGVAPG.

This is observed, and the fragment has a mass of 1019 Da from the deuterium exchanged species (F), while the mass of the fragment arising from the unlabeled species is only 1014 Da. The mechanism adopted for the TMPP⁺-Ac-VGVAPG (Species F) for the loss of C-terminal glycine is shown in Figure 4.14.

E. Genesis of an and bn ions due to Cleavage at the Site of the Proline Residue:

The CAD-MS/MS and MALDI-PSD results from analysis of the TMPP $^+$ -Ac derivatives of the labeled peptides suggest that the major fragmentation pathway in the formation of *a_n and *b_n ions is due to the shift of the amide hydrogen over to the neutral fragment of the peptide as shown in Figure 4.4. Yet, in the ESI-CAD-MS/MS spectra, there is always a low intensity signal at the m/z values corresponding to the *a_n and *b_n ions. The following table concisely presents the m/z values of the *a_5 and *b_5 peaks observed for the various labeled and unlabeled species.

Table 4.6. List of m/z values for *a₅ and *b₅ Ions Observed From the Labeled Variants of TMPP⁺-Ac-VGVAPG:

Peptide	*a ₅	*b ₅
(+)-VGVAPG	968	996
(+)-VG ^α VAPG	970	998
$(+)$ - $V^{\alpha}GV^{\alpha}APG$	970	998
$(+)$ - $V^{\beta}GV^{\beta}APG$	970	998
(+)-VGVA ^β PG	971	999
$(+)$ - $^{\eta}V^{\eta}G^{\eta}V^{\eta}AP^{\eta}G$	972	999

The shift in mass for the two ions in the case of the species with deuterium labels at α - or β - carbon suggests that these protons do not shift during the formation of the *a₅ and *b₅. But, the data from the amide hydrogen-labeled species is different (compare row 7 with row 2). For the as ion, if there were no shift of amide hydrogens, then the m/z value of the fragment ion (m/z 972) should be 4 Da higher than that for the fragment ion formed from the unlabeled species (m/z 968). This expectation is in agreement with the observed result, which suggests that the fragmentation does not involve any of the neighboring residues, but the proline residue itself. This type of β-hydrogen shift is primarily responsible for fragmentation in high-energy CAD analysis. Such a mechanism is not the most predominant in low-energy CAD, and may not be favored energetically. Hence, a very weak signal is observed, which is <10% of the relative intensity of the base peak in the mass spectrum. However, the fact that there is a signal is intriguing and the results from mass spectrometric analysis of the labeled peptides support that this signal is real. The following scheme shows a plausible pathway for forming an as ion involving the proton from the cyclic side chain of proline.

Figure 4.15. Mechanism for formation of the *a₅ ion due to cleavage at proline residue.

The data from the above table also indicate that in the case of the formation of the *b₅ ion, the shift in mass in the case of the amide labeled peptide and the unlabeled peptide is not 4 Da (as observed for the *a₅ ion), but only 3 Da. This suggests that one of the deuterons on the amide nitrogen from the neighboring residue is possibly shifted away resulting in the formation of the *b₅ ion. A reasonable mechanism depicting this process is shown in Figure 4.16. This pathway involves a six-centered intermediate, and forms a six-membered ring, which is a stable system. This is a more stable structure than

the structure of the *a_5 ion, which may explain why the signal due to the *b_5 ion is slightly larger than the signal due to *a_5 (ca. 12% of the base peak).

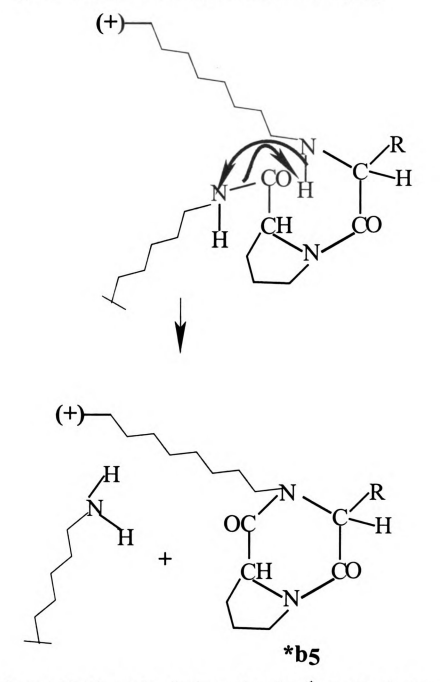


Figure 4.16. Mechanism for formation of the $^{\circ}b_{5}$ ion due to cleavage at proline residue.

The above discussions indicate that the formation of the *a_3 ion does not involve a shift of the amide hydrogen whereas the formation of the *b_5 does.

IV. Conclusions

The results from the mass spectrometric study of the TMPP $^+$ -Ac derivatives of the deuterium-labeled forms of the peptide VGVAPG show that the major pathway during the formation of the *a_n and the *b_n ions involves the shift of the amide hydrogen of the residue at which the cleavage occurs. This suggests that the structure of the *b_n ion is not a ketone as suggested previously, but is an aziridinone. Minor signal due to the cleavage at the proline residue suggests that ions do form due to cleavage at this site during CAD-MS/MS in a trap, although there is no amide hydrogen present. The shift in masses for the fragment ion *a_5 implies that the ion formation dues to cleavage at proline involves a proton shift from the ring structure of the side chain in proline. However, the *b_5 ion forms due to the shift of a neighboring amide hydrogen with a resultant structure including a six-membered ring. The data also serve as evidence for previously proposed mechanism for the loss of C-terminal residue.

V. References

- 1) Dongre, A.R.; Jones, J.L.; Somoygi, A.; Wysocki, V.H. J. Am. Chem. Soc., 1996, 118, 8365.
- 2) Johnson, R.S.; Krylov, D.; Walsh, K.A. J. Mass Spectrom., 1995, 30, 386.
- 3) Lias, S.G.; Liebman, J.F.; Levin, R.D. J. Phys. Chem. Ref. Data, 1984,13,695.
- 4) Tang, X.-J.; Thibault, P.; Boyd, R.K. Anal. Chem, 1993, 65, 2824.
- 5) Hunt, D.F.; Yates, J.R.; Shabanowitz, J.; Winston, S.; Hauer, C.R. Proc. Natl. Acad. USA, 1986, 83, 6233.
- 6) Meot-Ner, M. J. Am. Chem. Soc., 1984, 106, 278.
- 7) Aue, D.H. and Bowers, M.T. Gas Phase Ion Chemistry, Bowers, M.T. ed. (Academic, New York), 1979, pp.1-51.
- 8) Nair, H.; Wysocki, V.H. Int. J. Mass Spectrom. Ion Processes, 1998, 174, 95.
- 9) Jones, J.L.; Dongre, A.R., Somogyi, V.H.; Wysocki, V.H. J. Am. Chem. Soc., 1994, 116, 8368.
- 10) Schwartz, B.L.; Bursey, M.M. Biol. Mass Spectrom., 1992, 21, 92.
- 11) Roepstorff, P.; Fohlman, J. J. Biomed. Mass Spectrom., 1984, 11, 601.
- 12) Biemann, K.; Martin, S.A. Mass Spectrom. Rev., 1987, 237, 992.
- 13) Mueller, D.R.; Eckersley, M. Richter, W.J. Org. Mass Spectrom., 1988, 23, 217.
- 14) Kenny, P.; Nomoto, K.; Orlando, R. Rapid Commun. Mass Spectrom., 1992, 6, 95.
- 15) Tang, X.; Boyd, R.K. Rapid Commun. Mass Spectrom., 1992, 6, 651.
- 16) Roth, K.D.W.; Huang, Z.-H.; Sadagopan, N.; Watson, J.T. Mass Spectrom. Rev., 1998, 17, 255.
- 17) Keough, T.; Youngquist, R.S.; and Lacey, M.P. *Proc. Natl. Acad. Sci. USA*, 1999, 96, 7131.
- 18) Burlet,O.; Orkiszewski, R.S.; Ballard, K.D.; Gaskell,S.J. Rapid Commun. Mass Spectrom., 1992, 6, 658.

- 19) Ligon, W.V. Anal. Chem., 1986, 58, 485.
- 20) Huang, Z.-H.; Wu, J.; Roth, K. D. W.; Yang, Y.; Gage, D. A.; Watson, J. T. Anal. Chem. 1997, 69, 137.
- 21) Liao, P.-C.; Huang, Z.-H.; Allison, J. J. Am. Soc. Mass Spectrom. 1997, 8, 501.
- 22) Sadagopan, N.; Watson, J.T J. Am. Soc. Mass Spectrom. 2000, 11, (in press).
- 23) Wagner, D.S. Ph.D. Dissertation, Michigan State University, East Lansing, MI, 1992.
- 24) Barany, G.; Merrifield, R.B. The Peptide Analysis, Synthesis, Biology (Gross, E. and Meinhofer, Jed.), Academic Press, New York, 1980.
- 25) Lin, T.; Glish, G.L. Proceedings of the 45th ASMS Conference on Mass Spectrometry and Allied Topics, Palm Springs, California, June 1-5, 1997.
- 26) Thorne, G.C.; Ballard, K.D.; Gaskell, S.J. J. Am. Soc. Mass Spectrom. 1990, 1, 249.